Carbon Nanotube Quality Impact on Epoxy Composites Thermal Conductivity

Aleksandar Grujicic

A Thesis
in
The Department
of
Mechanical and Industrial Engineering

Presented in Partial Fulfillment of the Requirements
for the Degree of Master of Applied Science (Mechanical Engineering) at
Concordia University
Montreal, Quebec, Canada

March 2014

CONCORDIA UNIVERSITY

School of Graduate Studies

This is to certify that the Thesis prepared

By: **Aleksandar Grujicic**

Entitled: "**Carbon Nanotube Quality Impact on Epoxy Composites Thermal Conductivity"**

and submitted in partial fulfillment of the requirements for the Degree of

Master of Applied Science (Mechanical Engineering)

complies with the regulations of this University and meets the accepted standards with respect to originality and quality.

Signed by the Final Examining Committee:

_____Chair
Dr. S. Narayanswamy

_____Examiner
Dr. M. Pugh

_____Examiner
Dr. T. Vo-Van External
Department of Physics

_____Supervisor
Dr. S.V. Hoa

Approved by: _____
Dr. S. Narayanswamy, M.A.Sc. Graduate Program Director
Department of Mechanical and Industrial Engineering

_____2014 _____
Dr. C. Trueman, Interim Dean
Faculty of Engineering & Computer Science

ABSTRACT

Carbon Nanotube Quality Impact on

Epoxy Composites Thermal Conductivity

Aleksandar Grujicic

Composite materials thermal conductivity is a challenging area. This is particularly applicable in the through thickness direction. Obstacles on the path of improvement are numerous. To overcome issue of carbon nanotube distribution within composite a new approach was adopted. Carbon nanotubes were added to thin carbon fibre fabric, creating a new material to be impregnated by matrix. This was achieved with employment of ultrasound to obtain a basic building block for the layer-by-layer method. Laminate was prepared from prepreg layers utilising ancillary materials stack-up sequence optimised for thermal conductivity improvement through nanomaterials. Autoclave cured materials were examined for thermal conductivity. The highest value was achieved at 125 ^{o}C. The highest improvement over reference carbon fibre / epoxy composite material was obtained at 25 ^{o}C. Three different carbon nanotube materials were used in the research. Least damaged carbon nanotubes yielded the best results. Simple calculations completed on carbon nanotube / epoxy composites confirmed the least damaged carbon nanotubes – the carbon nanotubes of the highest quality - as the best heat transport medium.

Dedication

To my Parents

Mami i Tati

Table of Contents

List of Figures……...……..ix

List of Tables……xiv

Chapter 1.....1

1. Motives for the Present Study……..……1

1.1. Introduction…….……1

1.2. Motivation……2

1.3. Thesis Layout……..4

Chapter 2……..6

2. Literature Review……...……..6

2.1. Carbon Nanotubes……6

2.1.1. Discovery……6

2.1.2. Definition……7

2.1.3. Physical Properties……..…….8

2.2. Thermal Conductivity……..9

2.2.1. Heat Transfer by Phonons……9

2.2.1.1. Phonon – phonon interaction…….……10

2.2.1.2. Scattering by lattice imperfections…….……10

2.2.1.3. Boundary scattering……...……10

2.2.2. Graphite……..……11

2.2.2.1. The Structure of Graphite……..11

2.2.2.2. The Thermal Properties of Graphite……..11

2.2.3. CNT……15

Thermal transport……...……15

2.2.3.1. Thermal conductivity……..…16

2.2.4. Functional Composites……..…….27
2.2.4.1. Polymer + CNT……..27
2.2.4.2. Polymer + CNT + CF…….……35
2.2.4.3. CF + CNT……..38
2.2.4.4. CF + CNT + Polymer…….……39
2.2.5. Graphene……..……..40
2.2.5.1. Graphene thermal conductivity……..……40
2.3. Summary……43
2.4. Problem definition……...……..44
2.5. Thesis Objective……..…47
Chapter 3……..……..49
3. Materials and Manufacturing Procedure……49
3.1. Selected Materials…….…….50
3.1.1. Carbon Fibre Fabrics……..……51
3.1.2. CNTs……..…51
3.1.3. Matrix……...……..51
3.2. Samples Manufacturing…….52
3.2.1. Type A Samples manufacturing…….53
3.2.2. Type B Samples manufacturing……...……..53
3.2.3. Type C Samples Manufacturing……...…….54
3.2.4. Properties Improvement Samples Manufacturing…….57
3.2.4.1. The Effect of Ancillary Materials Stacking Sequence……..….65
3.3. Sample Quality……...70
Chapter 4…….....……..75
4. Testing……..……..75

4.1 Thermal Conductivity Testing……..……..75
4.1.1 Thermal Diffusivity……...……76
4.1.1.1. Measurement Principle……..……76
4.1.1.2. Coupon Preparation……..…….76
4.1.1.3. Measurement…….…….78
4.1.2. Density……...……78
4.1.2.1. Measurement……..78
4.1.3. Specific Heat……...…79
4.1.3.1. Cp Determination Process……..79
4.1.3.2. Measurement……...……81
Chapter 5……...…….82
5. Results and Discussion…….…….82
5.1. Type B samples…….…….82
5.1.1. BR Samples……82
5.1.1.1. CNTs Loading Level Impact…….……83
5.1.1.2. Temperature Impact……..…….87
5.1.2. BP Samples……...…….89
5.1.2.1. CNTs Loading Level Impact…….89
5.1.2.2. Temperature Impact……...……92
5.1.3. BSP Samples……..94
5.1.3.1. CNTs Loading Level Impact…….94
5.1.3.2. Temperature Impact……...……97
5.1.4. CNTs Quality Impact…….99
5.1.5. Conclusion…….……..105
5.2. Type D Samples……...…106

5.2.1. DR Samples……106
5.2.1.1. CNTs Loading Level Impact……107
5.2.1.2. Temperature Impact……110
5.2.2. DP Samples……112
5.2.2.1. CNTs Loading Level Impact……113
5.2.2.2. Temperature Impact……115
5.2.3. DSP Samples……117
5.2.3.1. CNTs Loading Level Impact……118
5.2.3.2. Temperature Impact……120
5.2.4. CNTs Quality Impact……121
5.2.5. Conclusion……127
5.3. Conclusion……129
Chapter 6……132
6. Conclusion, Contributions and Future Work……132
6.1. Conclusion……132
6.2. Contributions……134
6.3. Future Work……135
References……137

List of Figures

Fig. 1.1: Schematic presentation of most common methods to produce nanocomposites and proposed new method involving ultrasound…….……3

Fig. 2.1: First nanotubes observed [1]…….....6

Fig. 2.2: A single atom thick sheet of graphite. Vectors a and b are unit vectors of the two-dimensional lattice. The figure defines the lattice points coordinates [5]...7

Fig. 2.3: Thermal Conductivity of the SWNT with d=1nm……..17

Fig. 2.4: As-measured effective thermal conductivity (κ) versus temperature (T) for the two SWNT, one DWNT, and four MWNT samples in this work. Filled symbols and unfilled symbols are results measured before and after Pt–C deposited at the contacts, respectively [17]……..…….……18

Fig. 2.5 The individual MWNT length versus bundle length - SEM image [21]…..….20

Fig. 2.6: CNT forests measured thermal diffusivity [24]…….……..…..….22

Fig. 2.7: Effect of temperature-controlled lengths on the thermal conductivity of SWNTs [28]….....…25

Fig. 2.8: Thermal conductivity for a) (5,5) and b) (20,20) SWNT…..…..……...…25

Fig. 2.9: Thermal conductivity of MWNT/DGEBA epoxy composites…...……...29

Fig. 2.10: TEM images of a) acid oxidised and b) microtome cut SWNT [36]……30

Fig. 2.11: Thermal conductivity with pristine and functionalised MWNTs [37]……..31

Fig. 2.12: Thermal conductivity of CNT-epoxy composites processed at 0 and 25 T, compared with pristine epoxy sample processed at 25 T. The measurement was in the magnetic field alignment direction [41]……..33

Fig. 2.13: Axial thermal conductivity as a function of CNT mass fraction for CNT fibre / epoxy and T300 CF / epoxy composites. Included are TCs for as spun CNT fibre and T300 fibre as well as for pure epoxy [42]……..……34

Fig. 2.14: In-plane (circles) and through-plane (diamonds) thermal conductivities of the MWCNT-PBI fibre mats as a function of MWCNT content [44]……..…….35

Fig. 2.15: Thermal conductivity of composites with raw MWNTs and thermally treated MWNTs [45]…….……36

Fig. 2.16: Thermal conductivity of composites with a) LMWNTs b) SMWNTs [49].....38

Fig. 3.1: DSC determination of prepreg production parameters…..…..……...55

Fig. 3.2: Curing cycle for matrix system Epon 862 / Epicure W…...……..56

Fig. 3.3: CNTs dispersion: a) CNTs in DI water; b) Sonication in ice bath..……..57

Fig. 3.4: Adding CNTs into carbon fibre preform: a) Carbon fibre preform; b) Carbon fibre preform submerged in CNT - DI water solution; c) Arrangement in ultrasonic bath…….……..58

Fig. 3.5: Schematic presentation of CNT incorporation into CF fabric……58

Fig. 3.6: New material - Carbon fibres with CNTs added with the aid of ultrasound: a) CNTs attached to carbon fibres; b) Increased stiffness of modified carbon fibres……...……...60

Fig. 3.7: Schematic presentation of new material created from CFs and CNTs: a) 3D presentation; b) Frontal 2D view……...61

Fig. 3.8: Prepreg preparation from new material and matrix…….……..62

Fig. 3.9: CONCOM autoclave…...……..63

Fig. 3.10: Sample after curing in autoclave…….……..63

Fig. 3.11: New material after impregnation with matrix and curing in autoclave - CNTs attached to carbon fibres and impregnated in matrix can be seen as bright pixels……...……..64

Fig 3.12: SEM image of sample with accumulated matrix against the tool plate. CNTs are bright pixels…….…..65

Fig. 3.13: Thermal conductivity change with sanding of bottom, than top side of coupons……..…..……...67

Fig. 3.14: Schematic presentation of sample stacked up for curing in autoclave. Detail in circle is shown enlarged in Fig. 3.15…….....68

Fig. 3.15: Schematic presentation of improved stacking sequence that eliminates insulating matrix accumulation…….68

Fig. 3.16: Stacking Sequence Effect…….69

Fig. 3.17: TGA plot analysis showing reinforcement residue wt%.....72

Fig. 3.18: Optical microscope image of laminate at magnification of 500x…….72

Fig. 3.19: SEM images of properties improvement samples at a) 5k magnification and b) 50k magnification……..74

Fig. 4.1: Thermal diffusivity measurement principle [71]…..……76

Fig. 4.2: Typical Cp plot……...……...80

Fig. 5.1: Thermal conductivity at 25 ^{o}C plot for A and BR samples as a function of CNT loading……...……...……84

Fig. 5.2: Thermal conductivity at 75 ^{o}C plot for A and BR samples as a function of CNT loading……...……...……85

Fig. 5.3: Thermal conductivity at 125 ^{o}C plot for A and BR samples as a function of CNT loading……..86

Fig. 5.4: Thermal conductivity of A and BR samples as a function of temperature..…87

Fig. 5.5: Thermal conductivity at 25 ^{o}C plot for A and BP samples as a function of CNT loading……...…89

Fig. 5.6: Thermal conductivity at 75 ^{o}C plot for A and BP samples as a function of CNT loading……...……90

Fig. 5.7: Thermal conductivity at 125 ^{o}C plot for A and BP samples as a function of CNT loading……...…….…..91

Fig. 5.8: Thermal conductivity of A and BP samples as a function of temperature……93

Fig. 5.9: Thermal conductivity at 25 oC plot for A and BSP samples as a function of CNT loading……...……...95

Fig. 5.10: Thermal conductivity at 75 ^{o}C plot for A and BSP samples as a function of CNT loading……..……96

Fig. 5.11: Thermal conductivity at 125 ^{o}C plot for A and BP samples as a function of CNT loading……..……97

Fig. 5.12: Thermal conductivity of A and BSP samples as a function of temperature…..98

Fig. 5.13: 1 wt% samples thermal conductivity as a function of temperature…….……101

Fig. 5.14: 2 wt% samples thermal conductivity as a function of temperature…….……103

Fig. 5.15: 3 wt% samples thermal conductivity as a function of temperature…..……104

Fig. 5.16: Thermal conductivity at 25 ^{o}C plot for C and DR samples as a function of CNT loading…….……108

Fig. 5.17: Thermal conductivity at 75 ^{o}C plot for C and DR samples as a function of CNT loading…….……109

Fig. 5.18: Thermal conductivity at 125 ^{o}C plot for C and DR samples as a function of CNT loading……....110

Fig. 5.19: Thermal conductivity of C and DR samples as a function of temperature….111

Fig. 5.20: Thermal conductivity at 25 ^{o}C plot for C and DP samples as a function of CNT loading……..…113

Fig. 5.21: Thermal conductivity at 75 ^{o}C plot for C and DP samples as a function of CNT loading……..…114

Fig. 5.22: Thermal conductivity at 125 ^{o}C plot for C and DP samples as a function of CNT loading……..……..115

Fig. 5.23: Thermal conductivity of C and DP samples as a function of temperature…..116

Fig. 5.24: Thermal conductivity at 25 ^{o}C plot for C and DSP samples as a function of CNT loading……..……..118

Fig. 5.25: Thermal conductivity at 75 ^{o}C plot for C and DSP samples as a function of CNT loading……..……..119

Fig. 5.26: Thermal conductivity at 125 ^{o}C plot for C and DSP samples as a function of CNT loading……120

Fig. 5.27: Thermal conductivity of C and DP samples as a function of temperature.….121

Fig. 5.28: 1 wt% samples thermal conductivity as a function of temperature…….……123

Fig. 5.29: 2 wt% samples thermal conductivity as a function of temperature…….124

Fig. 5.30: 3 wt% samples thermal conductivity as a function of temperature…….……125

Fig. 5.31: Comparison of highest thermal conductivities obtained with different CNTs materials……..……...126

Fig. 5.32: Good distribution of CNTs in the CFRP nanocomposites. Surface is featuring tough material characteristics……..127

List of Tables

Table 3.1: Matrix properties..……...……...…..52

Table 3.2: Samples schedule……...……..….52

Table 3.3: Three roll mill sequence……..……...……..……53

Table 3.4: Type B sample schedule.……...……...54

Table 3.5: Type D sample schedule……..…….……64

Table 3.6: Thermal conductivity of the samples as produced, then progressively sanded……...……66

Table 3.7: Thermal conductivity of samples made using standard stacking sequence and improved stacking sequence…….……...…….....69

Table 3.8: Sample groups' thicknesses….....……..…….71

Table 5.1: Thermal conductivity for Type A and BR samples.……...…..……...…83

Table 5.2: Thermal conductivity for Type A and BP samples.……..……...89

Table 5.3: Thermal conductivity for Type A and BSP samples.……...……..……..94

Table 5.4: Thermal conductivity for Type C and DR samples.…….…..107

Table 5.5: Thermal conductivity for Type C and DP samples……...…….....112

Table 5.6: Thermal conductivity for Type C and DSP samples.…...……..…117

Chapter 1

1. Motives for the Present Study

1.1. Introduction

Composite materials are replacing traditional materials like metals in nearly every imaginable domain. The reason for it resides in the fact that composite materials can have similar mechanical properties to metals while their weight is significantly lower. This property is important for many applications, notably automotive and aerospace industries. However, the application of composite materials in certain areas remains challenging. One of these areas is elevated temperature operating conditions. Parts operating in the elevated temperature environment are required to dissipate heat well. The physical property that determines part heat dissipation quality is part material thermal conductivity.

Materials used to produce composite materials parts are different fibres, one being carbon fibre, and a large variety of plastics, either thermoset or thermoplastic. Carbon fibres can be made from pitch or polyacryilonitrile precursors. Pitch based carbon fibres possess excellent thermal conductivity, however, their mechanical properties limit their application. On the other hand, widely used polyacrylonitrile (PAN) based carbon fibres are excellent heat conductors along the fibre, however fibre thermal conductivity perpendicular to the fibre is far smaller. The plastics used to give form to parts made from carbon fibres are in general terms thermal insulators. Combined together, carbon fibres and plastics have better thermal conductivity than the plastics, nonetheless

insufficient for engineering applications where heat dissipation is the determining factor in material choice.

At the end of the twentieth century, carbon nanotubes attracted significant attention of the scientific community. A method was discovered to produce them in quantities sufficient for characterization and application related research. Carbon nanotubes were found to be a material with exceptional mechanical, thermal and electrical properties. Such properties made them prime candidate to add to existing composite materials in order to obtain truly multifunctional composite materials with high electrical and thermal conductivity in all directions as well as improved mechanical properties.

Large amount of effort was put into improving composite materials thermal conductivity in order to obtain multifunctional composites with the addition of carbon nanotubes. However, carbon nanotubes high thermal conductivity did not result in very high thermal conductivity of composite materials. This was particularly applicable in the through thickness direction while certain methods were giving good results for in plane thermal conductivity. Many obstacles were identified on the road to the envisioned goal. Interface, both carbon nanotube – matrix and carbon nanotube – carbon nanotube, non-perfect crystal lattice of a carbon nanotube, high anisotropy of carbon nanotubes, dispersion quality are some of the issues encountered when improved thermal conductivity was sought.

1.2. Motivation

Carbon nanotubes have very high thermal conductivity, ~10^4 W/mK, higher than any other material found to date. Thermal conductivity is higher in individual carbon nanotubes than in assembled forms of bundles (< 10^3 W/mK), yarns, arrays, mats etc.

Nonetheless, even in these assembled forms, thermal conductivity is still very high, promising improvement of material to which either individual or assembled carbon nanotubes are added. At the same time, mechanical and electrical properties are expected to be improved as well, giving multifunctional composite material. To improve polymer thermal conductivity, carbon nanotubes were added to matrix. Compatibility between carbon nanotubes and matrix has to exist to achieve significant improvement. Good dispersion is a requirement as well. Damaged carbon nanotubes would yield smaller improvement. Impregnating carbon fibres with polymer matrix enriched with carbon nanotubes did not give expected result. One reason was carbon nanotube filtration, even from the matrix with well dispersed carbon nanotubes.

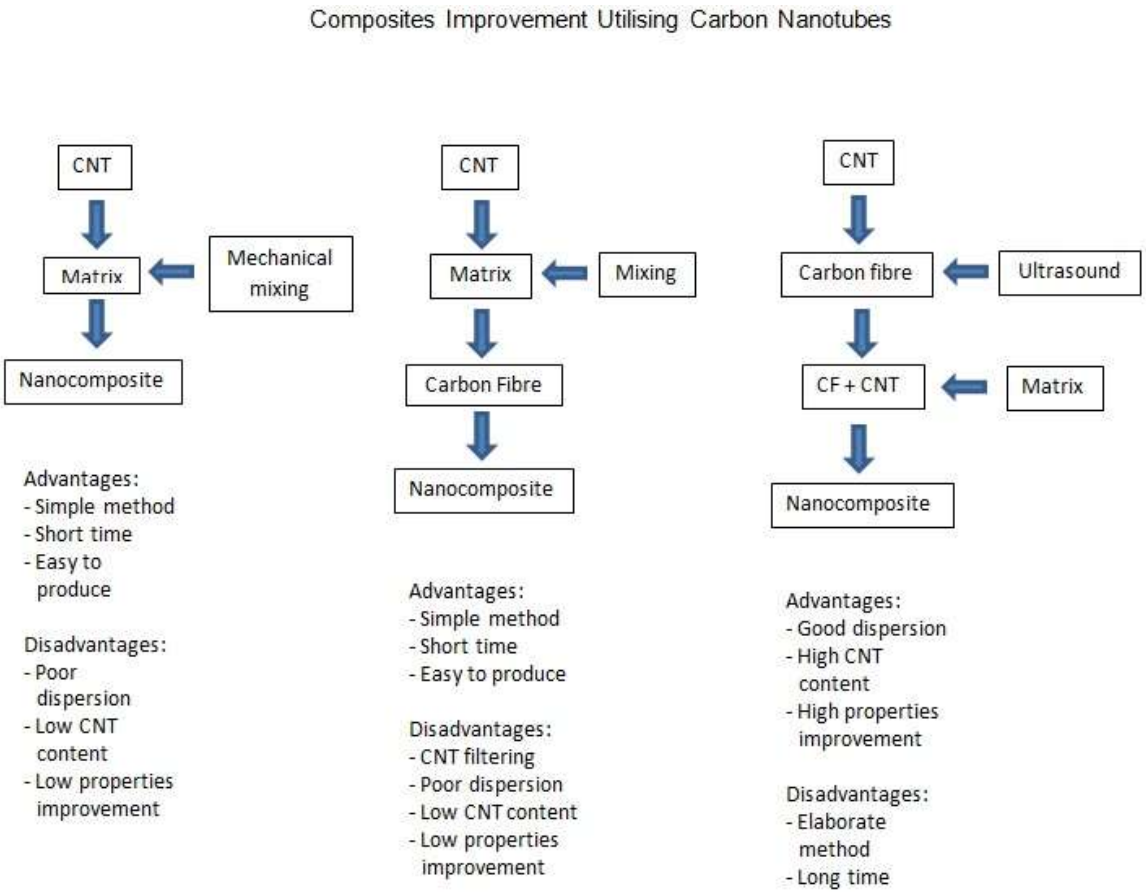

Fig. 1.1: Schematic presentation of most common methods to produce nanocomposites and proposed new method involving ultrasound.

To resolve the dispersion in polymer issue, proposed was layer-by-layer method, where very thin layers of carbon nanotubes were assembled with very thin polymer layers, one by one. Another, most recent approach was to grow carbon nanotubes on carbon fibres, thus improving thermal conductivity.

Therefore, the expectations with respect to thermal conductivity improvement could be met with the selection of appropriate approach to the carbon nanotube selection and material fabrication. To support the relevance of carbon nanotube quality and quantity to thermal conductivity improvement, numerous experiments were completed using single wall carbon nanotubes as the filler of choice. Carbon fibre reinforced epoxy thermal conductivity in through thickness direction was improved 140.4% at 25 ^{o}C with 3 wt% loading, significantly better than the best result reported to date, ~44% at room temperature with 11.68 wt% loading [51]. Schematic presentation of most common methods to produce nanocomposites and proposed new method involving ultrasound is given in Fig. 1.1.

1.3. Thesis Layout

The first chapter provides summary of broad background leading to research of thermal conductivity in composites. Reasons for incorporating carbon nanotubes are provided as well as issues met in the course of such attempts.

Current state of the art was reviewed in chapter number two. Short scientific background of thermal transport in graphite was given, followed by focusing on carbon nanotubes. The topic was then expanded to provide values of thermal conductivity in carbon

nanotubes and their assembled forms, followed by description of scientific effort to apply intrinsic properties in the real life applications.

At the beginning of the following chapter, numbered three, employed material description and properties are provided. Selected path to manufacture new material with improved thermal conductivity was described afterwards. Details are provided with respect to sample schedule, manufacturing and preparation for testing along with sample quality examination results.

The fourth chapter is giving an overview of tests performed to evaluate manufactured material properties.

Testing results were reviewed in chapter number five. Discussion of results and conclusions drawn were presented in this chapter as well. Important achievements are emphasised and supported with scientific evidence.

Work completed and results obtained in the course of the thesis are summarised in the last, chapter number six. Contributions to the body of knowledge are pointed out, followed by recommendations for future work.

Chapter 2

2. Literature Review

2.1. Carbon Nanotubes

2.1.1. Discovery

Carbon Nanotubes (CNTs) were discovered in 1952 by Russian scientists Radushkevich and Lukyanovich [1,2]. The discovered nanotubes [Fig. 1] were Multiwall Carbon Nanotubes (MWNT), 50 nm in diameter [2].

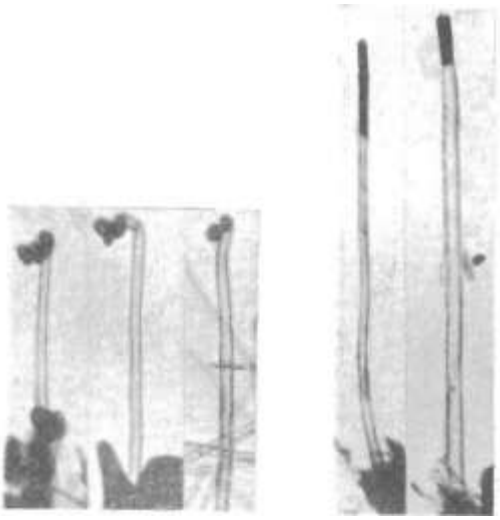

Fig. 2.1: First nanotubes observed [1].

Single Wall Carbon Nanotubes (SWNT) were first observed by two independent teams [2]: a Japan team S. Iijima and T. Ichihashi [3] and a US team Bethune et al. [4]. Both teams reported tubular structures with the diameter in the 1 nm range and the walls being of a single atom dimension thickness [4]. The Japanese team confirmed the carbon hexagon helical arrangement via electron diffraction from a single tube [3].

Tubule structure can be described uniquely following Hamada notation [5].

2.1.2. Definition

Carbon nanotubes are an allotrope of carbon [5]. *sp*2 bonded carbon atoms are forming a graphene sheet [6]. CNTs can be represented as a sheet of graphite rolled in a cylinder [5]. In some cases, tubule diameters are small enough to exhibit the effects of one-dimensional (1D) periodicity [6]. If the structure consists of a single cylinder, the CNT is a Single Wall Carbon Nanotube (SWNT). Where multiple cylinders are present, concentric about the tube axis, the CNT is a Multiwall Carbon Nanotube (MWNT). If only two concentric tubules are present, it is a Double Wall Carbon Nanotube (DWNT). Hexagons consisting of carbon-atoms are arranged about the tube axis helically [5]. The realization that the ends of carbon nanotubes must be fullerene-like (C_{30}) "caps" explained the fact that the diameter of a carbon nanotube could only be as small as a fullerene molecule [8].

Taking one atom thick sheet of graphite [Fig. 2.2] as a material to begin with, it is possible to construct an infinite number of CNTs by superposing a randomly chosen lattice point on a chosen origin. Each of these microtubules would be uniquely defined by a lattice point superposed on a chosen origin. Hence, a lattice point of a graphite sheet can be used as an index of the atomic structure of the graphitic microtubule. The index is denoted as $A(n_1, n_2)$, where (n_1, n_2) represents the lattice point [5].

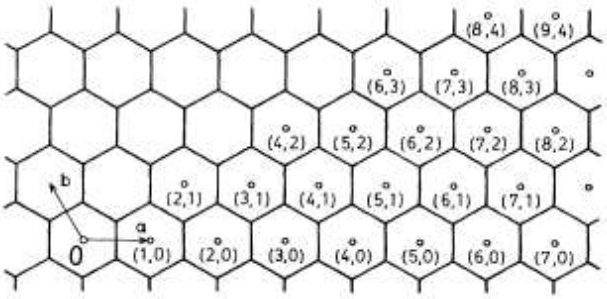

Fig. 2.2: A single atom thick sheet of graphite. Vectors a and b are unit vectors of the two-dimensional lattice. The figure defines the lattice points coordinates [5].

2.1.3. Physical Properties

Thermal conductivities of earlier discovered allotropes of carbon, type IIA diamond (2320 W/mK at 300K [9]) and graphite sheets – pyrolytic graphite (1950 W/mK in parallel and 5.70 W/mK in perpendicular direction at 300K [9]) are the highest measured at moderate temperatures [10]. The highest values measured for these two allotropes were at very low temperatures. For type IIA diamond it was 11900 W/mK at 70K while for pyrolytic graphite the highest value of 4970 W/mK in parallel direction was measured at 100K and in perpendicular direction it was 18.1 W/mK at 80K [9]. As carbon nanotubes are in essence a graphite sheet rolled into a cylinder, they could be expected to possess thermal conductivity similar to those of graphite sheet and diamond [10].

Graphitic tubules may possess as well unusual mechanical, electronic and optical properties with a wide range of technological applications (e.g. nanoscale devices, light-weight and high strength composite materials etc.) because of their crystalline perfection, various possible helical structures, the dimensionality and the high efficiency of production [7].

Another possible application is heat dissipation on micro and macro scale. Thermal conductivity is the determining factor when choosing material for thermal management. For this reason, among physical properties, this thesis shall put an emphasis on thermal conductivity.

2.2. Thermal Conductivity

2.2.1. Heat Transfer by Phonons [11]

A crystal lattice is an array of points in three-dimensional space where individual atoms lie. Imperfections in the crystal lattice structure are inevitable. These could be vacant points, inserted or substituted atoms.

In the crystal lattice structure, heat is carried under the gradient of temperature. This is achieved through vibrations of the lattice. Thermal energy of the solid is distributed amongst the vibration modes of the crystal. Each mode can be represented as a standing wave and analysed into traveling waves in opposite directions. Such waves are called sound waves if longitudinally polarised. Thus, energy can be carried through the lattice with velocity of the order of velocity of sound. The quanta of the lattice vibrational field are named phonons.

Phonons can be divided into acoustic and optical, based on their frequencies or wavelengths. Acoustic phonon wavelengths correspond to the ordinary elastic waves of the continuum while optical phonon frequencies correspond to electromagnetic radiation frequencies in infra-red. Optical phonon frequencies are significantly higher than the acoustic phonon frequencies. These frequencies are nearly that of a free molecule, and the effect on the surrounding lattice would be very small. Hence, optical modes do not play a significant role in the transport of energy through the lattice.

The resistance to the heat transport is coming from phonon-phonon interactions and scattering from imperfections in the lattice.

2.2.1.1. Phonon – phonon interaction

In phonon-phonon interaction, two phonons interact and get destroyed and the third one is created.

To understand the process, let a phonon move through the lattice. With the vibration of the lattice, some atoms move apart, other get closer than when in equilibrium. If another phonon is moving through the lattice while the vibration from the previous one is still affecting atoms to be out of their equilibrium state, it would be met with the different spacing between the atoms that would reflect it. The reflected phonon wave vector would equal the sum of the first two wave vectors.

2.2.1.2. Scattering by lattice imperfections

Certain types of imperfections can be treated as independent characteristic modes of error in the construction of the ideal lattice.

The imperfections can be isolated point imperfections like vacancies, inserted atoms and impurities. An atom can be inserted into, removed from or substituted for another in the crystal lattice.

Where imperfection exists crystal lattice properties are different from the ideal lattice properties. This difference in lattice properties is a cause of scattering of phonons.

2.2.1.3. Boundary scattering

At the crystal lattice boundary a phonon may be unable to continue in the same direction with the same velocity and energy if the structure on the other side of the boundary does not possess the same elastic properties. The amount of scattering would depend on the mismatch in properties.

2.2.2. Graphite [12]

Mentioned is possibility that CNT physical properties are similar to the physical properties of graphite.

The physical properties of graphite were extensively researched. Kelly [12] provided a summary.

The thermal conductivity of CNT is of particular interest. In order to better understand the thermal conductivity of CNT, first we will take a closer look at the thermal conductivity of graphite.

2.2.2.1. The Structure of Graphite

The graphite normal structure is the hexagonal one with symmetry. It consists of a stack of parallel hexagonal net planes. The unit cell contains four atoms in a planar stacking sequence. The natural valency of carbon is four, as in diamond, but this is not inflexible - in graphite coplanar trigonal bonds are formed with neighbouring carbon atoms in the hexagonal net sheet structure. The individual hexagonal nets are tightly bonded, but the nets are only weakly bonded together. The graphite crystal is highly anisotropic.

2.2.2.2. The Thermal Properties of Graphite

The thermal properties of a solid reflect the crystal lattice vibration spectrum and hence the interatomic forces. In general the properties involve an average over a wide range of wavelengths in the spectrum and tend therefore to be rather insensitive to the spectrum. At low temperatures it is necessary to consider the electronic contribution to the property.

2.2.2.2.1. The Lattice Vibration Spectrum

The vibrational modes propagating along the hexagonal crystal axis are the longitudinal and transverse acoustic modes. The maximum frequency in the longitudinal mode was found to be 3.84×10^{12} Hz for a pyrolitic graphite. Sample imperfection with mosaic spread mixes into the transverse acoustic mode observations a proportion of the in-plane lattice vibrations.

The simplest treatments of the lattice spectrum theories, akin to the Einstein and Debye models, the high degree of anisotropy of graphite lattice suggested that the atomic vibrations are of two kinds only, those in which atomic movements are parallel to the hexagonal axis (out-of-plane) and those in which they are perpendicular to it (in-plane vibrations).

The symmetry of the graphite lattice requires that only two principal thermal conductivities are necessary to describe the crystallite, measured parallel (Kc) and perpendicular (Ka) to the hexagonal axis. At an angle ϕ to the hexagonal axis $K(\phi)=K_c\cos^2\phi+K_a\sin^2\phi$ and as usual the same symmetry applies to the extruded or moulded polycrystalline body, i.e. equation $K(\phi)=K_c\cos^2\phi+K_a\sin^2\phi$ applies with $K_{\parallel}$ replacing K_c and $K_{\perp}$ replacing K_a.

A formulation assumes that an atom in the graphite lattice is subject to four kinds of restoring force when displaced:

a) A force due to change $\Delta\theta$ in the angle enclosed by two covalent bonds in the basal planes.

b) A force due to a change Δl_1 in the nearest neighbour bond length.

c) A force due to the change Δl_2 in the separation of nearest neighbours in adjacent layers.

d) A force due to the displacement Δh of an atom out of its plane defined by the three nearest neighbours.

2.2.2.2.2. Thermal Conductivity Levels

2.2.2.2.2.1. In plane

A number of forms of carbon and graphite exist. The materials are natural graphite, pyrolitic carbon and graphite, polycrystalline nuclear and electrode graphites, and non-graphitising carbons. The review of the experimentally established thermal conductivities of different forms of carbon and graphite follows.

Lattice conduction forms the dominant mechanism in many carbons.

A study of a number of Canadian natural graphite samples (the closest approach to single crystal graphite) found maximum thermal conductivity of 2800 W/mK at ~80K parallel to the basal planes over the range of 5K to 300K.

The thermal conductivity parallel to the axis of a carbon filament produced by deposition from methane on to a hot carbon wire showed a maximum value of between 2000 and 3000 W/mK at ~150K.

2.2.2.2.2.2. Perpendicular to the deposition planes

Kelly [12] provided as well a summary of the thermal conductivity measurements perpendicular to the samples deposition planes, published by several authors. The first group of results extends from 10K to 300K with a peak of ~ 20 W/mK at 75K.

Comparison with the same author results parallel to the deposition plane shows that the anisotropy ratio increases from ~50 at 10K to a constant value of ~325 above ~150K.

2.2.2.2.2.3. The imperfections

The imperfections affect the low temperature conductivity, however are of much less effect at high temperatures. Data have been reported in the form of diffusivity data.

The data show a diffusivity parallel to the deposition plane falling from 30 mm^2/s at 1300 ^oC to 16 mm^2/s at 2000 ^oC. In the same temperature range the diffusivity of each of three samples measured perpendicular to the deposition planes was independent of temperature with values between 0.2 mm^2/s and 0.35 mm^2/s. The specific heat at these temperatures varies from 23.4 J/molK at 1300 ^oC to ~25.9 J/molK at 2000 ^oC, so that the conductivity parallel to the deposition planes falls from ~1590 W/mK to ~ 940 W/mK. The conductivity perpendicular to the basal plane varies from ~10 W/mK to ~18 W/mK, almost independent of temperature.

Measurements for materials based upon natural graphite of high perfection but with only partial orientation showed that the magnitude of conductivity varied with the direction of measurement relative to the symmetry direction. Each direction showed a peak between 100K and 200K of magnitude 50 to 300 W/mK.

The low temperature studies reveal an electronic component. Over the major part of the temperature range the lattice contribution is dominant.

Consider first the lattice contribution parallel to the basal planes. Generally accepted explanation of the peak in the conductivity curve in lattice conductors is that below peak conductivity is limited by crystallite boundary scattering and above the peak by phonon-

phonon scattering. The resistance due to the latter is essentially independent of the defect structure for not too large defect concentrations, while the conductivity in the former is generally supposed to be proportional to the crystallite size and the specific heat.

For temperatures 300-1000K, the main contribution is found to be due to the longitudinal acoustic mode, the optical modes making little contribution directly but being important in scattering.

2.2.3. CNT

Thermal transport

The overall phonon spectra of graphitic tubules resemble that of a graphite sheet, especially when the tubule diameter is large. The low frequency modes, which are the signature of the tubule structure, are sensitive to the diameter. The normal modes of a graphitic tubule can be approximately classified into radial modes and tangential modes [7].

Radial modes would correspond to the modes parallel to the hexagon axis and the tangential modes would be perpendicular to the hexagon axis.

The higher frequency tangential modes in the graphitic tubules with a general helicity cannot be classified into pure z modes (modes with eigenvectors along the tubule axis) and θ modes (modes with eigenvectors along the circumference of the tubule) according to their vibrational eigenvectors. Employing tight-binding molecular dynamics, it was determined that phonon modes in tubules are softened by the curvature when compared to graphite [7].

In a highly anisotropic material like CNTs, thermal conductivity is most sensitive to the high velocity and high-scattering-length phonons. Hence, it is likely that even in nanotube bundles, the thermal conductivity should directly probe on-tube phonons and be insensitive to inter-tube mechanical coupling [13].

2.2.3.1. Thermal conductivity

Following conclusions that CNTs thermal conductivity can be similar to those of graphite and diamond [6, 7] significant effort was put in attempt to determine the thermal conductivity of CNTs. Experimental and numerical methods were employed.

2.2.3.1.1. Experimental

Both SWNT and MWNT thermal conductivities were measured. Experimental determination of thermal conductivities of various forms gave better insight in differences between individual CNTs, aligned and non aligned bundles, mats and forests.

2.2.3.1.1.1. Individual CNTs

Individual MWNT thermal conductivity value experimentally established in 2001 by Kim et al. [14] was measured using a microfabricated suspended device. Observed thermal conductivity was more than 3000 W/mK at room temperature.

With respect to individual SWNT thermal conductivity, experimental results yielded high values as well.

Pop et al. [15] probed the thermal conductivity of individual SWNTs for the first time by exploiting electron transport characteristics under strong self-heating and obtained κ= ~3600 W/mK at T=300 K.

Another team [16] found individual SWNT thermal conductivity in 2005. Thermal conductance of a 2.76 μm long individual suspended single-wall carbon nanotube was very close to the calculated ballistic thermal conductance of a 1 nm diameter SWNT. Thermal conductivity was calculated from the thermal conductance and obtained values were summarised in Fig. 2.3.

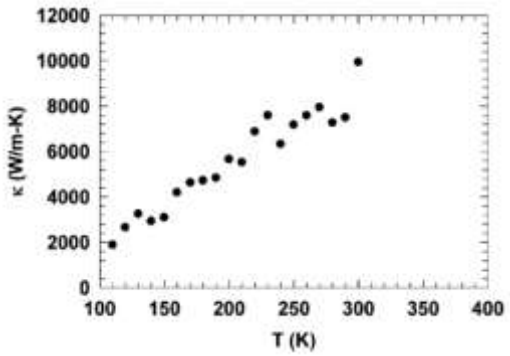

Fig. 2.3: Thermal Conductivity of the SWNT with d=1nm.

The highest obtained value for thermal conductivity was 10000 W/mK, deducted from Fig. 2.3.

Further measurements were made with mixed results, compared with the established values.

An attempt [17] was made to establish the structure–thermal property relationship by conducting thermal conductance and TEM measurements on the same individual SWNT, double-walled (DWNT), and MWNT directly grown between two suspended microthermometers by thermal chemical vapor deposition (CVD). For one SWNT thermal conductance, diameter, and chirality were all characterized, and thermal conductance of a DWNT is measured. Intrinsic thermal conductivity values determined

for the three MWNT samples correlate well with the different structural defect concentrations observed by TEM.

A total of seven CNT samples are reported in the quoted work. These samples are denoted as S1 and S2 for the two SWNT samples, D1 for the DWNT sample, and M1, M2, M3, and M4 for the four MWNT samples.

Thermal conductance (G_s) of the as-grown CNTs was measured using the suspended microthermometer device.

Effective thermal conductivity κ is obtained as $\kappa = G_s L/A$ where A and L are the cross-sectional area and suspended length of the as-grown CNT sample, respectively.

Obtained effective thermal conductivity results for the two SWNT, one DWNT, and four MWNT samples are shown in Figure 2.4.

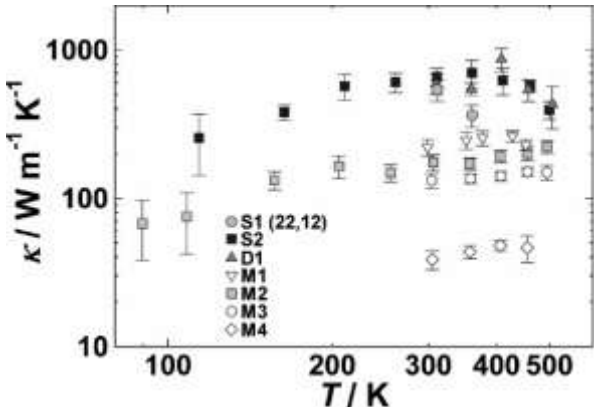

Fig. 2.4: As-measured effective thermal conductivity (κ) versus temperature (T) for the two SWNT, one DWNT, and four MWNT samples in this work. Filled symbols and unfilled symbols are results measured before and after Pt–C deposited at the contacts, respectively [17].

It could be seen that κ could be as high as 1000 W/mK for DWNT, however, the average level for SWNTs is closer to 650 W/mK. MWNT thermal conductivity varies between ~40 and ~300 W/mK.

These values are lower than MWNT thermal conductivity measured in [14] and SWNT thermal conductivities measured in [15,16].

Further measurements of CNT thermal conductivity ensued.

Individual MWNT obtained by CVD thermal conductivity was measured. The obtained value is 600±100 W/mK. Low structural quality of CVD grown MWNT can explain the obtained thermal conductivity, low when compared with earlier measurement results [18].

2.2.3.1.1.2. Bundles

Following thermal conductivity determination for individual CNTs, thermal diffusivity and conductivity of CNT bundles were determined. Higher thermal diffusivity means higher thermal conductivity.

Transient electrothermal technique (TET) was employed by Guo et al. [19] to measure thermal diffusivity of SWNT bundles. Obtained diffusivity of a bundle measured to be around 65 μm thick is 27.3 mm^2/s.

Another measurement of SWNTs bundle thermal diffusivity was completed utilizing a transient photon-electro-thermal (TPET) technique based on step laser heating and electrical thermal sensing. Measured thermal diffusivity for the SWNT bundle is 25.3 mm^2/s, much less than thermal diffusivity of graphite in the layer direction [20].

Pulsed laser-assisted thermal relaxation technique was used to measure thermal diffusivity of multiwall carbon nanotube bundles [21]. Measured thermal diffusivity ranges from 10.5-15.0 mm^2/s. Measured thermal diffusivity is low in significant part due to the random alignment of the CNTs in the bundle. First order estimation was conducted

by the authors to evaluate the real thermal diffusivity of single MWNT based on the alignment shown in Fig. 2.5. Two typical MWNT are picked and analyzed. One is between points A and B and the other is between points C and D. The shortest distance – in axial direction - between A and B is 1.125 μm. However, the length of the black curve in the figure from A to B is 3.542 μm which is the MWNT real length. Keeping in mind that thermal diffusivity α is proportional to the square of length in data processing, thermal diffusivity of the single MWNT (A-B) is estimated to be 145 mm^2/s, which is about order of magnitude higher than thermal diffusivity of the MWNT bundle measured to be 14.6 mm^2/s. Similarly, taking the MWNT between C and D for analysis, the MWNT length between C and D is 6.389 μm, while the C-D straight line length is 2.583 μm. Thermal diffusivity of this single MWNT is estimated to be 89.3 mm^2/s. For more curved CNTs, and many are visible in Fig. 2.5, their thermal diffusivities will be much larger than 89.3 mm^2/s. Based on the above estimations, authors concluded that the real thermal diffusivity of MWNTs should be about ten times the value measured for a bundle. If the effect of the thermal contact resistance between CNTs is taken into consideration, the real thermal diffusivity of single MWNTs can be even higher.

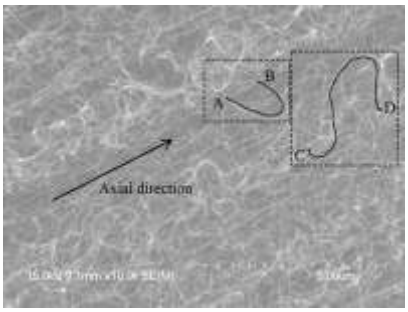

Fig. 2.5 – The individual MWNT length versus bundle length - SEM image [21]

Following measurement of individual MWNT, thermal conductivity (TC) measurement was completed for bundles. MWNT bundles were separated from highly oriented yarns drawn from the sidewall of a 300–350 μm tall MWNT forest, which was synthesized by a catalytic chemical vapor deposition method (CVD). Thermal conductivity measurements yield the value of 150±15 W/mK. This value is four times lower than individual MWNT κ measured. The reason for it is coupling in nanotube bundles [18].

2.2.3.1.1.3. Yarns

Another form of CNT based material is yarn.

Thermal conductivity of array-spun multi-walled carbon nanotube yarns (CNT fibres) was measured to obtain the value of 60±20 W/mK. 10 μm yarn was measured using parallel thermal conductance technique. Thermal conductivity was observed to decrease with increasing yarn diameter. Authors consider structural differences to be the drivers of the conductivity reduction process [22].

2.2.3.1.1.4. Mats

Hone et al. measured thermal conductivity of thick films of aligned single wall carbon nanotubes and nanotube ropes. These samples were produced via filtration/deposition from suspension in strong magnetic fields with a mosaic spread that ranged from 28° to 35°, pending the sample thickness. Obtained thermal conductivity of nanotubes is large, even in bulk samples: aligned bundles of SWNTs show a thermal conductivity of > 200 W/mK at room temperature in parallel direction [23].

On the other hand, highly oriented transparent nanotube sheets were drawn from the sidewall of a 300–350 μm tall MWNT forest, to continue evaluation of different, ever

more macroscopic CNT forms. Thermal conductivity was measured and yielded the value of 50±5 W/mK. This value represents further decrease from the one obtained for the bundles of MWNTs, which on their part had four times lower TC values compared to single MWNT. Thermal conductivity reduction comes from tube–tube interconnections and sheet imperfections like dangling fiber ends, loops and misalignment of nanotubes [18].

2.2.3.1.1.5. Forests

Diverse carbon nanotube forests with tailored structures were synthesized by water-assisted chemical vapor deposition growth (supergrowth) from engineered catalysts. Carbon nanotube forests composed from nanotubes with different size and wall number were synthesized as a function of varying production conditions. Superior thermal diffusivity was obtained from predominantly SWNT forests. It was found that thermal diffusivity values decreased with increasing wall number. From Fig. 2.6 can be seen that thermal diffusivity of CNT forests vary from ~20 to near 40 mm^2/s, pending the CNT type dominating the forest composition.

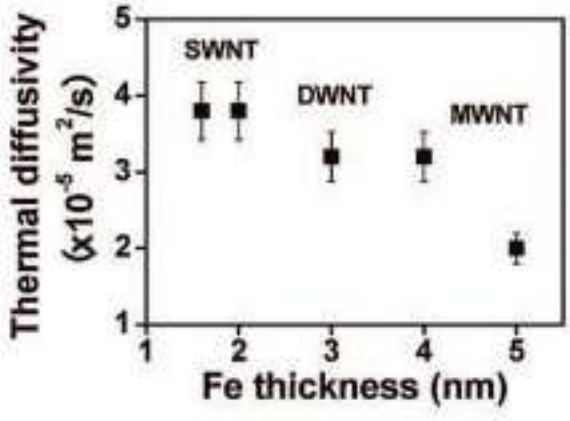

Fig. 2.6: CNT forests measured thermal diffusivity [24].

In general, phonon transport is more sensitive to defects than electron transport. The authors concluded the differences in thermal diffusivity levels are due to this property [24].

Chemical vapour deposition was employed to produce supergrowth SWNT forests with thickness of 1 mm. Thermal diffusivity measurement of the as-grown samples completed in thickness direction gave values from 47-77 mm^2/s. Obtained thermal diffusivity is on the same order as isotropic graphite [25].

The value measured in [25] is slightly higher than the value obtained in [24]. However, some authors reported lower values for CNT forests, as follows.

MWNT arrays were grown by CVD and characterised for thermal conductivity properties. Obtained values for κ at room temperature along the growth direction of the MWNTs are in the range of 0.5–1.2 W/mK, with the shortest array having the highest thermal conductivity.

When compared to shorter arrays, due to the longer growth times, taller arrays have more defects and amorphous carbon. This increase in defects is most likely the cause of thermal conductivity reduction with the array height increase.

In the direction perpendicular to the MWNT cylinder, the thermal conductivity was ten times lower. This datum is evidence of MWNT imperfection providing for contact between MWNTs. However, the imperfection is not limited to straightness.

When the fact that the array is not densely packed is employed to scale up thermal conductivity along the alignment direction by 35, a factor of typical literature value, a value for comparison with the individual MWNT is obtained. This value is 18-42 W/mK, at the low end of literature reported values [26].

2.2.3.1.2. Numerical Methods

In parallel with experimental effort to determine the thermal conductivity of an individual CNT and CNT forms, numerical approach was attempted with mixed result.

2.2.3.1.2.1. Individual CNTs

Molecular dynamic simulations provided results for predicted single wall carbon nanotubes thermal conductivity in the range 37000 W/mK at 100 K to 6600 W/mK at room temperature. Results were compared to the results obtained for a graphene monolayer showing very similar behavior for both carbon allotropes. Results for graphite depict interlayer interactions effect reducing graphite thermal conductivity by an order of magnitude compared with the previous two.

Strong tube–tube coupling decreases high-temperature thermal conductivity of SWNT bundles by an order of magnitude relative to isolated tubes; weak coupling may imply no significant reduction in thermal conductivity when tubes are bundled into ropes [27].

Single wall carbon nanotubes thermal conductivities were determined using non-equilibrium molecular dynamic simulations [28]. Thermal conductivities length dependence of single wall carbon nanotubes were studied in a vacuum. Analysis was completed on single wall carbon nanotubes with 12.3 nm, 24.6 nm, and 36.9 nm lengths with varying fixed end temperatures. Apparent thermal conductivity values increase with the increase of lengths of the temperature-controlled sections, and they converge to constant values – Fig. 2.7.

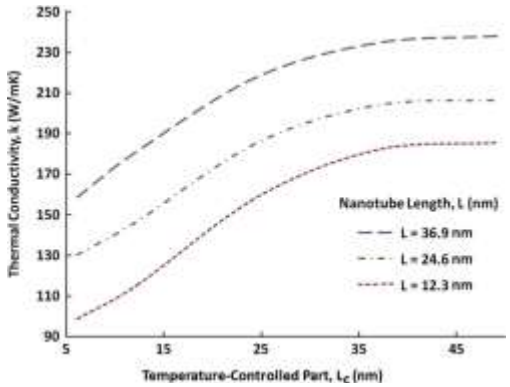

Fig. 2.7: Effect of temperature-controlled lengths on the thermal conductivity of SWNTs [28].

From Fig. 2.7 is possible to estimate values of plateau thermal conductivities. For respective tubules, these are 185, 207 and 240 W/mK.

The thermal conductivity of SWNTs and MWNTs was calculated using a kinetics model. Results show the SWNT thermal conductivity being a function of tube chirality with the (5,5) tube having maximum thermal conductivity an order of magnitude larger than the (20,20) SWNT along the tube axis. The maximum values for the respective tubes are approximately 35000 and 3500 W/mK. Chirality dependence is even more emphasised at 300 K, slightly above room temperature where thermal conductivity for the former is measured to be ~30000 W/mK and for the latter ~1750 W/mK, as shown in the Fig. 2.8.

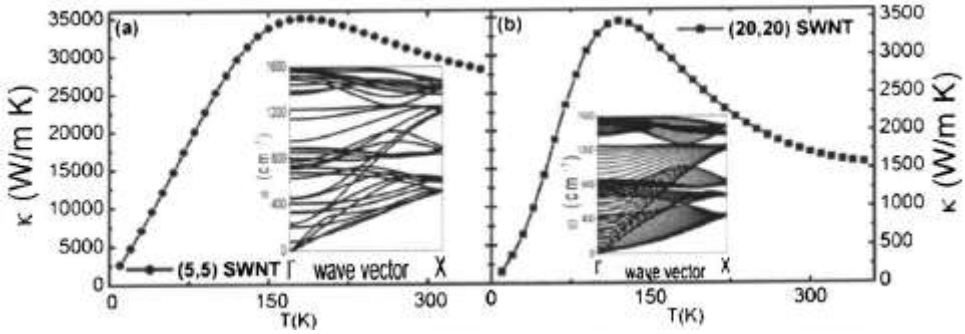

Fig. 2.8: Thermal conductivity for a) (5,5) and b) (20,20) SWNT.

When discussing thermal conductivity of an individual multiwall carbon nanotube, because of the weak intertube interaction, it is possible to use the constituent wall

properties to calculate κ of a MWNT. On the other hand, phonon scattering processes in a MWNT are different from those in an individual SWNT. In a defect-free MWNT phonons remain in a single shell - the intertube interactions in a perfect MWNT would be very low. This is called weak intertube coupling. In a tube with defects in interstitial space between the walls, phonons travel from one wall to another and strong intertube coupling exists.

Calculations were compared with experimental results for an individual 14 nm diameter MWNT. If the strong intertube coupling is intrinsic, measured thermal conductivity would be comparable to that of the outmost wall. If the outmost tube is a (100, 100) SWNT (~13.5 nm in diameter), its thermal conductivity would not be larger than 100 W/mK, which is far smaller than a measured value of 3000 W/mK. If, however, the intertube coupling is weak, thermal conductivity is nearly a sum of κ_i of the constituent walls. If the number of walls can be counted by transmission electron microscope it would be possible to verify the consistency between calculated and measured κ. As it was not the case, the only conclusion drawn is that the intertube coupling in this MWNT is weak [29].

2.2.3.1.2.2. Bundles

Study of SWNT bundles shows κ along the axis is two orders of magnitude larger than that perpendicular to the axis. Thus, phonon propagation would remain remarkably one dimensional in such an ideal bundle with weak intertube interaction [29].

2.2.4. Functional Composites

Following theoretical estimations, experimental results and numerical simulations, all giving very high values of CNTs and their macroscopic forms thermal conductivity, scientific effort was directed towards obtaining functional polymer based nanocomposites incorporating CNTs. The reason behind this effort was thermal management on micro and large scale.

The effort was again going in two directions: experimental work and numerical simulations. Here is to be presented work that yielded either the highest values of thermal conductivity or provided valuable contribution to the research field.

2.2.4.1. Polymer + CNT

This portion of review will begin with composites containing CNTs and polymers. First, let's take a look into experimental work.

2.2.4.1.1. Experimental

In the early stages substantial effort was made to exploit CNTs high thermal conductivity to convert essentially insulating polymers into conductors. Many difficulties were met on the way to achieve this goal. For that reason the improvement was insignificant and far below the expected one based on the law of the mixture.

One of the early successful trials was when industrial epoxy samples loaded with 1% unpurified HiPCO SWNTs material showed a 70% increase in thermal conductivity at 40K, rising to 125% at room temperature. The loading values were not reduced to

account for Fe impurities but were based on the mass of as-grown SWNT material. Samples were prepared via mixing and sonication [30].

Notifying difficulties in dispersion of CNTs in resins, in particular at high loadings, Kotov et al. [31] proposed sequential layering of CNTs and polyelectrolytes. This process greatly diminished phase segregation and rendered SWNT composite highly homogeneous. This layer-by-layer (LBL) technique rendered composites with SWNT content of 50±5 wt% as opposed to earlier attempts that were below 10 wt%.

Another approach was taken to address the CNTs dispersion in the polymer matrix. Actually, in lieu of attempting homogeneous dispersion, team Du et al. [32] created highly heterogeneous sample. Freestanding SWNT framework was prepared to reduce CNT/CNT interfacial resistance, earlier identified as a primary cause for only modest increases in thermal conductivity relative to the polymer matrix. The resulting composite showed the thermal conductivity improved 220 % compared to pure PMMA for 7 wt% loading to ~0.4 W/mK. The substantial improvement was attributed to more effective heat transfer within the nanotube-rich phase.

Nanocomposites were prepared from MWNT and epoxy resin. Thermal conductivity testing showed an essentially linear increase with the MWNT content, independent of the degree of dispersion and the MWNT type, functionalised or as received. Thermal conductivity could be increased by about a factor of 5 using 10 wt% MWNT, compared to the pure resin matrix [33].

Different results can be achieved by employing different materials. PMMA resin appears to be more susceptible to thermal conductivity enhancement.

CVD produced SWNTs and MWNTs were purified in acid and ultrasonicated to disperse them. Coagulation method was used to prepare composites with PMMA. Thermal conductivity testing gave κ=2.43 W/mK for 1 wt% SWNTs and κ=3.44 W/mK for 4 wt% MWNTs composites. This represents ten and fifteen fold improvement over neat resin, respectively [34].

2.2.4.1.1.1. Functionalization

Experimental

H_2SO_4/HNO_3 treated and triethylenetetramine (TETA) grafted MWNTs were used as a filler to synthesise nanocomposites with DGEBA epoxy resin. Thermal conductivity improvement with respect to composites made with as-received MWNTs is attributed to improved interfacial heat transport due to TETA functionalization, as well as to improved dispersion. The results are presented in Fig. 2.9.

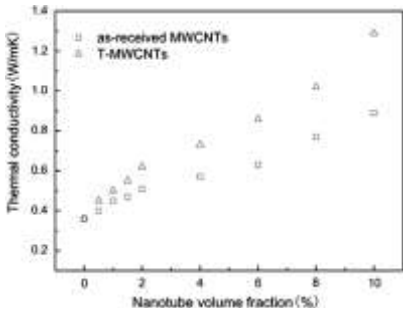

Fig. 2.9: Thermal conductivity of MWNT/DGEBA epoxy composites

The values in the figure show κ=~0.36 W/mK for DGEBA and the maximum value of ~1.3 W/mK for TETA grafted MWNT composite with 10 wt% loading. This represents substantial increase in thermal conductivity [35].

Factors that play a role in this enhancement could be the high initial thermal conductivity of epoxy and compatibility between the epoxy and functional groups grafted onto MWNTs, apart of improved dispersion and interfacial heat transport.

From TEM images in Fig. 2.10 is possible to see functionalization impact on a CNT. Acid oxidised CNT has etched surface while microtome cut SWNT has smooth surface.

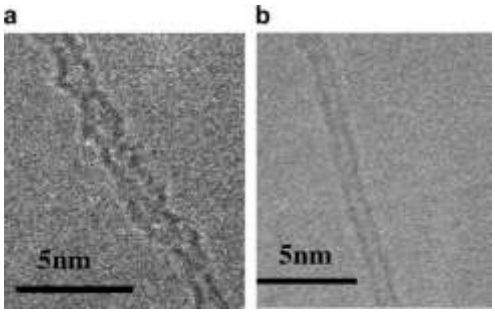

Fig. 2.10: TEM images of a) acid oxidised and b) microtome cut SWNT [36].

It means that functionalization in general damages CNTs.

In order to alleviate CNTs surface damaging, the functionalization approach was modified.

MWNTs were functionalised without damaging MWNTs surface via Friedel–Crafts modification [37]. Functionalised MWNTs were dispersed in epoxy via mixing with solvent. Benzenetricarboxylic acid grafted multi-walled carbon nanotubes (BTC-MWNTs) and epoxy matrix were employed to form a fully heat flow network.

The experimental results presented in Fig. 2.11 show increase in thermal conductivity for undamaged surface MWNTs composites compared to pristine MWNTs composites. This increase is ~ 3 times in composites with 1 vol% and ~ 2 times for composites with 3 and 5 vol%. This increase is due to: a) rigid linkage between MWNTs and epoxy matrix, b) good dispersion of MWNTs in matrix.

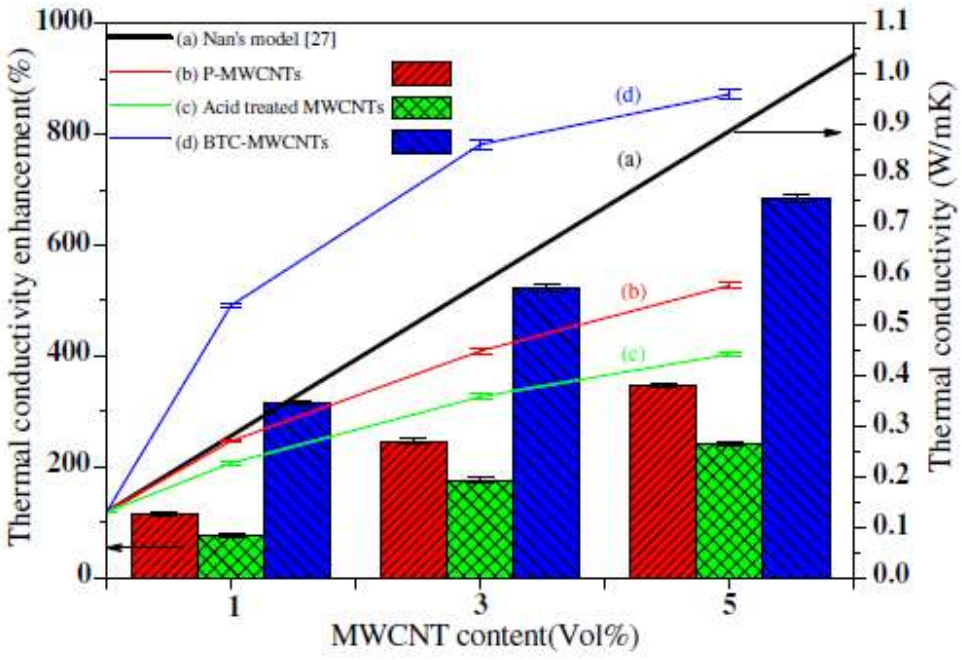

Fig. 2.11: Thermal conductivity with pristine and functionalised MWNTs [37].

It is important to note the decrease of the thermal conductivity for samples prepared with acid treated MWNTs. This is likely due to damage to the MWNT surface.

Adding CNTs to polymer matrix in high loadings could represent a formidable task. Carbon nanotubes are not an inexpensive material either. Hence, improving thermal conductivity with low loading of CNTs is another approach towards comercialisation of nanocomposites.

A successful attempt to increase thermal conductivity with low loading of CNTs was achieved with UV/O_3 functionalised MWNTs. The next step was deposition of aniline. After the aniline was deposited, Ag was added to MWNTs. Nanocomposites were synthesised with PMMA and nanomaterial obtained after described functionalization. Thermal conductivity was measured to obtain 0.48 W/mK for 0.25 wt% loading, thus improving 0.18 W/mK polymer thermal conductivity ~ 2.7 times [38].

Numerical

Numerical simulation was employed to predict functionalised CNTs nanocomposites thermal conductivity. Molecular dynamic simulations were predominant direction of this effort.

Using molecular dynamic simulations thermal conductivity of SWNT on which biphenyl rings have been chemically attached was calculated. Simulation was completed for pristine and CNTs with various percentage of CNT atoms with a bonded biphenyl group. The functionalization of nanotubes reduces their thermal conductivity, and at densities as low as 10.0 % thermal conductivity is reduced dramatically [39].

Using a classical molecular dynamics method the deposition process of metal species onto a SWNT was simulated to estimate its resulting physical strength and thermal diffusivity. The physical strength of the metal-coated SWNT was found to be similar to that of an uncoated SWNT. The thermal diffusivity decreased by 90% [40].

The above is confirmation that modified CNTs can be employed successfully for improvement of polymer properties, however, the attention shall be given to compatibility of constituent materials.

2.2.4.1.1.2. Magnetic alignment

Randomly dispersed CNTs were giving mixed results, pending many factors. Therefore, CNTs alignment was employed to exploit CNTs intrinsic properties.

Purified SWNTs were mixed with epoxy resin Thixotropic/PR2032. Dispersion was achieved via ultrasonication and mechanical mixing. Magnetic alignment was then applied in the 25 T magnetic field. Thermal conductivity measurement results are

presented in Fig. 2.12. CE-25$T_{||}$ is the composite processed in magnetic field, CE-0T is composite not processed in magnetic field, and E-25T is pristine matrix processed in magnetic field. Magnetically aligned composite sample reached κ=~6.5 W/mK in the direction of magnetic field alignment at room temperature, an enhancement of ~3 times, compared to neat aligned epoxy.

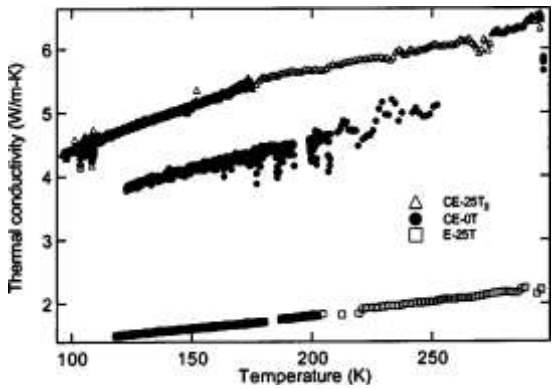

Fig. 2.12: Thermal conductivity of CNT-epoxy composites processed at 0 and 25 T, compared with pristine epoxy sample processed at 25 T. The measurement was in the magnetic field alignment direction [41].

2.2.4.1.1.3. CNT Fibres

CNTs/epoxy composites were produced. First, CNTs were assembled parallel to each other into fibres during CVD production process. High volume fraction composites were then made via direct polymer infiltration. Thermal conductivity was tested. The results are presented in the Fig. 2.13.

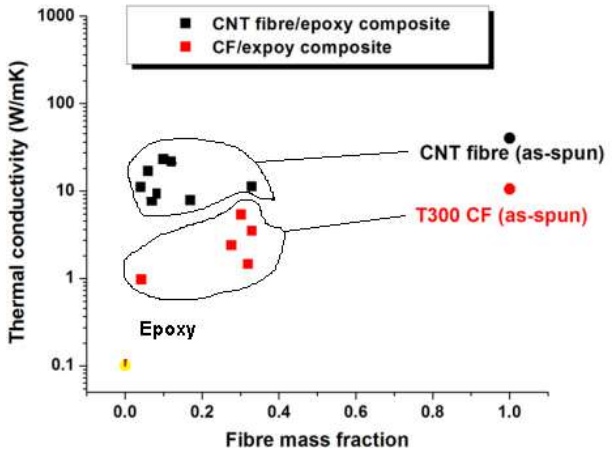

Fig. 2.13: Axial thermal conductivity as a function of CNT mass fraction for CNT fibre / epoxy and T300 CF / epoxy composites. Included are TCs for as spun CNT fibre and T300 fibre as well as for pure epoxy [42].

The highest thermal conductivity values are 23 W/mK for 10 wt% CNT fibre and 5.3 W/mK for 30 wt% CF.

2.2.4.1.1.4. Electrospun fibres

Following good results achieved with CNT fibres, attempts were made to further improve properties while the production process would be simplified. Polymer electrospinning is well documented and not really involved process. Some teams adopted this approach.

CNT-loaded polymer fibres were electrospun from the dimethyl acetamide solution. Through the applied electric field, alignment of the CNTs in the fibres was achieved. The liquid crystal properties of cellulose acetate (CA) also enhanced the alignment of carbon nanotubes in a fibre. Combining CNTs (2 wt%) with graphite particles (10 wt%) as nanosized fillers improves the network of thermally conductive nanoparticles. Thermal conductivity of 6 W/mK was reached. It represents nearly 16 times increase compared with pure CA thermal conductivity of 0.38 W/mK. The enhancement was attributed to alignment of CNTs in polymer fibres [43].

MWNT- polybenzimidazole polymer nanofibre composites were produced by core–shell electrospinning. Thermal conductivity testing was performed to characterise the material. Results are presented in Fig. 2.14.

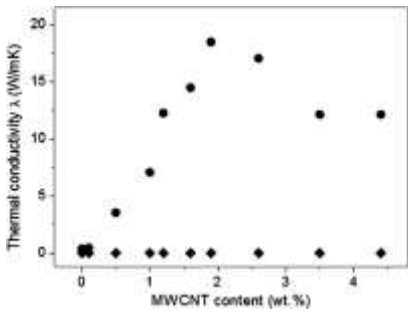

Fig. 2.14: In-plane (circles) and through-plane (diamonds) thermal conductivities of the MWCNT-PBI fibre mats as a function of MWCNT content [44].

Maximum in plane thermal conductivity of 18 W/mK for 1.94 wt% CNT loading, and approximately 0 W/mK through thickness thermal conductivity, independent of CNT loading, were deducted from the Fig. 2.14.

2.2.4.2. Polymer + CNT + CF

As CNT loaded polymer composites were not fulfilling expectations with respect to conductivity properties, the same was the case with mechanical properties. Hence, attention was turned towards improvement of carbon fibre reinforced plastics (CFRP) with the addition of CNTs.

Carbon fibre (CF) / phenolic matrix composite thermal conductivity was increased from 250 to 393 W/mK by adding 7 wt% of crystalline MWNT, average diameter of 80 nm, length 10-20 nm (Fig. 2.15). MWNTs were produced on an industrial scale by chemical vapor deposition method and subsequent thermal treatment.

MWNTs were dispersed in the resin with the aid of ultrasound. Thus created solution was used to impregnate pitch based carbon fibres. CF/phenolic resin ratio was kept at 1 wt%, and MWNT content was varied: 5, 7 and 10 wt%.

As-produced MWNTs (not heat treated) resulted in reduced thermal conductivity values for the composites, thus indicating that catalytically grown MWNTs, possessing intrinsic structural defects are not adequate for the fabrication of highly thermal conducting composites. To become filler that enhances composite thermal conductivity, MWNTs require thermal treatment to improve their structural integrity because the presence of defects on the sidewalls of carbon nanotubes obstructing the propagation of phonons is annealed out during the thermal treatment.

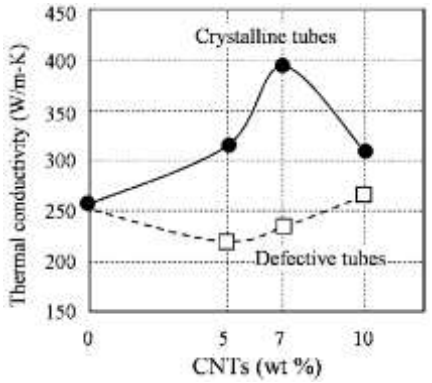

Fig. 2.15: Thermal conductivity of composites with raw MWNTs and thermally treated MWNTs [45].

The above studied thermal conductivity is specified schematically to be in the carbon fibre alignment direction.

Amine groups (NH_2) functionalised MWNTs were deposited using electrophoretic deposition process on the CFs from which the sizing was removed. The MWNT content was determined relatively to the solvent used, in which 0.005 and 0.01 wt% of CNTs was ultrasonically dispersed. CFs were PAN based fibres 5 satin weave harness. Composites

were cured with epoxy resin. The volume fraction of the matrix was 88% and of the fibres 12%. Raman spectroscopy revealed possible covalent bonding between CFs and MWNTs. Thermal conductivity was measured using thermal flash unit with CFs all oriented in the direction of the light pulse. Matrix-CF composites had κ=1.87 W/mK. For composites prepared with solution containing 0.005 wt% of CNTs, the increase was to 2.24 W/mK (20%) and for 0.01 wt% of CNT solution composite κ=3.41 W/mK, the increase of 83% [46].

Some attempts were not as successful as others. These are important in order to understand the available paths that could lead to desired results.

Carbon fibre prepreg surface was sprayed with carboxylic acid groups functionalised SWNTs. Thus modified prepregs were stacked up and cured to form a composite material. SWNTs remained between layers, causing no improvement in thermal conductivity [47].

PAN based CFs/epoxy prepreg was selected as the reference material to evaluate through thickness thermal conductivity improvement with addition of SWNTs, chopped mesophase pitch base CF K-1100, and carbon black (CB).

The reference material was fabricated as a crossply composite.

The fillers were added by wet application on both surfaces of a prepreg sheet via immersion. The filler quantity was determined based on the spreadability of the solution applied. Following curing under the same conditions as for the reference material, the thermal conductivity was measured. The maximum thermal conductivity was obtained

for SWNTs, 1.453 W/mK, slightly more than for the K-1100, 1.444 W/mK. Addition of CB yielded TC increase to 1.212 W/mK from 1.091 W/mK for reference material [48].

Long MWNTs (LMWNT - over 1 mm in length) and their longer extended networks were used to improve thermal conductivity of CF/epoxy composites. LMWNTs were mixed with Epon 862 epoxy using three roll mill at 0.5, 1.0, 5.0 and 10.0 wt%. The mixture was then incorporated into the carbon fibre fabric. Thermal conductivity testing results are presented in Fig. 2.16. It can be seen that only samples with 10 wt% of LMWNT make the difference in TC. The maximum κ=1.4 W/mK. However, the maximum κ=1.5 W/mK for short MWNTs at 0.5 wt% CNT loading (Fig. 2.16). This is due to induced loading.

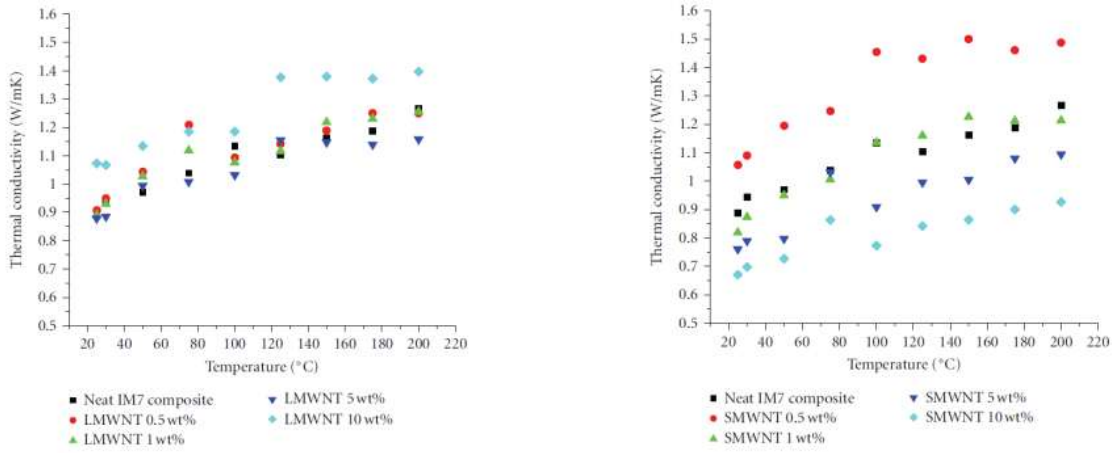

a) b)

Fig. 2.16: Thermal conductivity of composites with a) LMWNTs b) SMWNTs [49].

2.2.4.3. CF + CNT

Successful attempts to improve CFRP thermal conductivities with the addition of CNTs were scarce. Many attempts did not achieve their objectives due to filtration effect.

The focus shifted towards the modification of CFs and CF preforms with the addition of CNTs.

The first logical step was to grow CNTs directly on fibres.

CNTs were grown on PAN (T1000GB) and pitch (K13D) based carbon fibres using CVD method. Thermal diffusivity of obtained hybrid materials was measured. From thermal diffusivity measurements, thermal conductivities were calculated to be 18.6±1.7 and 956.6±30 W/mK, respectively, an increase from original thermal conductivities of 12.6±1.9 and 745.5±16.0 W/mK [50].

2.2.4.4. CF + CNT + Polymer

Following CNT growth on CFs, in order to form CFRP, polymer was added to the modified preform to improve its properties.

Chemical vapour deposition was employed to grow MWNTs on CF plain weave cloth substrates, woven from PAN based T-300 tows. Four batches of preforms with 1.98, 4.44, 4.96 and 11.68 CNT wt% were prepared. From these preforms and neat cloth composite laminates were made with epoxy matrix LY-556/HT972. CF and MWNT-CF preform volume fraction was kept at 30%. Both in-plane and through thickness thermal conductivities were improved for the CNT modified preforms. The highest conductivities were measured on preforms with 11.68 wt% of CNTs. The in-plane TC was enhanced from 17.68 W/mK to 29.05 W/mK, an increase of ~64%. The through thickness TC was increased from 1.82 W/mK to 2.61 W/mK, the improvement of ~44% [51].

It is worth noting that in-plane TC had visible increase for 4.96 wt% and significant increase for 11.68 wt%, whereas the transversal TC began showing visible increase with

1.98 wt% MWNT loading, with the next three samples having similar TC, per diagram depicting TC measurement results.

2.2.5. Graphene

2.2.5.1. Graphene thermal conductivity

New nano-sized carbon material – graphene - was produced, isolated, identified and characterised recently by Novoselov and Geim [52]. The graphene is a 2D material and has excellent thermal conductivity properties. Measured thermal conductivity for a single layer graphene is in the range ~ $(4.84 \pm 0.44) \times 10^3$ to $(5.30 \pm 0.48) \times 10^3$ W/mK [53]. This datum was encouraging and resulted in efforts to improve thermal conductivity of composites through graphene as filler, alone or in combination with CNTs. Significant enhancement in thermal conductivity of nanocomposites made with this material was reported.

Graphite nano platelets (GNP) were combined with SWNTs yielding higher thermal conductivity improvement (3.35 W/mK) than either GNP or SWNTs loaded composite up to 20 wt% filler loading. Above 25 wt% loading, GNP loaded composites exhibited higher thermal conductivity than hybrid filler composite reaching value higher than 6.5 W/mK for 40 wt% GNP loading, being improvement of ~30 times compared to pristine epoxy [54].

Standard thermal conductivity of ~1–5 W/mK achieved with conventional thermal interface materials (TIMs) requires high volume fractions of the filler (~70%). Multi layer graphene and liquid phase exfoliated graphene were used as filler materials in TIMs. Thermal conductivity measurement result indicated more than 23 times improvement with 10% graphene volume fraction [55].

Advantage of flat over wrinkled GNP as a filler for thermal conductivity improvement was observed. 10 vol% flat GNP loaded into epoxy composite increased pristine epoxy thermal conductivity (0.19 W/mK) five fold [56].

Another very high value of thermal conductivity was obtained with combined GNP and CNT filler. In this case, the authors were using equal amounts of both fillers to load epoxy with up to 50 vol% nanomaterial. The result is thermal conductivity at room temperature of 7.30 W/mK. The large enhancement was, as in previous cases attributed to synergetic effects of the two fillers [57].

Another approach to exploit the combined properties of GNP and CNTs was to grow CNTs on GNP. A composite made with thus obtained filler gave better thermal conductivity than with either GNP or CNTs employed on its own. 20 wt% loading of hybrid material improved thermal conductivity 300% compared with the CNTs loading and 50 % compared with GNP loading. Through thickness thermal conductivity of 2.41 W/mK was achieved [58].

Functionalisation was another approach that was attempted to enhance epoxy thermal conductivity. One manner is non covalent functionalisation which does not induce a great damage to graphene flakes and renders them highly soluble. Authors designated the obtained product f-GFs. Adding 10 wt% of f -GFs into epoxy resin yielded thermal conductivity of 1.53 W/mK [59].

Thermal conductivity of functionalised graphite/epoxy composite with 20 wt% filler loading increased to 5.8 from 0.2 W/mK of pristine epoxy – 28 fold improvement.

However, the electrical property of epoxy composite prepared with chemically functionalised graphite declined [60].

Other studies determined that graphene improves epoxy electrical properties, however to lesser extent than CNTs.

Percolation network of MWNT and thermally reduced functionalised graphene sheets achieved in epoxy resin were investigated. Both rheological response of uncured and electrical response of cured material were evaluated. MWNT were forming percolation network at lower loading levels than graphene sheets, designating CNTs as better filler for electrical properties improvement [61].

How CNTs and graphene nanosheets affect electrical properties was investigated. It was found that pristine MWNT added to epoxy yielded the highest improvement in electrical conductivity, about two orders of magnitude higher than comparative composite with graphene nanosheets. Setting an arbitrary level as the electrical conductivity threshold, percolation network was achieved with 50 % more of graphene nanosheets than with MWNT: 0.3 wt% compared to 0.2 wt% respectively. This is clear indication of better suitability of CNTs as a filler to improve electrical conductivity compared to graphene [62].

As presented above, graphene is a promising material for thermal conductivity improvement. However, through thickness thermal conductivity of hybrid material comprising carbon fibres, graphene and polymer matrix was not reported. In the same time, CNTs appear to be the material of choice for electrical conductivity improvement. Hence, CNTs appear to be better suited to develop multifunctional composite material.

2.3. Summary

Following their discovery in 1952, CNTs did not attract much attention until 1991 when more details were published in the well known journal. CNTs are essentially cylinders formed of graphene sheets capped at their ends with halves of fullerene spheres. Those containing single cylinder are SWNTs and those with more cylinders are DWNTs or MWNTs.

After methodology was developed to produce CNTs in sufficient quantities for investigation, significant amount of work was invested in determining their properties. CNT properties were found to be similar to those of graphite, with thermal conductivity exceeding the highest known to date, the conductivities of pyrolitic graphite and diamond. Other physical properties were extremely high as well, promising new polymer reinforcement, possibly replacement for CFs. Predominantly molecular dynamic simulations were used to predict thermal properties of composites containing new filler. However, when experimental work took place, many obstacles were found to hinder efforts and obtained properties of CNT modified polymers were only moderately improved, negligible when compared with theoretical predictions via established rules and equations, like the rule of mixture.

Obstacles en route to better polymer composites were identified. The first group could be defined as manufacturing difficulties. Among those is poor dispersion of CNTs both in a solvent and in a polymer matrix due to high tube-tube attraction forces. Another one is high viscosity of CNT-polymer mixture. Handling difficulties presented additional issue. Poor quality of CNT/polymer interface, high interface resistance, both tube-tube and tube-polymer, were all cited as physics phenomena behind results not meeting

expectations. Nonetheless, the effort continued to provide for solutions for incremental improvements in sample manufacturing and thereafter properties measurements results. Such solutions were employment of ultrasound for CNT dispersion, magnetic alignment to address tube-tube interaction, LBL composite preparation to increase CNT loading while preserving homogeneous CNT dispersion, employment of non-damaged CNTs to reduce phonon scattering, creating CNT forests to improve alignment and reduce CNT-CNT contact and lately growing CNTs on CFs and CF preforms to address CNT filtering observed when CNTs were applied on prepregs or when CNT modified matrix was applied on CF preforms. Step by step, thermal conductivity was improved on macroscopic scale with testing results approaching functional materials thermal conductivity values. However, better results were obtained for the thermal conductivity in the direction of CNTs and CNT modified CFs than in the through thickness direction which remains challenging area with considerable space for improvement. Therefore, incorporation of CNTs in CFRP has a substantial potential for applications where heat dissipation is a concern.

2.4. Problem definition

From available reports can be concluded that parameters with the highest impact on CNT modified CFRP through thickness thermal conductivity are CNTs purity, quality and distribution.

Presence of impurities in CNT material adversely affects determination of CNTs physical properties from both technical and fundamental points of view [63].

To define CNT quality, let's begin with ideal CNT. The ideal CNT would be the one with perfect crystal lattice where hexagons are consisted of carbon atoms only, without any vacancies, inclusions or substitutions. Such carbon atom hexagons would be repeated always in the same manner with respect to the tubule axis while the same helicity would be maintained. Thus defined ideal CNT would be the perfect CNT with respect to heat transfer, i.e. the CNT with the highest quality as there would be no phonon scattering sites. Any CNT with a structure different from the ideal CNT structure would be the CNT with lower quality with respect to heat transfer. CNT quality with respect to heat transfer would degrade with increased number of imperfections in crystal lattice, CNT with the highest number of defects being the CNT with the lowest quality with respect to heat transfer due to the high number of phonon scattering sites.

Therefore, in order to increase CNT modified CFRP thermal conductivity, in particular in the through thickness direction, it is important to employ good quality CNTs. Such CNTs would have lower number of phonon scattering sites. At the same time, in the case of tube-tube contact, CNT coupling intensity would be lower, thus further facilitating heat transfer as phonons would remain on the tube, as opposed to jumping from one tube to another and back in which process energy carried by phonons would be dissipated partially or even completely.

Within the body of CNT structures available, some are better suited for heat transfer than another. Better heat transfer network would be formed from these CNTs than from others.

Another important parameter is the uniformity of CNTs structure. CNTs with the same structure would form better heat transfer network than CNTs that would differ in

structure one from another, i.e. if all CNTs would be e.g. (5,5) or (0,0) CNTs, there would be no mismatch in individual CNTs crystal lattice properties. Hence, the phonon boundary scattering would be minimised in case of phonon propagation from one tube to another. In the case of CNT structure different from one tube to another, phonon boundary scattering due to mismatch in crystal lattice properties would contribute to lower thermal conductivity improvement.

Based on above two paragraphs, CNTs most suitable for thermal conductivity improvement would be CNTs with uniform structure well suited for heat transfer.

The highest thermal conductivity was obtained, both numerically and experimentally, for a single SWNT. Any higher form of CNT assembly gave lower thermal conductivity value, decreasing further as the form was becoming more and more complex and approached macroscopic ones. If all CNTs were ideal CNTs as defined above, higher forms thermal conductivity should have been equal to thermal conductivity of the single ideal CNT, as the constituent CNTs would be, SWNT, DWNT or MWNT, disregarding the number of CNTs involved or mechanical coupling as all phonons would remain on tube. However, degradation in thermal conductivity with increasing number of building blocks – CNTs – provides evidence of imperfections presence and intertube coupling thereafter. Hence, to emulate thermal conductivity of a single CNT, it is necessary to disperse CNTs.

To disperse CNT higher forms like bundles and separate CNTs one from another, sonication was giving the best results. However, another issue appeared in polymer composite manufacturing process - agglomeration of dispersed CNTs. The highest CNT

weight content in a composite obtained with homogeneous CNT distribution – i.e. no agglomerations were observed – was achieved via LBL approach.

In order to avoid unnecessary intertube coupling, as long as effective heat transfer network of individual CNTs is maintained in a CFRP, CNTs need to be well dispersed. Reviewed results suggest that sonication and LBL method would be the most effective means towards this goal both for polymer composites and CFRP.

2.5. Thesis Objective

Reviewed literature provides insight in the potential of CNTs as a filler of choice for thermal interface materials and improvement of composite materials employed in areas where efficient heat dissipation is a valuable property. Carbon nanotubes are best suited to improve both electrical and thermal conductivity even as the former was not investigated. However, realization of such potential depends on several factors. Factors considered the most important for thermal conductivity improvement are CNT quality and CNTs dispersion homogeneity.

To demonstrate CNT quality importance for epoxy composites thermal conductivity, different quality CNTs were selected.

In order to obtain composite material of intended properties, it is important to select appropriate materials and manufacturing process. The most successful approach thus far was reported by Mathur et al. [51]. Achieved through thickness thermal conductivity was 2.61 W/mK, the improvement of ~44% over the reference material thermal conductivity of 1.82 W/mK. Bearing the above in mind, this thesis goal is to develop a multifunctional high performance hybrid composite material with heat dissipation properties

improvement beyond the current state of the art. To this extent carbon fibres, carbon nanotubes and epoxy resin are to be utilised.

In order to resolve filtering effect appearing when CNTs are added to CFRP, manufacturing process was suitably tailored. CNTs shall be first dispersed and incorporated into CF preforms using ultrasound, followed by impregnation by resin and manufacturing of prepreg, followed by laminate curing in autoclave.

Filtering effect is as well the reason behind the chosen thin, unidirectional carbon fibre fabric, made of 3k tows giving low specific weight per m^2. This material is used in aerospace industry, one of industries targeted with this research. The low specific mass and thickness are facilitating homogeneous distribution of CNTs inside the CF preform. The thin CF preform would emulate the substrate on which CNTs are to be attached, followed by impregnation with resin. Described process would be an emulation of highly successful LBL process, employed on CNTs and polymer, taking advantage of benefits rendered by it – CNTs well distributed throughout composite via thin layers.

Chapter 3

3. Materials and Manufacturing Procedure

In today's aerospace industry, requirements for ever lighter materials with superior properties, mechanical, electrical and thermal, are becoming more stringent faster than ever before. This trend could be expected to continue in the future.

Composite materials are no exception to these requirements. In fact, due to their unique properties – lighter, yet stronger than metals, they are becoming more prominent, and material of choice by leading aerospace manufacturers. To achieve such success, composites are to be produced following careful choice of constituting materials and manufacturing processes. This involves fibres, matrix and, as the latest material added for further composites improvement, CNTs.

Pending intended application and possible operational environment, appropriate combination of fibres, matrix (and CNTs) and manufacturing process should be selected. The selection process should take into consideration individual material properties, compatibility of fibres, CNTs and matrix, process utilised to include CNTs in the material, and composite part manufacturing procedure.

In this chapter, described are materials selected for specimen production, their properties, process used to incorporate CNTs into the material produced, and samples production method. The quality of the produced samples was evaluated and the results are presented in the later sections of the chapter.

3.1. Selected Materials

Many applications of composite materials require heat dissipation facilitation. One possible application is aircraft industry where certain parts are exposed to constant thermal flux. To alleviate the possibility of overheating and consequent damage, those parts are required to have good thermal conductivity. Trend is to introduce composite materials to as many areas as possible in order to reduce weight, while maintaining mechanical properties of the replaced materials. Due to possible exposure to elevated temperatures and requirements for good thermal conductivity that facilitates heat dissipation, materials compatible with the intended application and environment, as well as one with another were chosen to make samples.

Unidirectional carbon fibre fabric was utilised as the base material. During preliminary investigation, fabric produced utilising 12k yarns was used. To complete full scale investigation, fabric produced utilising 3k yarns was selected. The principal reason for selection of the fabric produced from 3k yarns is an attempt to achieve homogeneous distribution of CNTs within the CF fabric and to emulate LBL composite manufacturing as described in [31].

To improve material properties, CNTs were selected as the most suitable for improvement of both electrical and thermal conductivity – a requirement in multifunctional composites.

Thermoset epoxy matrix was employed to give form to material and provide load transfer between fibres.

3.1.1. Carbon Fibre Fabrics

a) Carbon fibre fabric GA 090 is a carbon fibre fabric produced by Hexcel from 12k yarns. Material nominal weight is 305 $\frac{g}{m^2}$.

b) Carbon fibre fabric HexForce® G0947 D 1040 TCT is a carbon fabric produced by Hexcel from high strength PAN based carbon fibres. Warp material are 3k yarns made utilising HTA 5131 carbon fibres. The fibre density is 1760 kg/m^3 [64]. Weft yarns EC5 5.5 x 2 are made utilising glass fibres. Fabric content is 97% warp and 3% weft. Material thickness is 0.16 mm. Material nominal weight is 160 $\frac{g}{m^2}$.

3.1.2. CNTs

From available CNTs, SWNTs produced utilising HiPCO process were chosen as they promised the highest improvement of thermal conductivity [30]. Raw (R), purified (P) and super purified (SP) SWNTs were incorporated in the material to evaluate the difference and determine the best filler. Ash content was 16.5% for RCNTs [65], 8% for PCNTs [66] and 4% for SPCNTs [67].

3.1.3. Matrix

Matrix properties are presented in Table 3.1.

Table 3.1: Matrix properties.

Property	Value
Room temperature viscosity	~ 2.2 Pas [68]
Density	1174.5 kg/m^3
Working life	> 20 h [68]
Moisture absorption	2-2.5 wt% [68]
Operating temperature	170 ^{o}C [69]

Selected matrix is the system obtained by combination of bisphenol-F epoxy resin Epon 862 and aromatic amine curing agent Epicure W. This system has very long working life at room temperature and high operational temperature when cured. Low room temperature viscosity allows better manufacturing process, hand lay-up utilised in samples manufacturing was facilitated by this material property.

3.2. Samples Manufacturing

Four types of samples were produced. Pristine matrix (type A), control samples (type B), reference samples (type C) and properties improvement samples (type D). Control samples are consisting of matrix and CNTs only, while reference samples were combination of carbon fibres and matrix. Properties improvement samples were made of carbon fibre fabric, CNTs and matrix. Samples schedule is shown in Table 3.2.

Table 3.2: Samples schedule.

Sample Type	Sample Name	Sample Content
Type A	Pristine Matrix	Matrix
Type B	Control Samples	Matrix + CNTs
Type C	Reference Samples	Carbon Fibres + Matrix
Type D	Properties Improvement Samples	Carbon Fibres + CNTs + Matrix

3.2.1. Type A Samples manufacturing

Type A samples made of pristine matrix were obtained by combination of Epon 862 resin and W curing agent. The two were mixed in 100:26.4 weight ratio respectively. The mixing method applied was hand mixing. Following hand mixing the samples were degased in a vacuum oven for 30 minutes at 60 ^{o}C and -84.6 kPa. The samples were cured in an oven at 177 ^{o}C for 150 min.

3.2.2. Type B Samples manufacturing

Type B samples were made of matrix and CNTs. Three roll mill was used to mix CNTs with matrix. To obtain good dispersion of CNTs in the smatrix, a procedure was adopted based on work described in [70]. The sequence with respect to number of passes at selected gap is provided in Table 3.3.

Table 3.3: Three roll mill sequence.

Gap [μm]	Number of passes
50	1
20	1
10	4

The first two passes at the gap of 10 μm were with resin and CNTs and in the subsequent two curing agent was added.

Obtained mixture was subsequently degased in the vacuum oven for 30 minutes at -84.6 kPa and 60 ^{o}C. Following degassing the type B samples were cured in the oven at 177 ^{o}C for 150 min. Within type B samples, differentiation of samples is made based on CNTs material and wt%. Table 3.4 specifies sample B content and designations in further text.

Table 3.4: Type B sample schedule.

Sample Designation	CNT Type	wt%
BR1	RCNT	1
BR2	RCNT	2
BR3	RCNT	3
BP1	PCNT	1
BP2	PCNT	2
BP3	PCNT	3
BSP1	SPCNT	1
BSP2	SPCNT	2
BSP3	SPCNT	3

3.2.3. Type C Samples Manufacturing

Type C samples were made of carbon fibres and matrix. Hand layup technique was used to produce these $[0_2]$ samples. Carbon fibres fabric was cut in preforms with dimensions 0.22 x 0.022 m. The preforms would subsequently be impregnated by matrix. Preform impregnated with matrix was held in oven for 30 min at 60 ^{o}C thus giving prepreg material that could be stored in a freezer.

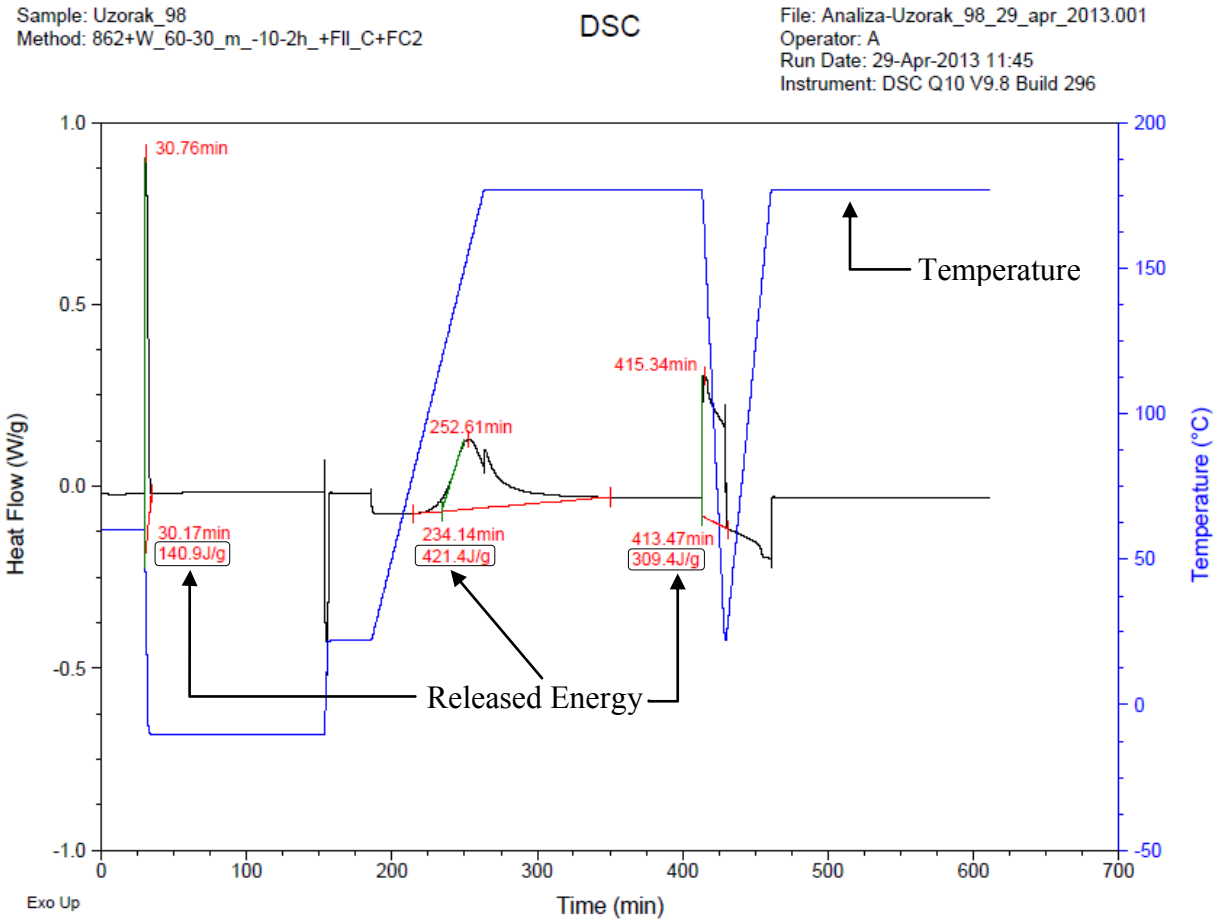

Fig. 3.1: DSC determination of prepreg production parameters.

Preparing a single layer of material to produce prepreg is significantly less involved than preparing multiple layers of material immediately laid up to produce laminate. The possibility to store material in the freezer allows for preparation of prepreg one day and laminates on another. In addition, partially cured prepreg material facilitates manipulation during stacking of laminate.

The prepreg production parameters, time and temperature, were determined with the help of differential scanning calorimeter (DSC). The instrument used to this purpose was TA DSC Q10. The same instrument was used throughout the experimental work in this research. DSC samples were examined during the cycle that emulated manufacturing

process in order to determine the process parameters yielding required degree of matrix cure (Fig. 3.1). The cure degree value of 15.6% is average value obtained from four samples.

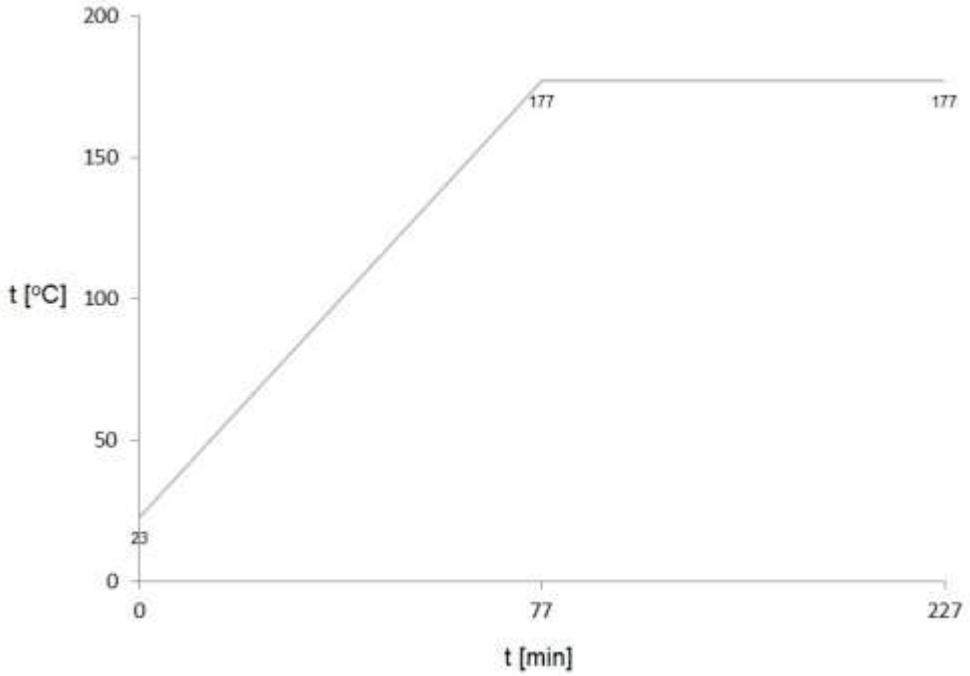

Fig. 3.2: Curing cycle for matrix system Epon 862 / Epicure W.

Thus obtained prepreg layers would be stacked up on the tool plate for autoclave curing. During the stacking, breather, bleeder and release film were applied both above and under the sample, release film being next to the sample and breather being against both the tool plate below and the bagging film above the sample. The bleeder was between release film and breather layers. Details are provided in the paragraph 3.2.4.1.

The sample prepared in such manner was cured in an autoclave at 177 ^{o}C for 150 min. Pressure (41.4 kPa) and vacuum (84.6 kPa) were applied to help compact the laminate, suppress voids and facilitate gasses extraction. The curing cycle is shown in Figure 3.2.

3.2.4. Properties Improvement Samples Manufacturing

Carbon fibre fabric was the base material utilised. Preforms were cut to dimensions 0.22 x 0.022 m.

CNTs were dispersed in de-ionized (DI) water. The entire quantity of CNTs to be incorporated could be processed at once. However, the best result was achieved with incremental addition of CNTs for the content exceeding 1 wt%. Increments could be either larger or smaller than 1 wt%. Better results were achieved with increments not exceeding 1 wt%. DI water was chosen over other solvents like acetone and ethanol for its higher boiling point. Due to that property, less solvent is used to manufacture samples. The solution was obtained by dispersing the CNTs utilising an ultrasonic processing unit in ice bath (Fig. 3.3). The ice bath was employed to keep processing parameters constant. In such manner solvent evaporation due to increased temperature was prevented as well.

a) b)

Fig. 3.3: CNTs dispersion: a) CNTs in DI water; b) Sonication in ice bath.

Thus obtained solution was poured over the carbon fibre preforms and processed in an ultrasonic bath in ice bath (Fig. 3.4). Again, ice bath was employed to maintain process parameters constant and to prevent solvent evaporation.

a) b) c)

Fig. 3.4: Adding CNTs into carbon fibre preform: a) Carbon fibre preform; b) Carbon fibre preform submerged in CNT - DI water solution; c) Arrangement in ultrasonic bath.

CNT incorporation into CF fabric process is schematically presented in Fig. 3.5.

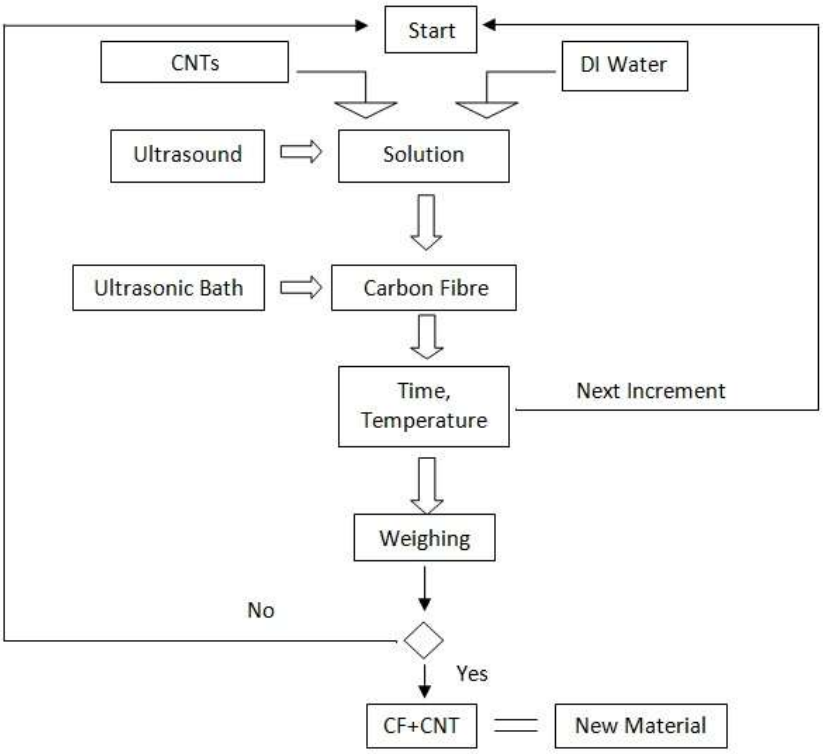

Fig. 3.5: Schematic presentation of CNT incorporation into CF fabric.

With the aid of ultrasound, CNTs were incorporated into carbon fibre preforms. To eliminate solvent, CF preforms with incorporated CNTs were held in oven at 120 ^{o}C for a minimum of 24 hours.

In case of incremental loading increase, the above described process was repeated until entire CNT quantity is processed. When all CNTs intended for incorporation in the preform were used, either whole quantity at once or through incremental addition, exact mass of incorporated nanomaterial was determined by weighing preform material. If the mass of incorporated CNTs did not satisfy the initial requirement, (e.g. 2 wt%) process was repeated from the beginning. When the process was repeated, the mass of CNTs processed was the difference between the required one and the one incorporated in the preform as determined via weighting. Once the mass of incorporated CNTs satisfies initial requirement, the process was stopped and new material (Fig. 3.6) stored.

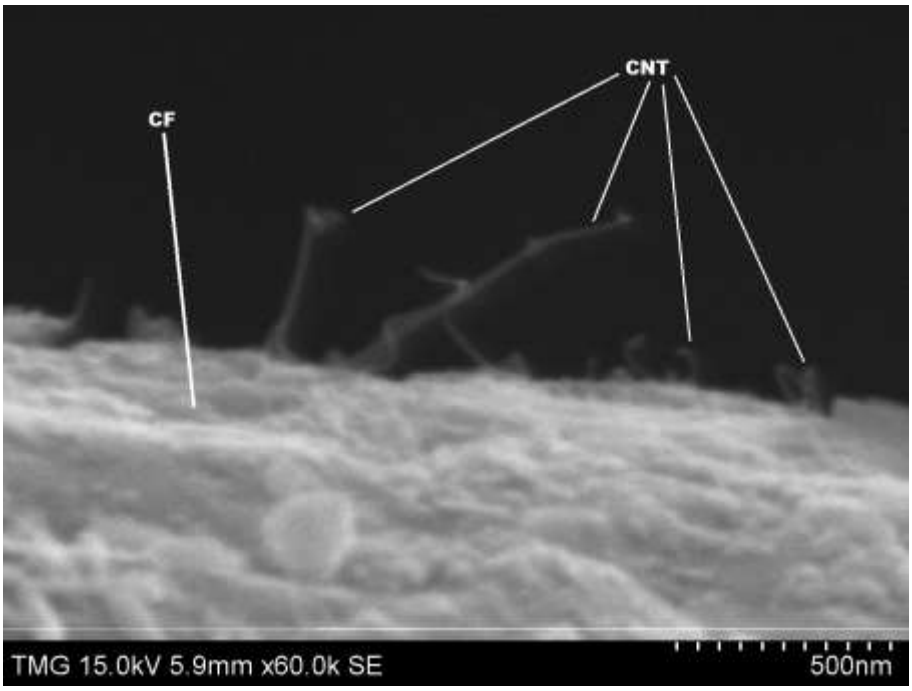

a)

b)

Fig. 3.6: New material - Carbon fibres with CNTs added with the aid of ultrasound: a) CNTs attached to carbon fibres; b) Increased stiffness of modified carbon fibres.

The mechanism of incorporation of CNTs into the CF preform is as follows. First, CNTs get attached to CFs, as shown in Fig. 3.6 a). Once CNTs are attached to CFs, other CNTs get loosely attached to CNTs attached to CFs, bridging CFs and CNTs attached to CFs, thus forming the heat transfer network. Schematically, the new material formed from CF preforms and CNTs is presented in Fig. 3.7.

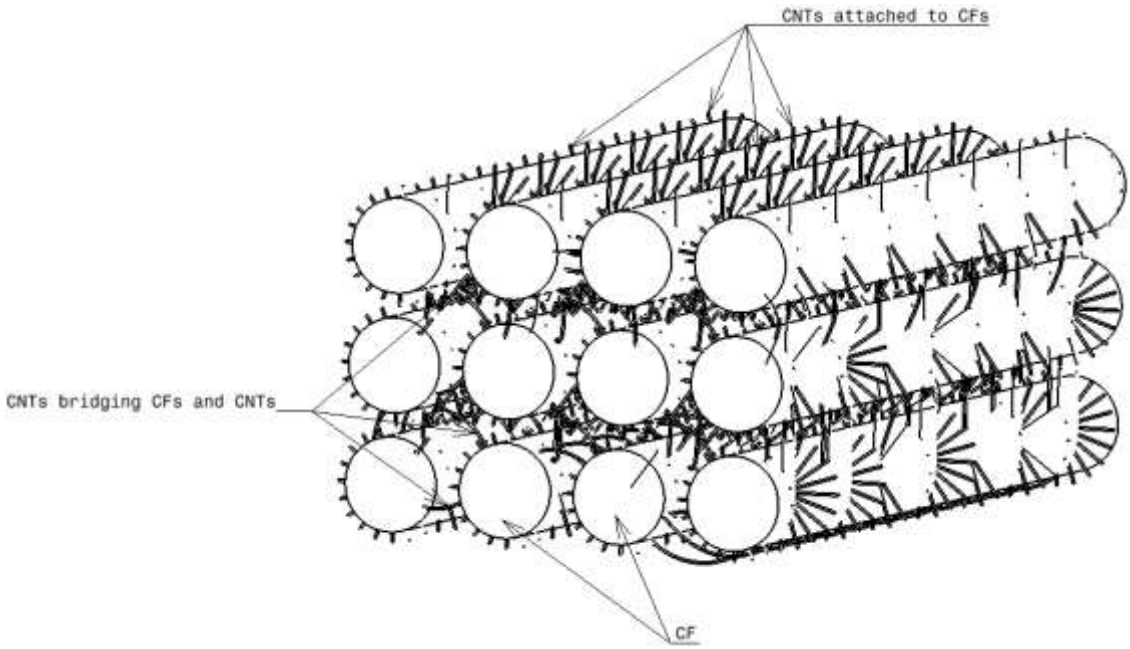

a)

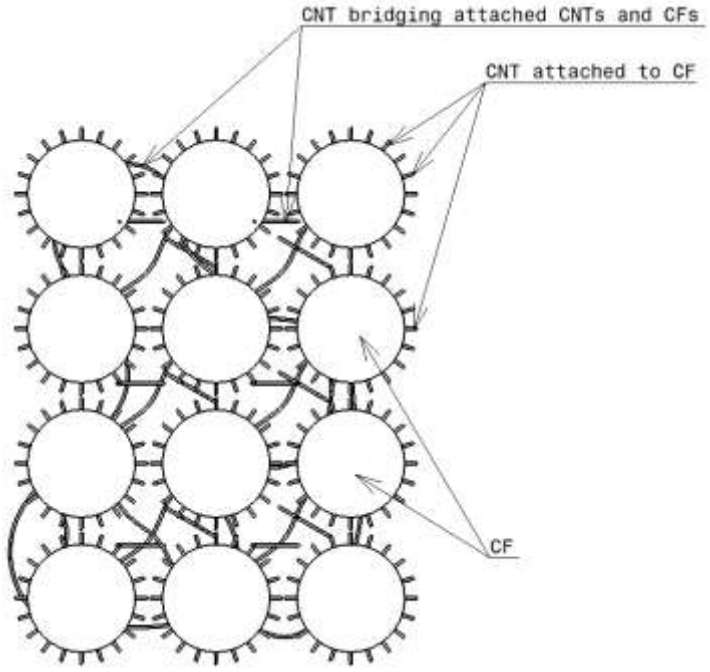

b)

Fig. 3.7: Schematic presentation of new material created from CFs and CNTs: a) 3D presentation; b) Frontal 2D view.

It is reasonable to expect that described procedure used to incorporate CNTs into CFs fabric can be utilised with other materials. In this case other materials could be either different nanomaterial, different fibre like glass fibre, different form of fabric or a different solvent. Fibres could be in the form of any fabric weave, tow or individual fibres. Different nanomaterials that could be used are different CNTs, graphene, nanoclay and even microcapsules. CNTs could be SW, DW or MWNTs, as produced, treated (acidic, centrifuge or heat treatment), functionalised or any their combination. Graphene could be in the form of graphene nanoplatelets, graphene oxide, graphene flakes or any other one like graphene with CNTs grown on them, as produced, treated (acidic, centrifuge or heat treatment), functionalised or any their combination. Mentioned nanomaterials could be combined one with another in any manner, for example any (or all) variety of graphene mentioned with any variety (or all) of CNT mentioned or anything in between. Any nanomaterial or combination mentioned could be incorporated in any carbon fibre or glass fibre form. To this purpose, different solvents could be used in addition to DI water, like acetone, ethanol, N-methylpyrrolidone (NMP), dimethylformamide (DMF) or others.

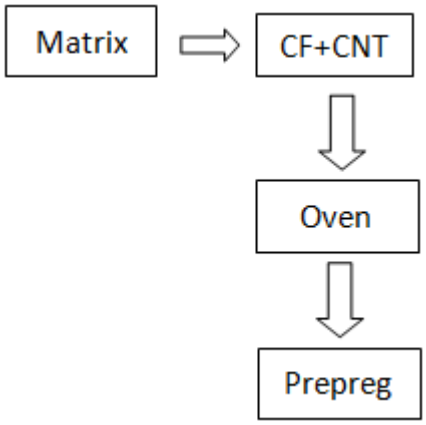

Fig. 3.8: Prepreg preparation from new material and matrix.

The next step was to impregnate the new material with the matrix utilising hand layup technique. The prepreg manufacturing procedure described above was again employed. Following partial cure in the oven for 30 min at 60 ^{o}C (degree of cure 15.6%), new prepreg material was created. The process is schematically presented in Fig. 3.8.

Thus prepared prepreg was stored in the freezer at -18 ^{o}C until the curing.

Thus obtained prepreg layers would be stacked up on the tool plate for autoclave curing.

Samples were stacked up and cured in the autoclave (Fig. 3.9) following the same stacking sequence and procedure as for the type C samples.

Fig. 3.9: CONCOM autoclave.

Fig. 3.10 depicts a sample on the tool plate in vacuum bag after the curing in the autoclave.

Fig. 3.10: Sample after curing in autoclave.

In Fig. 3.11 resultant material could be seen in SEM picture with 50k magnification. CNTs forming the heat transfer network can be seen as bright pixels. In the same time

fracture surface exhibits features of a tough material fracture surface. This is an improvement over standard brittleness of epoxy matrix.

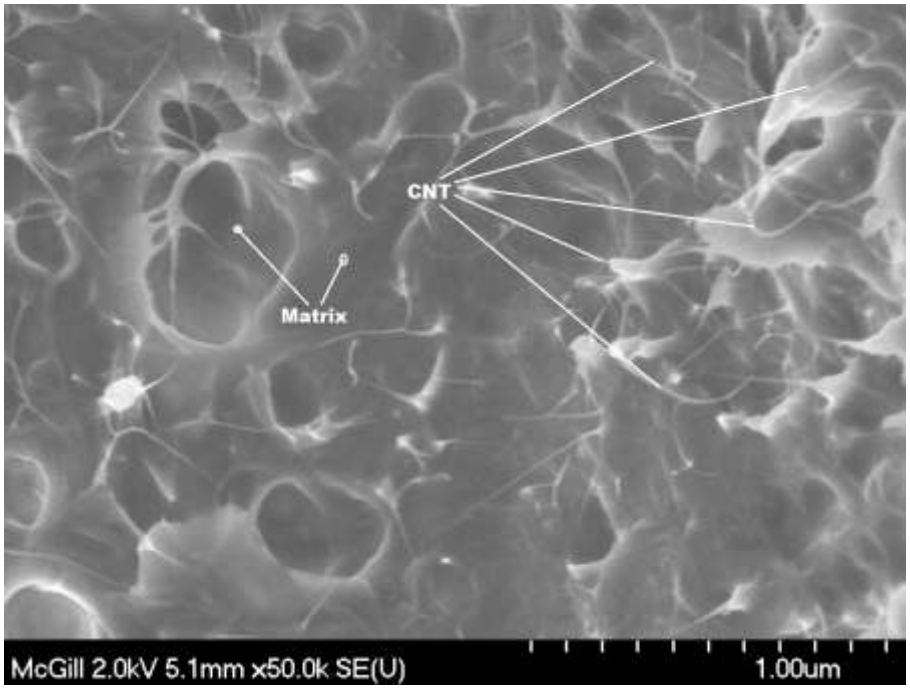

Fig. 3.11: New material after impregnation with matrix and curing in autoclave - CNTs attached to carbon fibres and impregnated in matrix can be seen as bright pixels.

Table 3.5: Type D sample schedule.

Sample Designation	CNT Type	wt%
DR1	RCNT	1
DR2	RCNT	2
DR3	RCNT	3
DP1	PCNT	1
DP2	PCNT	2
DP3	PCNT	3
DSP1	SPCNT	1
DSP2	SPCNT	2
DSP3	SPCNT	3

Within type D samples, differentiation of samples is made based on CNT type and wt%. Table 3.5 specifies sample content and designations in further text.

3.2.4.1. The Effect of Ancillary Materials Stacking Sequence

During the initial stage of preliminary research, the standard stacking sequence was used. Tool plate would be covered by a thin film of a release agent. On such prepared tool plate, a sample would be put. Release film would cover the sample, followed by bleeder and breather. Bagging film would complete the stacking sequence.

Both C and D type samples were produced in such manner. However, when type D samples were produced and examined under SEM, the stacking sequence was modified.

During SEM investigation of a type D sample stacked up for autoclave curing in the standard manner described above, an accumulation of matrix was observed on the sample surface that was against the tool plate during the curing process (Fig. 3.12).

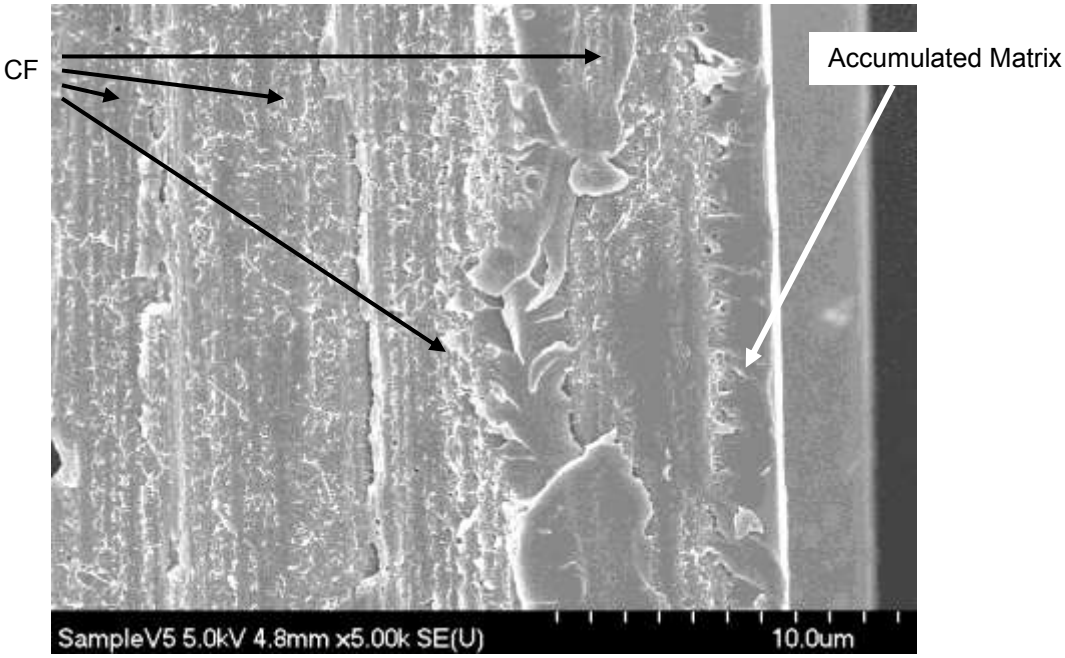

Fig 3.12: SEM image of sample with accumulated matrix against the tool plate. CNTs are bright pixels.

An assumption was that this layer of matrix would act as an insulating layer. To verify the assumption, thermal conductivity was measured for the same sample three times. The first time was on a coupon made from an as-produced sample (AP). The next step was to remove the accumulated matrix layer using sand paper. The second time thermal conductivity was measured on the sample with sanded bottom side (SB). Following the second measurement, the top side, cured covered with the release film, of the same sample was sanded. The third thermal conductivity measurement was completed on the coupon with both bottom and top sides sanded (SBT). Results are presented in Table 3.6 and Fig. 3.13.

Table 3.6: Thermal conductivity of the samples as produced, then progressively sanded.

		κ [w/mK]			κ - Relative Change [%]		
t [°C]	25	75	125		25	75	125
Sample							
AP	0.854±0.070	0.983±0.080	0.957±0.076				
SB	1.034±0.125	1.175±0.128	1.104±0.104		21.1	19.5	15.4
SBT	0.700±0.032	0.824±0.046	0.788±0.046		-18.1	-16.2	-17.7

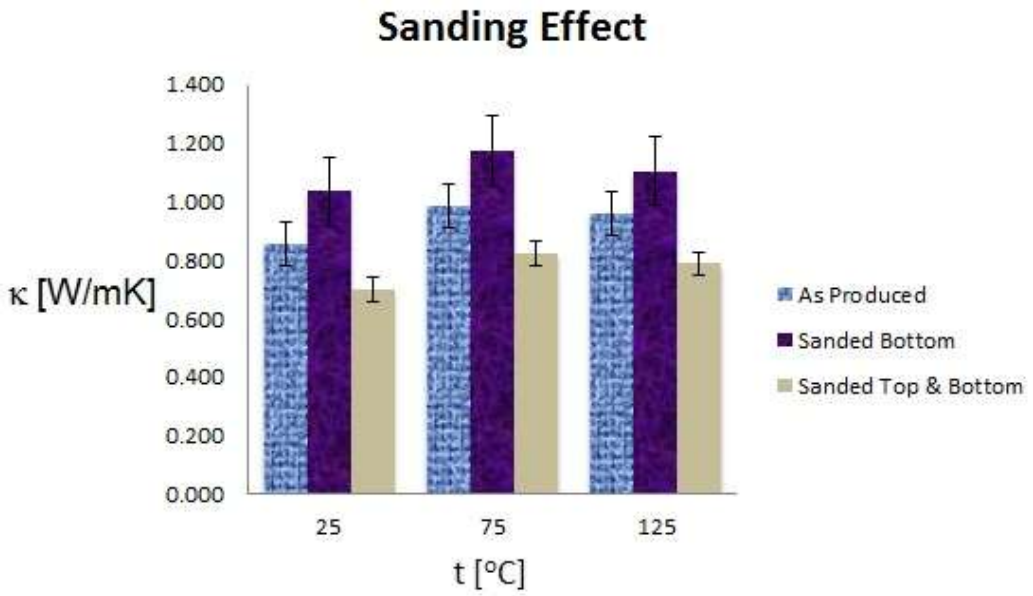

Fig. 3.13: Thermal conductivity change with sanding of bottom, than top side of coupons

The thermal conductivity change in type C samples was negligible after sanding, essentially non-existing. The change of thermal conductivity with sanding was observed only in samples with CNTs - type D samples. The change in thermal conductivity with sanding confirmed that accumulated matrix on the bottom of the sample was acting as the insulating layer. Removal of matrix from the bottom side of coupons increased thermal conductivity by approximately 20% at 25 ^{o}C and 75 ^{o}C. On the other side, the stacking sequence above the sample was the optimum configuration to exploit CNT effect on thermal conductivity, as even the minimum intervention on the top side was reducing thermal conductivity of the coupon. This stacking sequence allowed for CNTs to be on the surface of the sample, thus benefiting the through thickness thermal conductivity in the best possible manner. Hence, in order to eliminate matrix accumulation against the tool plate and formation of insulating layer, the standard stacking sequence was altered to apply release film, bleeder and breather both below and above the sample. Release film was next to the sample and breather was against both the tool plate below and the

bagging film above the sample. The bleeder was between release film and the breather layers. (Fig. 3.14 and Fig. 3.15).

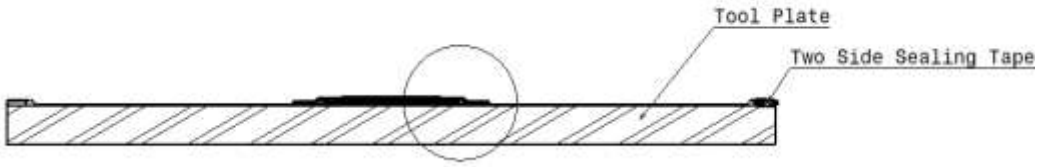

Fig. 3.14: Schematic presentation of sample stacked up for curing in autoclave. Detail in circle is shown enlarged in Fig. 3.15.

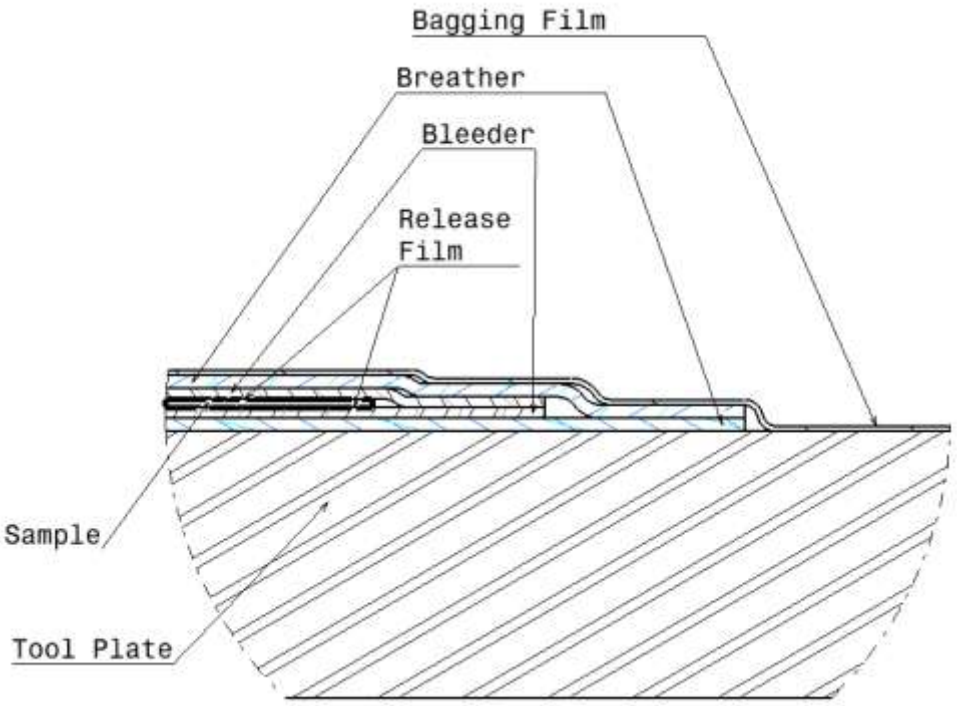

Fig. 3.15: Schematic presentation of improved stacking sequence that eliminates insulating matrix accumulation.

Thermal conductivity was measured on coupons made from thus produced samples (ISS). Obtained values (Table 3.7) were compared with the above provided results. Thermal conductivity values are very similar to thermal conductivity measured on coupons with sanded bottom side (Fig. 3.16).

Table 3.7: Thermal conductivity of samples made using standard stacking sequence and improved stacking sequence

		κ [w/mK]			κ - Relative Increase [%]		
t [°C]	25	75	125		25	75	125
Sample							
AP	0.854±0.070	0.983±0.080	0.957±0.076				
SB	1.034±0.125	1.175±0.128	1.104±0.104		21.1	19.5	15.4
ISS	1.008±0.153	1.174±0.173	1.209±0.177		18.0	19.5	26.3

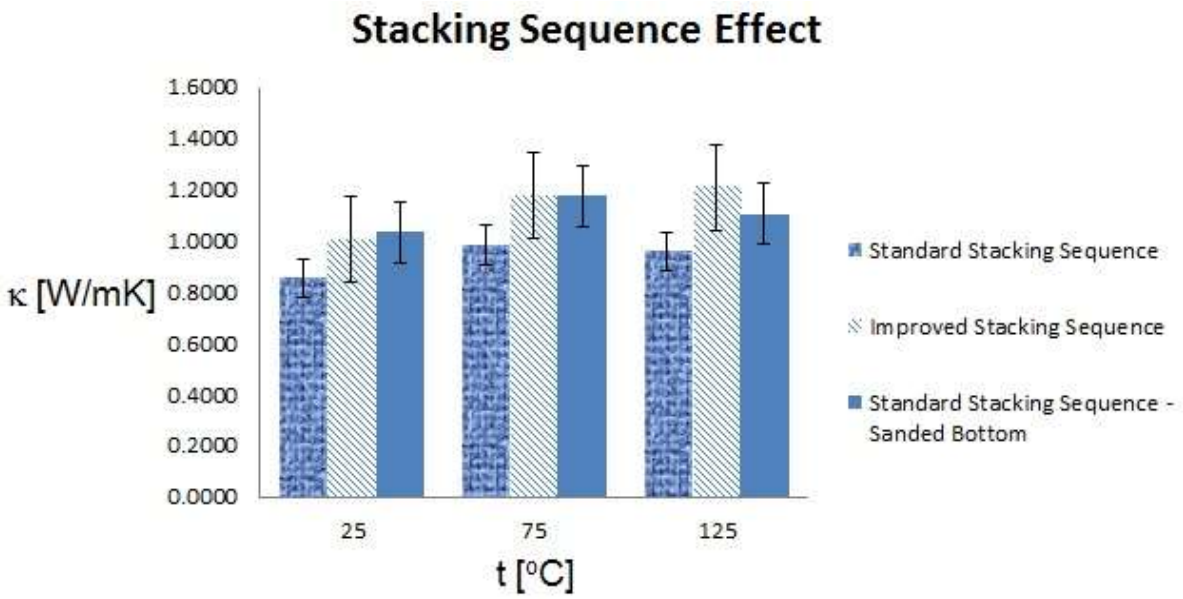

Fig. 3.16: Stacking Sequence Effect

The proximity in the obtained ISS and SB samples thermal conductivity is confirmation of the hypothesis that accumulated matrix was acting as the insulating layer and that it would be removed with modified stacking sequence. The stacking sequence optimised for thermal conductivity improvement using CNTs improved the thermal conductivity 18%-26.3%. It is reasonable to expect positive effect of thus modified stacking sequence on this and other transport properties, improvement of which is attempted via incorporation of CNTs, (SW, DW or MWNTs), other nanomaterials like graphene (in the form of

graphene nanoplatelets, graphene oxide, graphene flakes or any other one), any combination of any of the mentioned forms of CNTs and/or graphene forms, including CNTs grown on any of the mentioned forms of graphene.

This particular part of research was completed utilising GA 090 carbon fibre fabric. Hence the differences in thermal conductivity values presented here and in Chapter 5. The values presented in Chapter 5 are obtained with carbon fibre fabric HexForce® G0947 D 1040 TCT.

3.3. Sample Quality

Samples of good quality are the requirement for reliable research results. Samples are characterised by several parameters.

Cured sample dimensions is the first set of parameters evaluated following the sample curing. The next one would come when reinforcement (CFs+CNTs) volume fraction is determined via thermal gravimetric analysis (TGA). Absence of voids and resin rich areas is determined by optical microscopy. To evaluate CNT distribution within the sample, scanning electron microscopy (SEM) must be employed due to the nano size of the evaluated material constituent.

1. Sample Dimensions

Samples dimensions were determined with the aid of digital calliper and micrometer. Length and width corresponded to CF preforms' dimensions. The thickness was determined for individual samples. These values were used to calculate average sample thickness on two levels. The first level is the group of samples with the same CNT

material and wt%, e.g. type C samples or within type D samples, samples with 1 wt% of purified CNTs. Results are presented in Table 3.8.

Table 3.8: Sample groups' thicknesses

Sample type	Thickness [mm]	Sample type	Thickness [mm]
A	0.917±0.002	C	0.347±0.004
BR1	0.924±0.006	DR1	0.412±0.028
BR2	0.937±0.009	DR2	0.373±0.009
BR3	0.964±0.007	DR3	0.335±0.015
BP1	0.925±0.004	DP1	0.367±0.008
BP2	0.952±0.007	DP2	0.345±0.017
BP3	0.926±0.007	DP3	0.400±0.043
BSP1	0.913±0.008	DSP1	0.388±0.008
BSP2	0.975±0.009	DSP2	0.407±0.017
BSP3	0.942±0.009	DSP3	0.372±0.003

The second level is all samples. On the second level, average sample thickness for A and B type samples is T=0.934±0.018 mm and for C and D type samples T=0.375±0.033 mm.

2. Reinforcement Volume Fraction

Reinforcement volume fraction was determined through TGA ramp cycle from room temperature to 1000 ^{o}C at constant heating rate of 20 ^{o}C/min. Typical TGA plot obtained after this test is shown in Fig. 3.17.

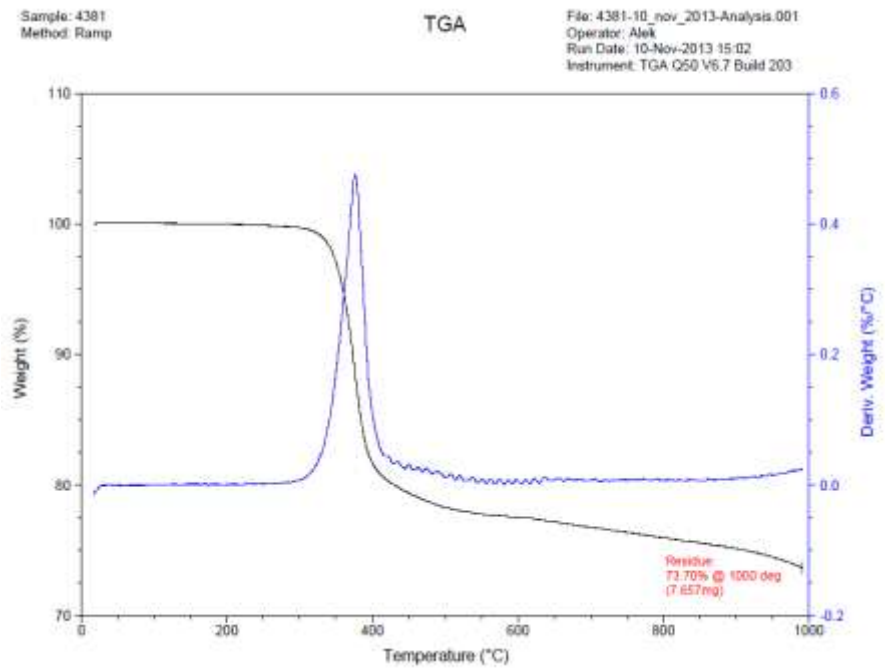

Fig. 3.17: TGA plot analysis showing reinforcement residue wt%.

Obtained residue value is 73.94±0.20 wt%. From this value reinforcement volume fraction can be calculated. Obtained value is 65.40±0.18 %.

3. Voids and Resin Rich Areas

Optical microscopy was utilised to verify samples for voids and resin rich areas. Typical images obtained during this stage of samples quality verification are shown in Fig. 3.18.

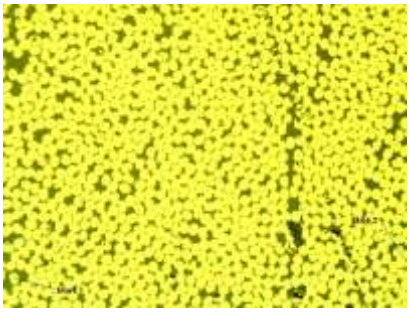

Fig. 3.18: Optical microscope image of laminate at magnification of 500x.

4. CNTs Distribution

CNTs distribution within composite material was verified via SEM. The following pictures (Fig. 3.19) depict CNTs attached to CFs and matrix impregnated. CNTs are easily distinguished as brighter pixels well distributed throughout the image a) while in the image b) CNTs can be as well seen embedded in matrix as a lighter shade of gray. From the pictures is clear that CNTs are homogeneously distributed throughout the sample. Surface on both pictures exhibits features of a tough material fracture surface.

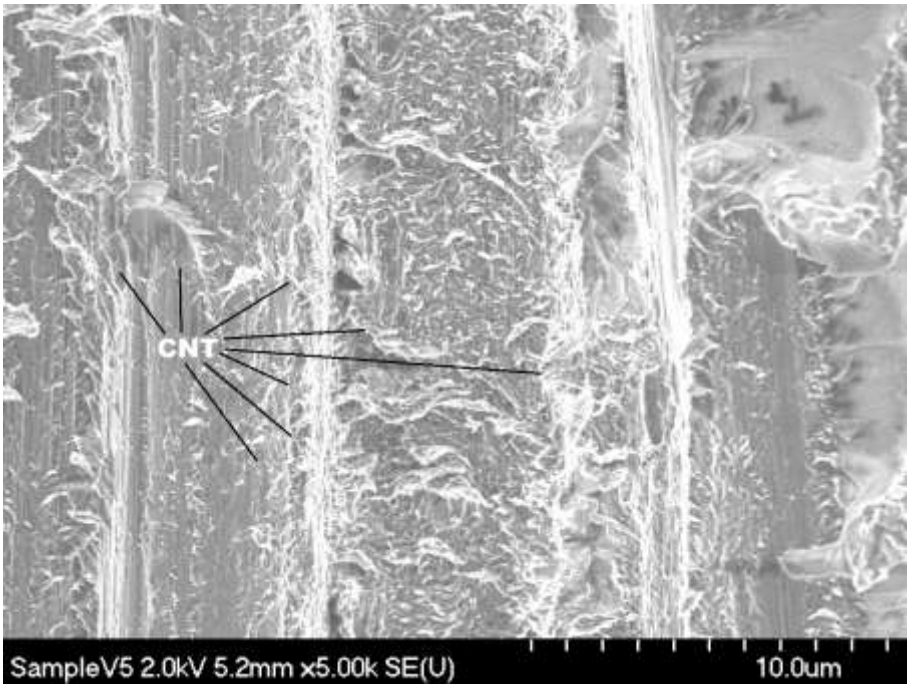

a)

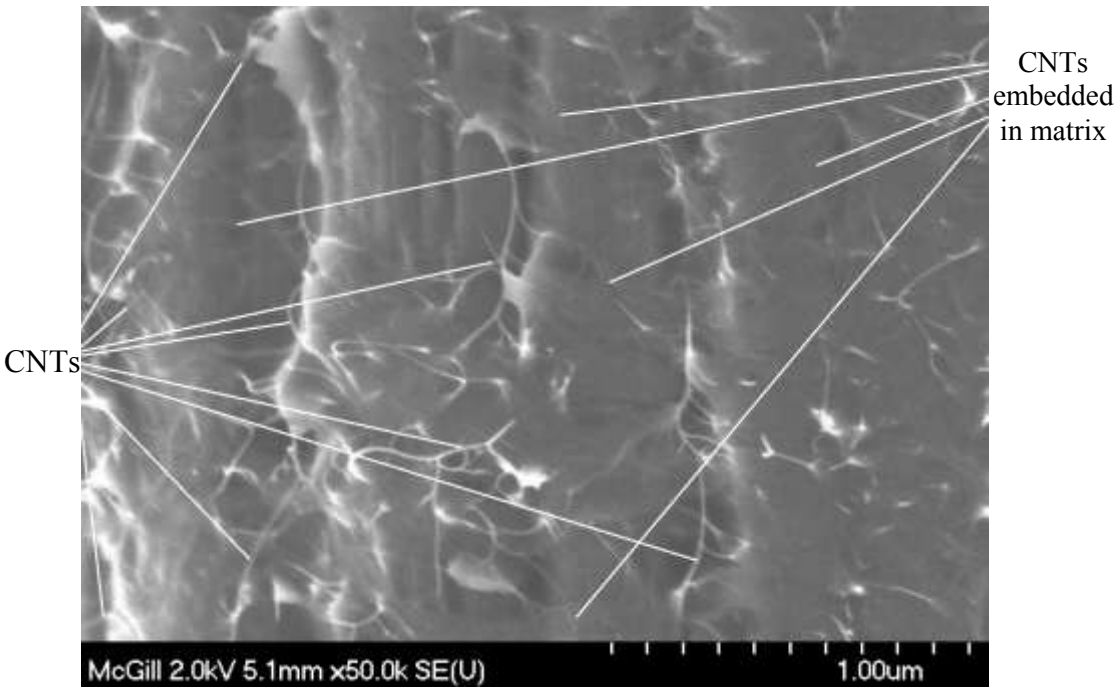

b)

Fig. 3.19: SEM images of properties improvement samples at a) 5k magnification and b) 50k magnification.

Chapter 4

4. Testing

Materials used to make parts with good heat dissipation shall possess good thermal conductivity. Therefore, thermal conductivity of obtained samples shall be verified.

4.1 Thermal Conductivity Testing

Thermal conductivity can be verified by variety of methods. For the purpose of this research, the method where thermal conductivity is obtained as a result of equation 4.1 was chosen.

$$\kappa = \alpha * \rho * Cp \qquad (4.1)$$

Where symbols denote:

κ – thermal conductivity

α – thermal diffusivity

ρ – density

Cp – specific heat.

Each of the above properties is determined independently of one another prior to combining them into equation 4.1. The following is the methodology employed to obtain these properties. While density is considered to be constant in the measured temperature range, thermal diffusivity and specific heat are temperature dependent, thus providing temperature dependent thermal conductivity.

4.1.1 Thermal Diffusivity

Samples thermal diffusivity was established with the flash method according to standards ASTM E-1461, DIM EN 821 and DIN 30905 [71].

4.1.1.1. Measurement Principle

A coupon placed in a coupon holder is irradiated by xenon flash tube. An infrared detector is used to measure temperature rise on the other side of the sample as a function of time. Thermal diffusivity is calculated using Cowan model. The calculation results are obtained in the form of a list. Schematic presentation of the instrument operating principle is shown in Fig. 4.1 [71].

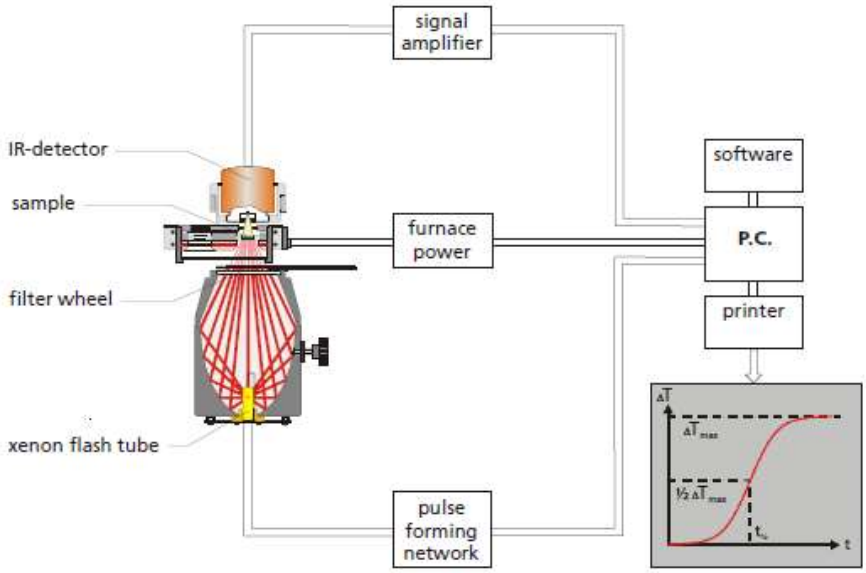

Fig. 4.1: Thermal diffusivity measurement principle [71].

4.1.1.2. Coupon Preparation

Coupons for thermal diffusivity measurement should conform to specifications provided by the instrument manufacturer [71].

The coupon holder limits coupon lateral dimensions to 12.7 mm. The thickness is recommended as a function of expected thermal diffusivity. For materials with low thermal diffusivity, coupon thickness should be 1 mm or less with the upper and lower surface as flat and parallel as possible. Samples flatness as well as top and bottom surfaces parallelism were assured via tooling and stacking sequence. For A and B type samples, machined metal tool plates were assuring sample face flatness while silicone moulds of uniform thickness were used to have bottom and top tool plates equally distant one from another, thus ensuring required parallelism. C and D type samples were prepared in a different manner, as described in Chapter 3. While metal machined tool plate was used for sample stack up and curing, layers of other materials were between the sample and the tool plate. This required more attention during sample layup and stack up. During layup, layers were placed precisely one on top of the other in order to minimize the possibility of slip between the layers during the initial stages of curing process. During stack up, attention was paid to placement of materials layers in order to avoid wrinkles and to provide for equal pressure distribution over samples. Coupons were cut from cured samples and measured to conform to the manufacturer's requirements. Details are provided in the section 4.1.2.

To enhance absorption of laser energy and emission of IR radiation to the detector, samples must always be coated with graphite. The purpose of the coating is to increase signal-to-noise ratio. The coating shall be uniform, approximately 5 μm thick. To conform to this requirement, four layers of liquid graphite lubricant resistant to high temperatures were sprayed on both sides of each coupon.

4.1.1.3. Measurement

Measurement is an automated process as well as thermal diffusivity calculation. When the instrument is prepared per manufacturer's instructions [71], coupons can be placed in the coupon holder. Up to four coupons can be placed in the coupon holder, however, it is recommended to have a reference material coupon in one of the slots in order to confirm reliability of the measurement.

Measurement is completed via software installed on a PC. Measurement parameters to be specified are desired testing temperature and number of shots per testing point.

Important coupon parameter to be entered before the measurement is the coupon thickness. The thickness is used in the calculation of the thermal diffusivity. The calculation of the thermal diffusivity is completed in the analysis software provided by the manufacturer. The results are obtained in the form of a list per coupon specifying thermal diffusivity for each specified temperature. Thermal diffusivity results units are mm^2/s.

4.1.2. Density

Density is a parameter required to calculate thermal conductivity per equation 4.1.

A coupon density is determined by dividing the measured mass of the coupon by the calculated volume of the coupon.

4.1.2.1. Measurement

The mass of a coupon was measured with analytical balance, with measuring precision of 0.0001 g. This balance was utilised throughout the research.

The volume of the coupon is determined by multiplying the coupon lateral dimensions with the coupon thickness. Coupons were cut from cured samples to dimensions W x L = 12.7 x 12.7 mm. W is the width and L is the length of a coupon. The coupons were cut from samples to approximate dimensions using a cutting knife. To obtain required dimensions, coupons were hand sanded using fine grain sand paper. Frequent verification of coupon dimensions allowed for good result. Upon finalisation of sanding, final coupon dimensions were determined with a digital caliper. The caliper had precision of 0.01 mm. This caliper was utilised throughout the research. Each dimension was measured at three points, both ends and the middle of the span of the respective dimension. Average value was calculated for each dimension. Thickness of the coupon was determined using a micrometer with precision of 0.001 mm. This micrometer was utilised throughout the research. Thickness was measured at five points, four corners and the imagined intersection of the coupon diagonals. The average value was calculated from these five measurements.

4.1.3. Specific Heat

Specific heat is another parameter required to determine thermal conductivity per equation 4.1.

A sample specific heat was determined via measurements completed with a DSC.

4.1.3.1. Cp Determination Process

Three measurements are taken into account to determine the specific heat of a sample. One is the baseline measurement, the second one is the reference material measurement and the third one is the sample measurement.

The baseline measurement is the test where there are no sample pans inside the DSC chamber.

The reference material measurement is the test where the reference (empty) pan is in its position, and the pan with the reference material is placed in the sample pan position.

The first two measurements are required to be completed only once. These two measurements are then used to determine Cp for each sample.

The sample measurement is the test where the reference pan is in its position and the tested sample is in the pan in the sample pan position.

The software provided by DSC manufacturer is used to calculate Cp for each sample utilizing the above three measurements. Calculated results for Cp are provided in the form of a list where Cp is function of temperature with the unit J/g^{o}C.

Typical Cp plot is presented in Fig. 4.2. Top curve is the heat capacity curve, while lower curve is total heat curve.

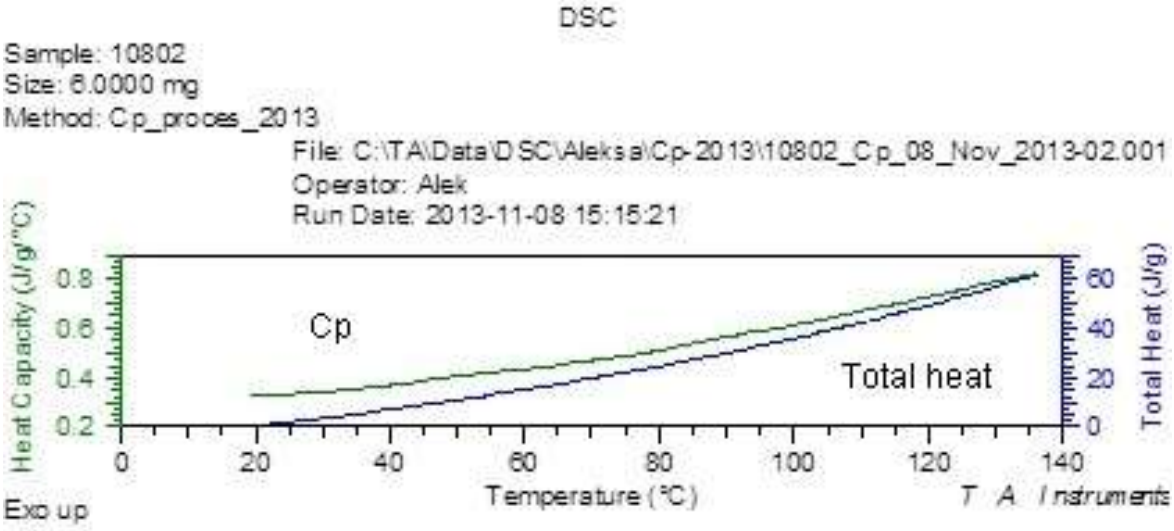

Fig. 4.2: Typical Cp plot.

4.1.3.2. Measurement

To complete the measurements as described in the Cp determination principle, samples need to be prepared.

As mentioned, there are no samples for the baseline measurement.

For the reference measurement empty pan is placed in the reference pan position and the pan with the reference material - sapphire – is placed in the sample position.

For each of the tested samples, material cut from the sample was placed in an Al pan and the pan was sealed.

All samples measurements, baseline measurement and reference measurement were completed per following procedure:

1. Equilibrate at 0 ^{o}C.
2. Isothermal for 10 min.
3. Ramp 20 ^{o}C/min to 140 ^{o}C.
4. Equilibrate at 140 ^{o}C.
5. Isothermal for 10 min.

Chapter 5

5. Results and Discussion

Thermal conductivity determination was carried out on all four types of samples: A, B, C and D. Each sample was tested at three different temperatures: 25, 75 and 125 ^{o}C. Within type B and type D samples, differentiation of samples based on CNTs weight loading [wt%] and type is made in the similar manner. The difference is that for type B samples wt% is determined with respect to the weights of matrix and CNTs whereas for type D samples wt% is determined relative to weights of CF preforms and CNTs.

Thermal conductivity results were organized per sample schedule. Thermal conductivity dependence of the CNTs content, both with respect to wt% loading and purification level was evaluated as well as a function of temperature. Results are presented for obtained values of CNT loaded samples thermal conductivity as well as with respect to pristine matrix (type B samples) and reference samples (type D samples).

5.1. Type B samples

Type B samples were manufactured from matrix and CNTs. Samples are differentiated with respect to incorporated carbon nanotube purification level and carbon nanotube weight loading.

5.1.1. BR Samples

Samples BR1, BR2 and BR3 contain 1 wt%, 2 wt% and 3 wt% of raw CNTs respectively.

Obtained thermal conductivity results for type A and BR samples are presented in Table 5.1.

Table 5.1: Thermal conductivity for Type A and BR samples.

		κ [w/mK]			κ - Relative Increase [%]		
t [°C]	25	75	125		25	75	125
Sample							
Type A	0.235±0.004	0.245±0.011	0.257±0.016				
BR1	0.303±0.008	0.314±0.008	0.314±0.008		29.1	28.4	22.4
BR2	0.313±0.013	0.324±0.015	0.324±0.012		33.2	32.7	26.4
BR3	0.326±0.014	0.336±0.011	0.335±0.012		38.7	37.2	30.4

Thermal conductivity varies both with CNTs weight content and temperature.

5.1.1.1. CNTs Loading Level Impact

To evaluate impact of CNTs loading level, defined as wt% of total sample weight, thermal conductivity was measured for pristine matrix and samples with each of the three different weight loadings: 1, 2 and 3 wt%. Obtained values are compared at each of the three temperature measurement points. Fig. 5.1 depicts results at 25 °C.

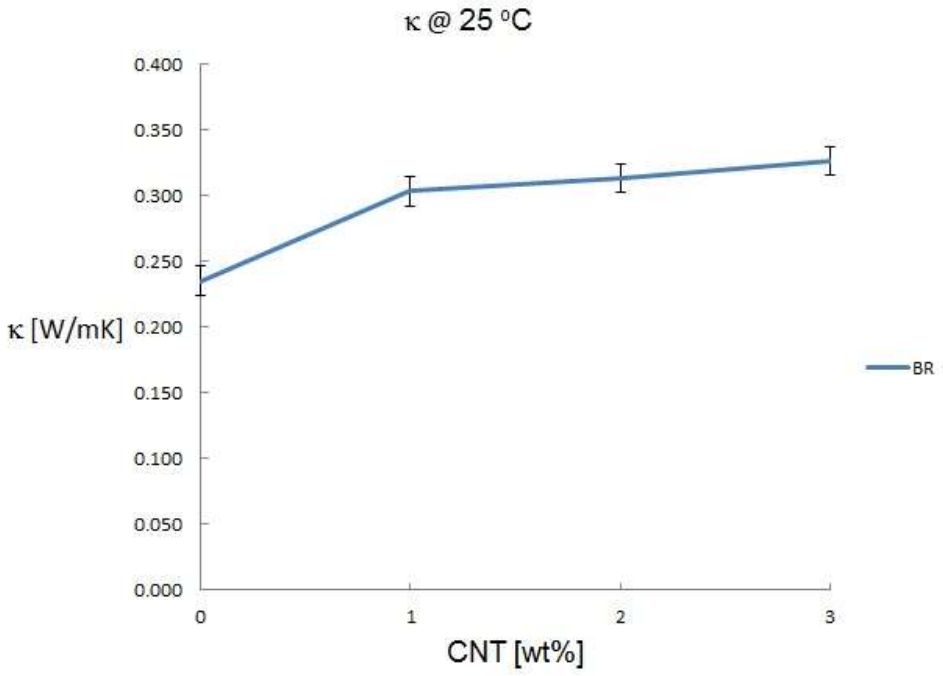

Fig. 5.1: Thermal conductivity at 25 °C plot for A and BR samples as a function of CNT loading.

Fig. 5.1 shows that percolation network is already established with 1 wt% of CNTs. Increase in thermal conductivity from type A samples is almost 30%. Further increase of CNT content continues to increase thermal conductivity, however at a much slower rate, as can be seen from the curve constant slope. Adding more CNTs increases thermal conductivity approximately 3.5% for each additional weight% added. The curve has constant slope, however, the increase in TC achieved from 1 wt% to 2 wt% and from 2 wt% to 3 wt% content is within the error margin. Increase in TC achieved from 1 wt% to 3 wt% is just outside the error margin.

For measurement point at 75 °C, thermal conductivity curve is presented in Fig. 5.2.

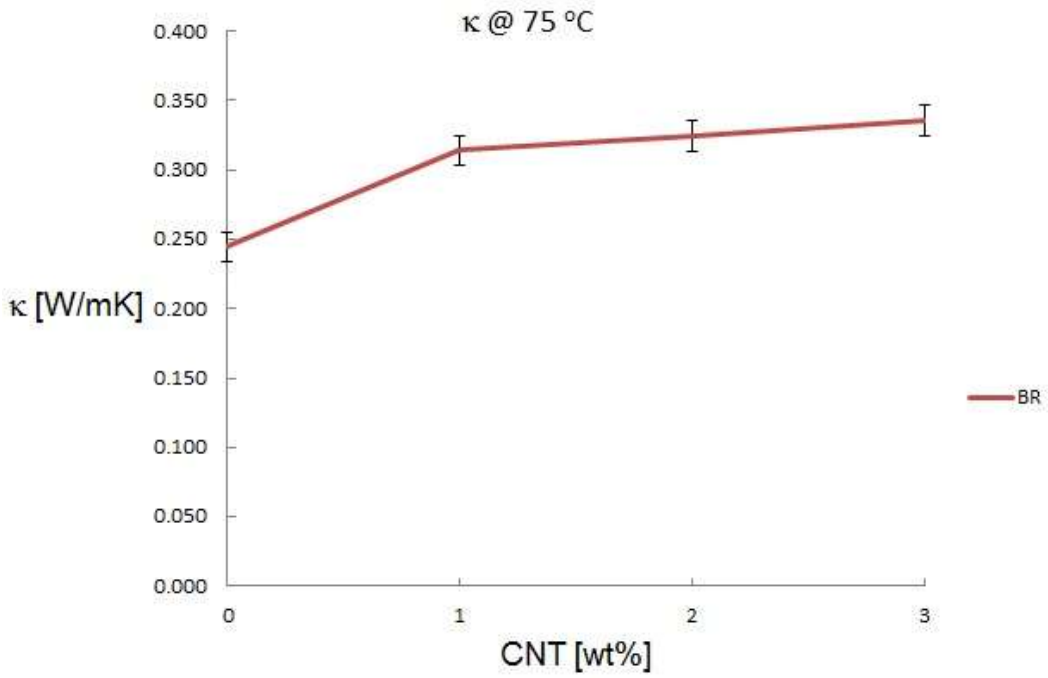

Fig. 5.2: Thermal conductivity at 75 °C plot for A and BR samples as a function of CNT loading.

Fig. 5.2 shows that thermal conductivity exhibits similar behavior at 75 °C with CNT content increase as it does at 25 °C. Efficient heat transfer network is established with 1 wt% of CNTs. The increase with respect to pristine matrix samples is approximately 30%. Further increase of CNT content continues to increase thermal conductivity, however at a much slower rate, as can be seen from the curve constant slope. Adding more CNTs increases thermal conductivity approximately 3.5% for each additional weight% added. The curve has constant slope, however, the increase in TC achieved from 1 wt% to 2 wt% and from 2 wt% to 3 wt% content is within the error margin. Increase in TC achieved from 1 wt% to 3 wt% is just outside the error margin.

For measurement point at 125 °C, thermal conductivity curve is presented in Fig. 5.3.

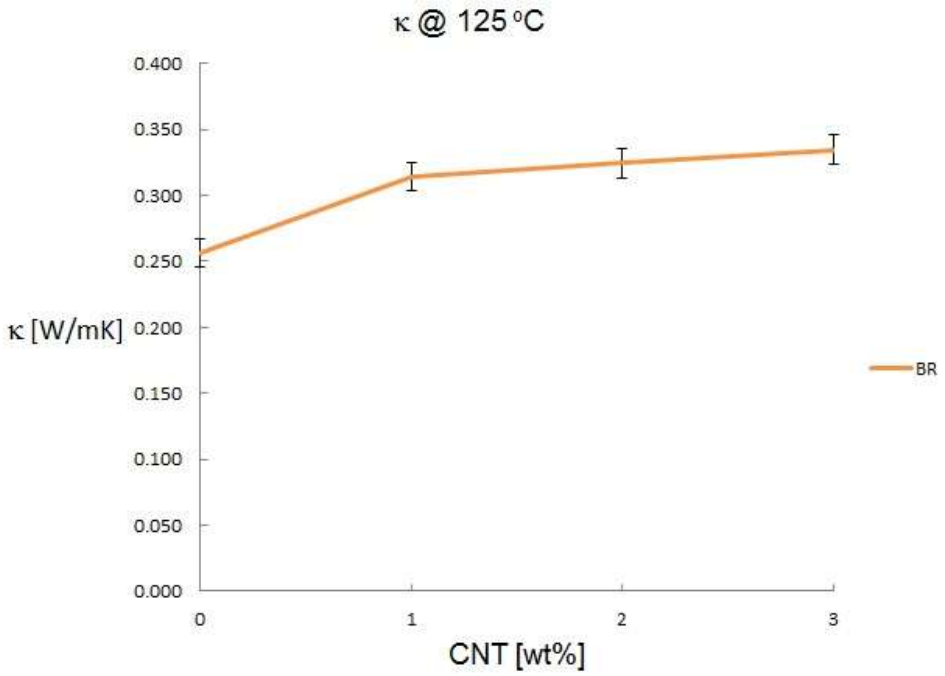

Fig. 5.3: Thermal conductivity at 125 °C plot for A and BR samples as a function of CNT loading.

Fig. 5.3 shows that thermal conductivity exhibits similar behavior at 125 °C with CNT content increase as it does at 25 °C and 75 °C. Efficient heat transfer network is established with 1 wt% of CNTs, with smaller increase with respect to pristine matrix samples of approximately 20%. Further increase of CNT content continues to increase thermal conductivity, however at a much slower rate, as can be seen from the curve constant slope. Adding more CNTs increases thermal conductivity approximately 3.5% for each additional weight% added. The curve has constant slope, however, the increase in TC achieved from 1 wt% to 2 wt% and from 2 wt% to 3 wt% content is within the error margin. Increase in TC achieved from 1 wt% to 3 wt% is just outside the error margin.

From the above presented, a conclusion can be drawn that RCNTs increase thermal conductivity of matrix when added in quantity of 1 wt% or more. Heat transfer network is readily established with 1 wt% of RCNTs. With higher loading levels, heat transfer

network is improved giving higher thermal conductivity levels. The TC increase is not large, however it should be noted that is steady for all loading levels verified at each temperature point. Per obtained data, thermal conductivity can be expected to increase further with increased RCNT content. With increased CNT quantity, number of heat transportation channels would be increased and thermal conductivity would rise, being a function of number of heat transportation channels.

5.1.1.2. Temperature Impact

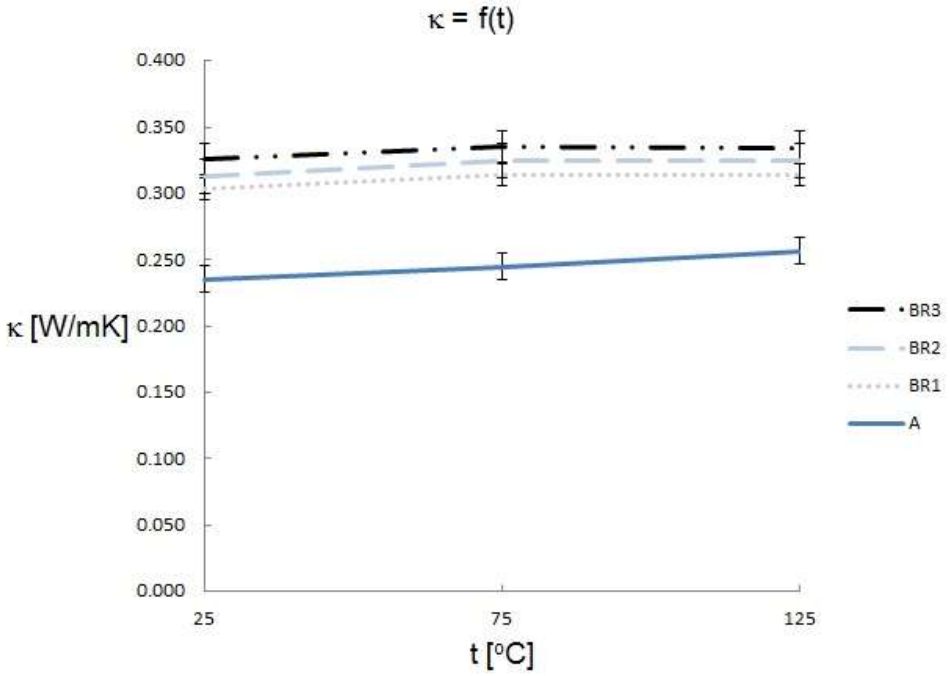

Fig. 5.4: Thermal conductivity of A and BR samples as a function of temperature.

To evaluate impact of temperature on thermal conductivity, thermal conductivity was measured at three different points: 25, 75 and 125 ^{o}C for pristine matrix and BR1, BR2 and BR3 samples. The thermal conductivity plot as a function of temperature in Fig. 5.4 depicts the results graphically.

While CNT loaded samples thermal conductivity exhibits the same behaviour with temperature change disregarding the loading level, pristine matrix thermal conductivity change with temperature increase is markedly different.

Pristine matrix thermal conductivity is increased with temperature increase throughout the investigated temperature range. Increase between 25 ^{o}C and 75 ^{o}C is approximately 4% and increase between 75 ^{o}C and 125 ^{o}C is somewhat larger, approximately 5%. The difference is visible as a change in the curve slope as well. However, the change is within the error margin.

Thermal conductivity increase is almost the same for samples with 1, 2 and 3 wt% of CNTs with temperature increase from 25 ^{o}C to 75 ^{o}C, approximately 3%. Still, this increase is within the error margin. However, being the same across the CNT loading range, it could be considered real. With further temperature increase to 125 ^{o}C, thermal conductivity is not increasing, probably due to higher phonon-phonon scattering which is always increased with increased temperature. Thus, the curve is flat between 75 ^{o}C and 125 ^{o}C.

As mentioned above, the thermal conductivity change with temperature increase is different for type A and type BR samples. Between 25 ^{o}C and 75 ^{o}C is almost the same, with increase of 4% and 3% respectively. However, with further temperature increase to 125 ^{o}C, type A samples thermal conductivity is rising by further 5% while there is no change in BR samples thermal conductivity. The difference is due to modified material properties with addition of CNTs.

5.1.2. BP Samples

Samples BP1, BP2 and BP3 contain 1 wt%, 2 wt% and 3 wt% of purified CNTs respectively. Samples made with PCNTs yielded thermal conductivity values that are given in Table 5.2.

Table 5.2: Thermal conductivity for Type A and BP samples.

		κ [w/mK]			κ - Relative Increase [%]		
t [°C]	25	75	125		25	75	125
Sample							
Type A	0.235±0.004	0.245±0.011	0.257±0.016				
BP1	0.292±0.008	0.301±0.008	0.302±0.008		24.1	23.0	17.6
BP2	0.320±0.006	0.341±0.012	0.346±0.014		36.2	39.6	34.8
BP3	0.356±0.005	0.375±0.009	0.382±0.013		51.3	53.4	48.7

Thermal conductivity varies both with CNTs weight content and temperature.

5.1.2.1. CNTs Loading Level Impact

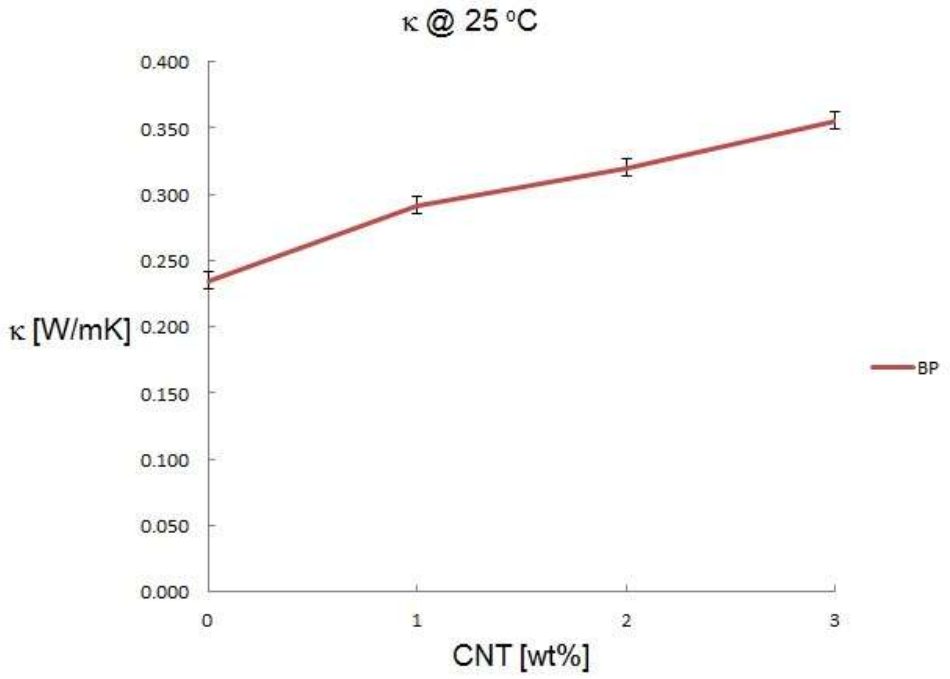

Fig. 5.5: Thermal conductivity at 25 °C plot for A and BP samples as a function of CNT loading.

To evaluate impact of CNTs loading level, defined as wt% of total sample weight, thermal conductivity was measured for pristine matrix and samples with each of the three different weight loadings: 1, 2 and 3 wt%. Obtained values are compared at each of the three temperature measurement points. Fig. 5.5 depicts results at 25 ^{o}C.

Fig. 5.5 shows that percolation network is already established with 1 wt% of PCNTs. Increase in thermal conductivity from type A samples is almost 25%. Further increase of CNT content continues to increase thermal conductivity, however at a slower rate, as can be seen from the curve almost constant slope. Adding more CNTs increases thermal conductivity approximately 10% for each additional weight% added. The increase in TC achieved from 1 wt% to 2 wt% and from 2 wt% to 3 wt% content is larger than the error margin, confirming the improvement in heat transfer network with addition of CNTs.

For measurement point at 75 ^{o}C, thermal conductivity curve is presented in Fig. 5.6.

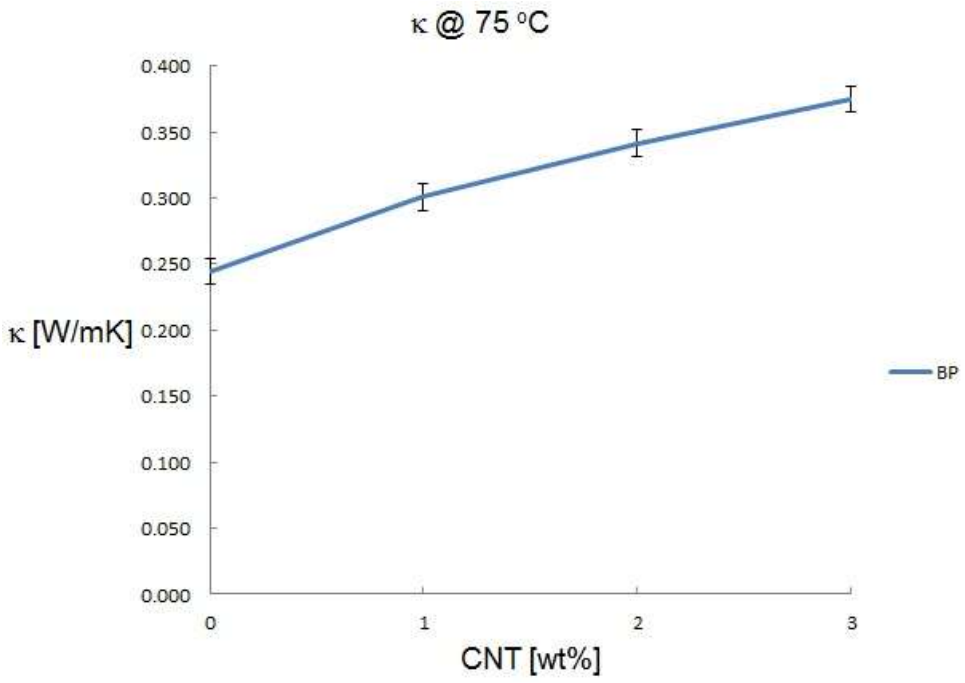

Fig. 5.6: Thermal conductivity at 75 ^{o}C plot for A and BP samples as a function of CNT loading.

Fig. 5.6 shows that percolation network is already established with 1 wt% of PCNTs. Increase in thermal conductivity from type A samples is almost 25%. Further increase of CNT content continues to increase thermal conductivity, however at a slower rate, as can be seen from the curve almost constant slope. Adding more CNTs increases thermal conductivity 13.5% and 9.9% for each additional weight% added. The increase in TC achieved from 1 wt% to 2 wt% and from 2 wt% to 3 wt% content is larger than the error margin, confirming the improvement in heat transfer network with addition of CNTs.

For measurement point at 125 ^{o}C, thermal conductivity curve is presented in Fig. 5.7.

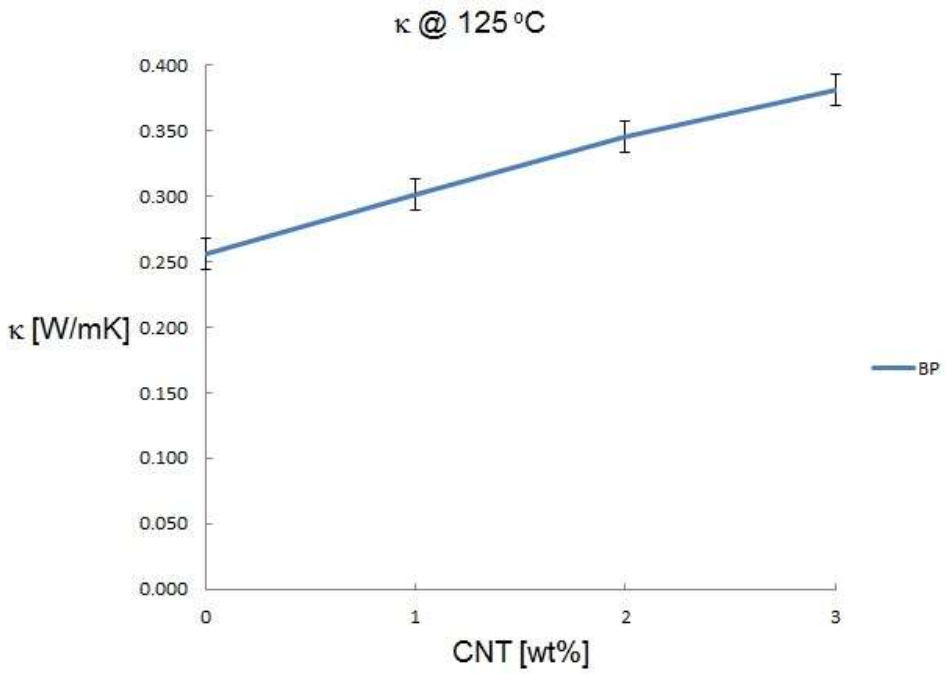

Fig. 5.7: Thermal conductivity at 125 ^{o}C plot for A and BP samples as a function of CNT loading.

Fig. 5.7 shows that percolation network is already established with 1 wt% of PCNTs. Increase in thermal conductivity from type A samples is almost 18%. Further increase of CNT content by 1 wt% continues to increase thermal conductivity, at just a bit slower rate (14.6%), as can be seen from the curve almost constant slope. Adding more CNTs

increases thermal conductivity additional 10.4%. The increase in TC achieved from 1 wt% to 2 wt% and from 2 wt% to 3 wt% content is larger than the error margin, confirming the improvement in heat transfer network with addition of CNTs.

From the above presented, a conclusion can be drawn that PCNTs increase thermal conductivity of matrix when added in quantity of 1 wt % or more. Heat transfer network is readily established with 1 wt% of PCNTs. With higher loading levels, heat transfer network is improved giving higher thermal conductivity levels. The TC increase is not large, however it should be noted that exists for all loading levels verified at each temperature point. Per obtained data, thermal conductivity can be expected to increase further with increased PCNT content. With increased CNT quantity, number of heat transportation channels would be increased and thermal conductivity would rise, being a function of number of heat transportation channels.

5.1.2.2. Temperature Impact

To evaluate impact of temperature on thermal conductivity, thermal conductivity was measured at three different points: 25, 75 and 125 ^{o}C for pristine matrix and BP1, BP2 and BP3 samples. Thermal conductivity plot as a function of temperature in Fig. 5.8 depicts results graphically.

While CNT loaded samples thermal conductivity exhibits similar behaviour with temperature change for each loading level, pristine matrix thermal conductivity change with temperature increase is markedly different, as described in 5.1.1.2.

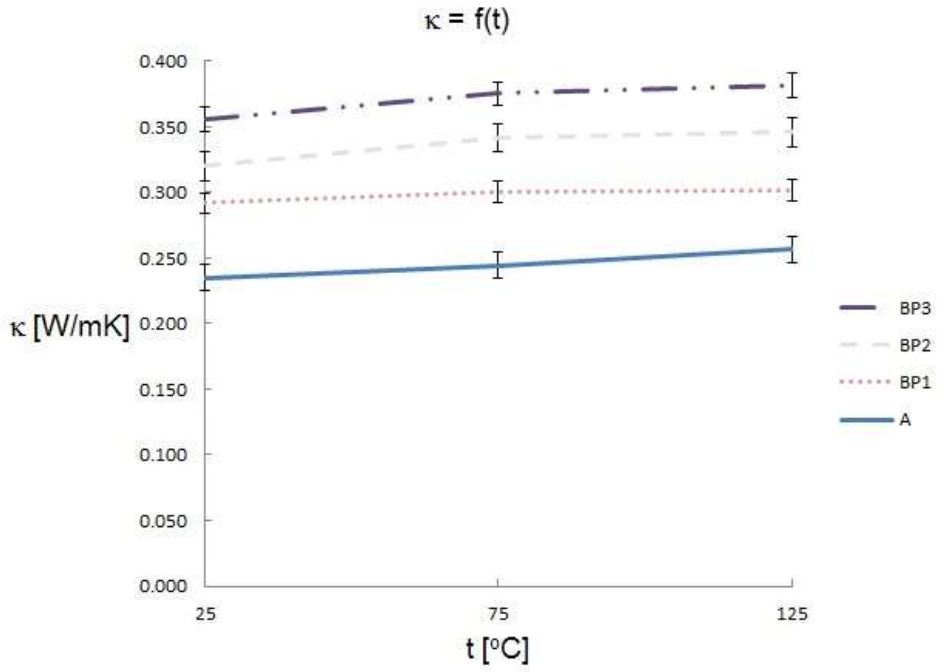

Fig. 5.8: Thermal conductivity of A and BP samples as a function of temperature.

BP1 sample thermal conductivity increases approximately 3% with temperature increase from 25 to 75 ^{o}C and is essentially constant with further temperature rise to 125 ^{o}C. This behaviour is different from the one that can be seen in thermal conductivity of samples with 2 and 3 wt%. For these two weight loadings thermal conductivity change with temperature is very similar. Thermal conductivity increase with temperature rise to 75 ^{o}C is somewhat higher than 5%, while further temperature rise to 125 ^{o}C leaves thermal conductivity nearly unchanged with rise of approximately 1.5%. When thermal conductivity change with temperature increase is discussed, it should be noted that only increase observed for samples with 2 and 3 CNT wt% with temperature rise from 25 to75 ^{o}C is larger than the error margin. Nonetheless, as it can be observed for samples with different loading levels, it could be considered real. At higher temperature of 125 ^{o}C, phonon-phonon scattering is increased, thus leaving thermal conductivity at the same level as at 75 ^{o}C.

As mentioned above, the thermal conductivity change with temperature increase is different for type A and type BP samples. Between 25 ^{o}C and 75 ^{o}C the nature of the change is similar, increase between 3 and 7 %. However, with further temperature increase to 125 ^{o}C, type A samples thermal conductivity is rising by further 5% while there is almost no change in BP samples thermal conductivity. The difference is due to modified material properties with addition of CNTs.

5.1.3. BSP Samples

Samples BSP1, BSP2 and BSP3 contain 1 wt%, 2 wt% and 3 wt% of super purified CNTs respectively.

Samples made with SPCNTs yielded thermal conductivity values that are given in Table 5.3.

Table 5.3: Thermal conductivity for Type A and BSP samples.

		κ [w/mK]			κ - Relative Increase [%]		
t [^{o}C]	25	75	125		25	75	125
Sample							
Type A	0.235±0.004	0.245±0.011	0.257±0.016				
BSP1	0.298±0.004	0.303±0.001	0.304±0.003		26.6	23.9	18.3
BSP2	0.258±0.006	0.274±0.002	0.284±0.005		9.8	12.1	10.7
BSP3	0.303±0.007	0.323±0.002	0.329±0.005		28.9	32.1	28.3

Thermal conductivity varies both with CNTs weight content and temperature.

5.1.3.1. CNTs Loading Level Impact

To evaluate impact of CNTs loading level, defined as wt% of total sample weight, thermal conductivity was measured for pristine matrix and samples with each of the three

different weight loadings: 1, 2 and 3 wt%. Obtained values are compared at each of the three temperature measurement points. Fig. 5.9 depicts results at 25 ^{o}C.

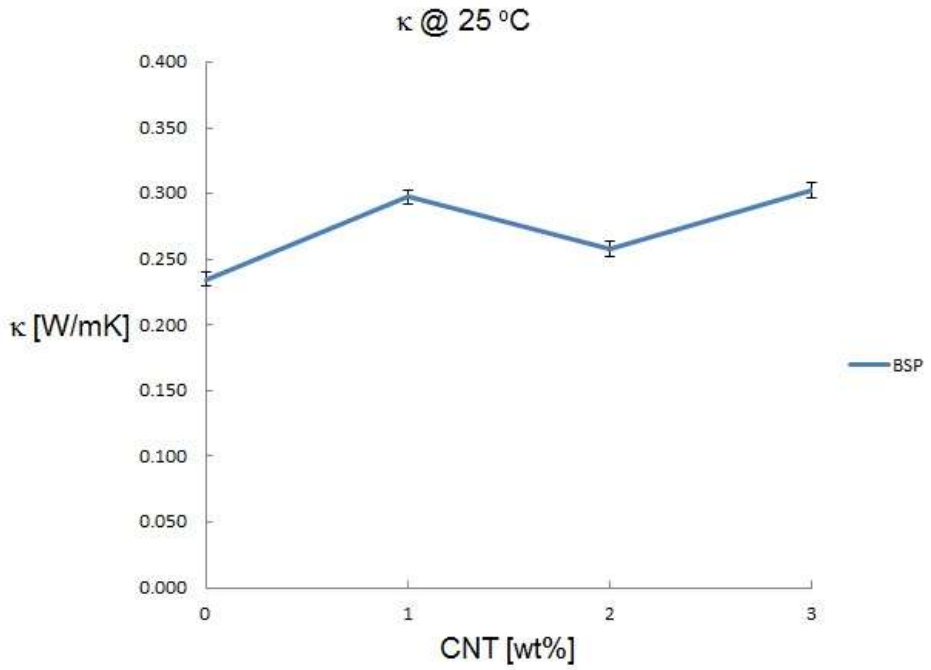

Fig. 5.9: Thermal conductivity at 25 ^{o}C plot for A and BSP samples as a function of CNT loading.

Fig. 5.9 shows that percolation network is already established with 1 wt% of SPCNTs. Increase in thermal conductivity from type A samples is almost 27%. CNT content increase to 2 wt% results in decrease in thermal conductivity from the one achieved with 1 wt%. This is considered an anomaly. Addition of the 3rd wt% of CNTs returns thermal conductivity to the expected level, above the one with 1 wt%. The difference is approximately 2%, within the error margin.

For measurement point at 75 ^{o}C, thermal conductivity curve is presented in Fig. 5.10.

Fig. 5.10 shows that percolation network is already established with 1 wt% of SPCNTs. Increase in thermal conductivity from type A samples is almost 24%. CNT content increase to 2 wt% results in decrease in thermal conductivity from the one achieved with

1 wt%. This is considered an anomaly. Addition of the 3rd wt% of CNTs returns thermal conductivity to the expected level, above the one with 1 wt%. The difference is approximately 7%, larger than the error margin, confirming improvement in heat transfer network.

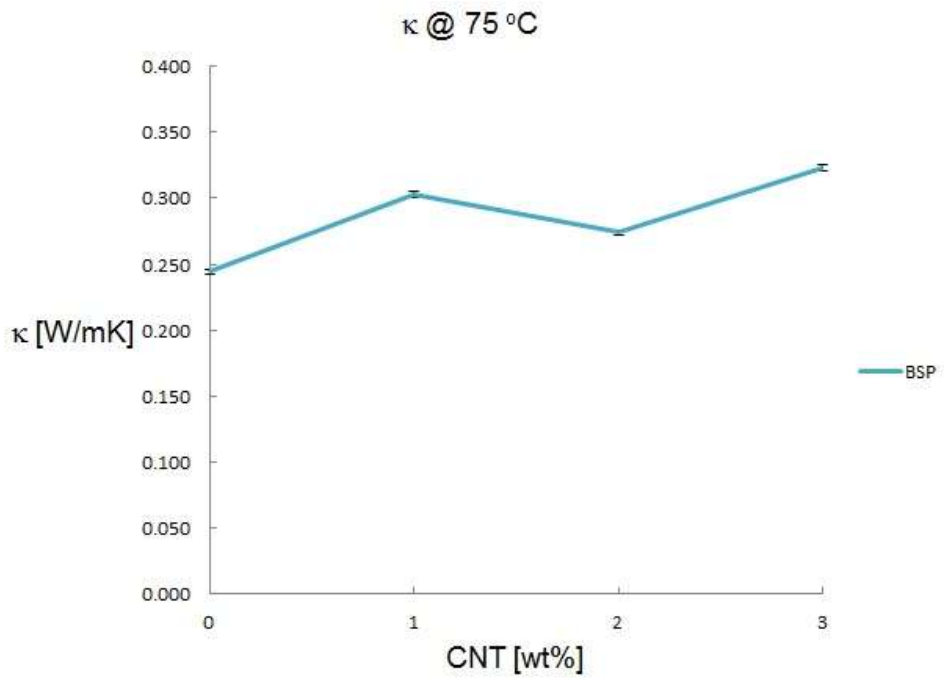

Fig. 5.10: Thermal conductivity at 75 °C plot for A and BSP samples as a function of CNT loading.

For measurement point at 125 °C, thermal conductivity curve is presented in Fig. 5.11.

Fig. 5.11 shows that percolation network is already established with 1 wt% of SPCNTs. Increase in thermal conductivity from type A samples is approximately 18%. CNT content increase to 2 wt% results in decrease in thermal conductivity from the one achieved with 1 wt%. This is considered an anomaly. Addition of the 3rd wt% of CNTs returns thermal conductivity to the expected level, above the one with 1 wt%. The difference is approximately 8.5%, larger than the error margin, confirming improvement in heat transfer network.

From the above presented, a conclusion can be drawn that SPCNTs increase thermal conductivity of matrix when added in quantity of 1 wt % or more. Heat transfer network is readily established with 1 wt% of SPCNTs. With higher loading level of 3 wt%, heat transfer network is improved giving higher thermal conductivity levels. Results obtained with 2 wt% are considered an anomaly. The TC increase is not large, however it should be noted at each temperature point. Per obtained data, thermal conductivity can be expected to increase further with increased SPCNT content. With increased CNT quantity, number of heat transportation channels would be increased and thermal conductivity would rise, being a function of number of heat transportation channels.

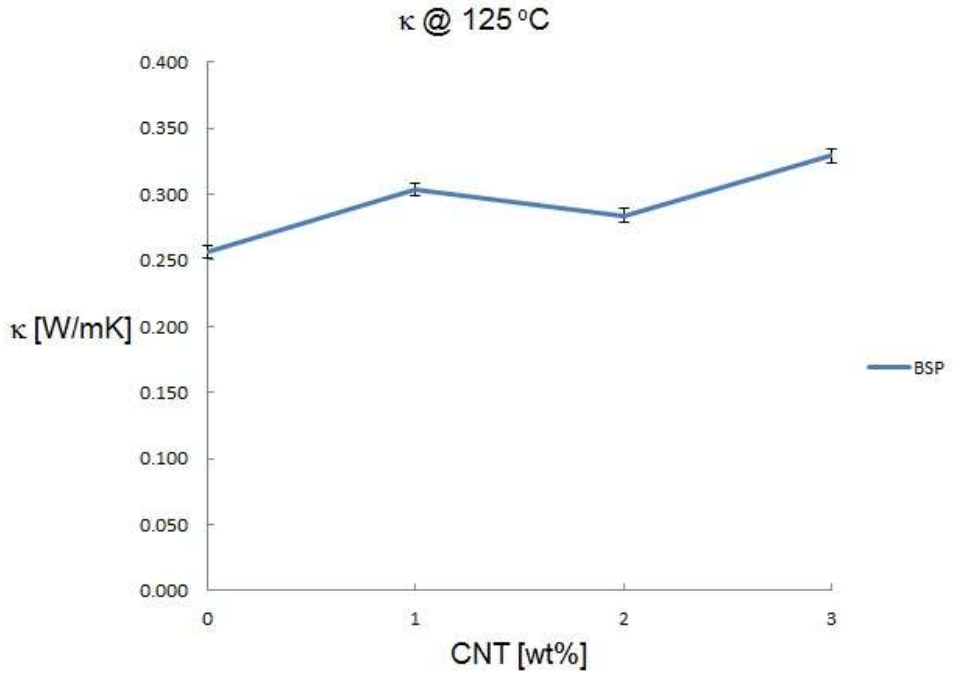

Fig. 5.11: Thermal conductivity at 125 °C plot for A and BP samples as a function of CNT loading.

5.1.3.2. Temperature Impact

To evaluate impact of temperature on thermal conductivity, thermal conductivity was measured at three different points: 25, 75 and 125 °C for pristine matrix and BSP1, BSP2

and BSP3 samples. Thermal conductivity plot as a function of temperature in Fig. 5.12 depicts results graphically.

While CNT loaded samples thermal conductivity exhibits similar behaviour with temperature change for each loading level, pristine matrix thermal conductivity change with temperature increase is markedly different, as described in section 5.1.1.2.

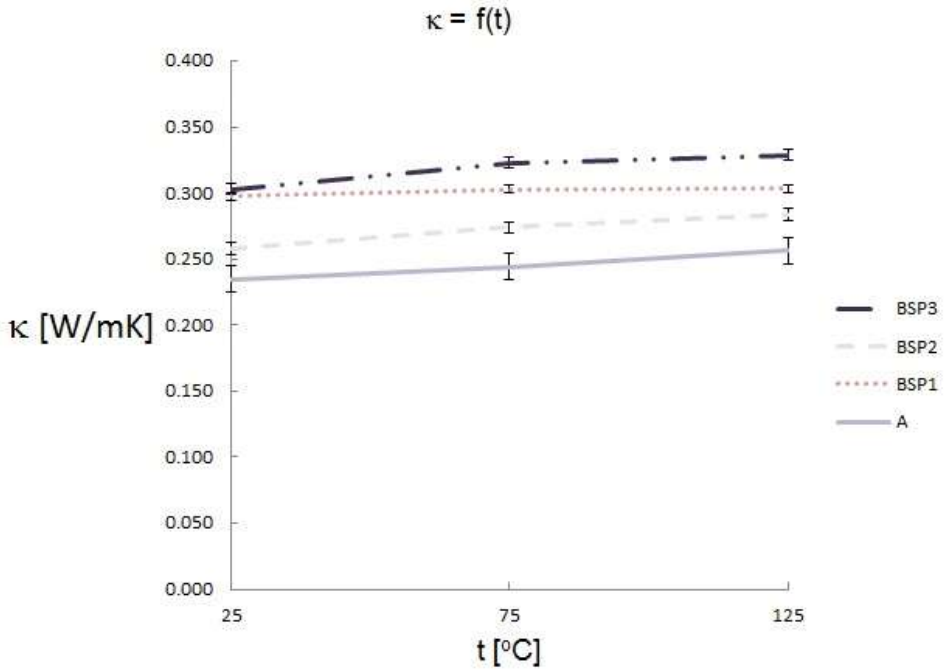

Fig. 5.12: Thermal conductivity of A and BSP samples as a function of temperature.

BSP1 sample thermal conductivity increases approximately 2% with temperature increase from 25 to 75 ^{o}C and is essentially constant with further temperature rise to 125 ^{o}C. This behaviour is different from the one that can be seen in thermal conductivity of samples with 2 and 3 wt%. For these two weight loadings thermal conductivity change with temperature rise to 75 ^{o}C is very similar. Thermal conductivity increase with temperature rise to 75 ^{o}C is approximately 6.5%. Further temperature increase to 125 ^{o}C

increases 2 wt% sample thermal conductivity by additional 3.6%, while the 3 wt% sample one is nearly unchanged with rise of approximately 2%.

When thermal conductivity change with temperature increase is discussed, it should be noted that only increase observed for samples with 2 and 3 CNT wt% with temperature rise from 25 to75 ^{o}C can be considered sufficiently outside the error margin. Nonetheless, as it can be observed for samples with different loading levels, it could be considered real. At higher temperature of 125 ^{o}C, phonon-phonon scattering is increased, thus leaving thermal conductivity nearly at the same level as at 75 ^{o}C.

Thermal conductivity change with temperature increase is different for type A and type BSP samples. Between 25 ^{o}C and 75 ^{o}C the nature of the change is similar, increase between 2% and 7 %. However, with further temperature increase to 125 ^{o}C, type A samples thermal conductivity is rising by further 5% while BSP samples thermal conductivity changes its behaviour and tends to be constant. The difference is due to modified material properties with addition of CNTs.

5.1.4. CNTs Quality Impact

In order to discuss CNT quality impact, it is important to define the CNT quality with respect to thermal conductivity.

In graphite crystal lattice heat is transferred by acoustic phonons. Boundary scattering and lattice imperfections like carbon atom displacement, either in plane or out of its plane, carbon atoms missing, inclusions in the form of either carbon or a different atom all lead to a reduction of the phonon mean free path and as a consequence a reduction in thermal conductivity [11,12]. Hence, higher number of defect sites means lower thermal

conductivity of a CNT. Therefore, a CNT without any imperfections would be the CNT with the highest thermal conductivity, i.e. the highest quality CNT.

The most common method for CNTs purification is acid treatment. In this manner, as described in literature, ash content is reduced. A negative side of the acid treatment is damaging of CNTs' side walls [36, 37].

It is reasonable to assume that lower levels of ash content would require acid treatment that would infer higher number of individual defects to CNTs, thus reducing CNTs thermal conductivity. Therefore, for CNTs produced by the same method and with the same production parameters, as produced CNTs would have the lowest number of defects and hence the highest thermal conductivity, thus being the CNTs of the highest quality with respect to thermal conductivity. CNTs purified via acid treatment would have lower thermal conductivity, therefore being the CNTs of lower quality.

In the case of CNTs used in the current study, based on the above, RCNTs would be the CNTs with the highest quality of the three. PCNTs would be the CNTs with the second highest quality and the SPCNTs would be the CNTs with the lowest quality with respect to heat transfer.

To evaluate CNTs quality impact on thermal conductivity, thermal conductivities of samples made with the same weight loading of different quality CNTs were compared across investigated temperature range.

Results for 1 wt% of CNTs are graphically presented in Fig. 5.13.

From Fig. 5.13 can be seen that thermal conductivities for samples made with 1 wt% of CNTs with different ash content are almost the same. BR1 samples exhibit somewhat

higher thermal conductivity at each temperature point, approximately 4%. However, the differences are within the error margin.

To explain this, we shall consider CNT purification level. Purification level affects thermal conductivity in two ways: CNT structure and ash content. Effect on CNT structure was given earlier – more purification affects structure progressively in adverse manner. Further analysis shall demonstrate effect on thermal conductivity. With more purification, ash content is being reduced. Let's consider the ash content within each of employed CNT materials. Ash content is 16.5%, 8% and 4% in R, P and SP CNTs respectively. Ash content affects thermal conductivity in two ways. First, higher ash content means less CNTs. Less CNTs means lower nominal heat transport potential available. Second, when CNTs are dispersed in polymer, ash is present as well. Ash particles are phonon scattering sites, effectively reducing number of available phonon paths. Higher ash content translates into higher number of phonon scattering sites.

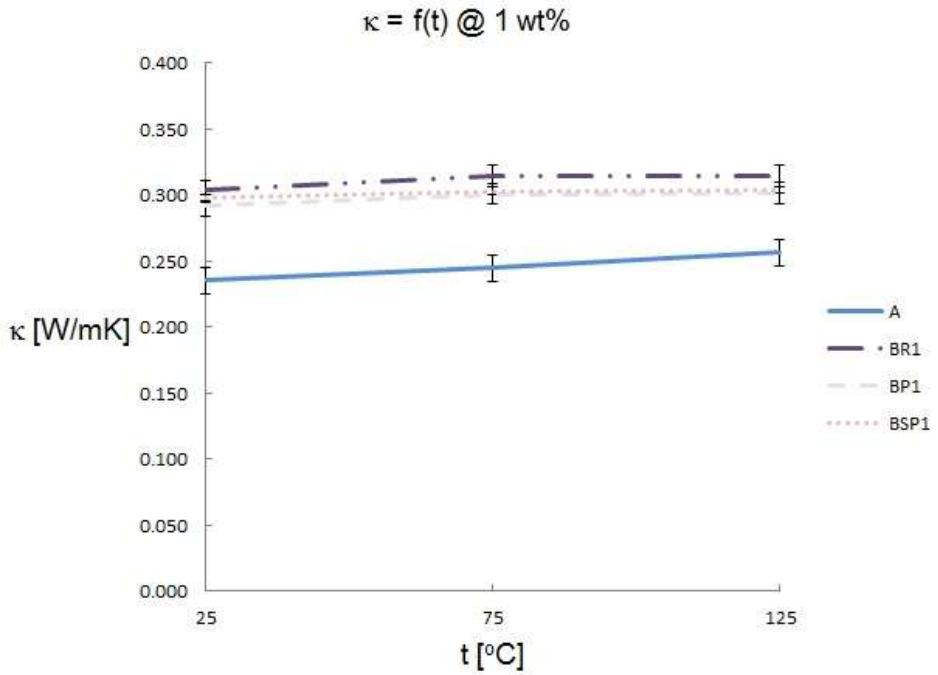

Fig. 5.13: 1 wt% samples thermal conductivity as a function of temperature.

If there would be only CNTs and ash, CNTs with 16.5% ash content would have 83.5% of CNTs, with 8% ash 92% CNTs and with 4% ash 96% CNTs. It means that 83.5% RCNTs with 16.5% of impurities transported 4% more heat energy than either 92% PCNTs with 8% of impurities or 96% SPCNTs with 4 % impurities.

To break this further down, consideration is to be given only to two CNT materials at the time. To begin with PCNTs and SPCNTs looks as a good idea as samples made with these two CNT materials have almost the same TC. Comparing CNT percentage, 92% vs. 96% means 4% less PCNTs than SPCNTs are available to transport heat energy. Consideration now has to be given to phonon scattering sites. Impurities content is 4% higher in PCNT material than in SPCNT one. It gives 4% more phonon scattering sites incorporated into BP than into BSP samples. Adding these two numbers, obtained is that 8% more heat is transported via individual PCNTs than via individual SPCNTs. If this simple calculation is extended to RCNTs, 21% more heat is transported through individual RCNTs than through individual PCNTs and 29% through individual RCNTs than through individual SPCNTs.

Results for 2 wt% of CNTs are graphically presented in Fig. 5.14.

From Fig. 5.14 can be seen that thermal conductivities for BR2 and BP2 samples are close one to another. BP2 samples exhibit somewhat higher thermal conductivity, from 2.2% at 25 ^{o}C to 6.6% at 125 ^{o}C. However, the difference is within the error margin. BSP2 samples thermal conductivity is anomalously low, as mentioned when loading level impact on thermal conductivity was considered. Therefore, consideration shall be given only to BR2 and BP2 samples. It appears that more heat energy is transported with 2 wt% of PCNTs than with 2 wt% of RCNTs.

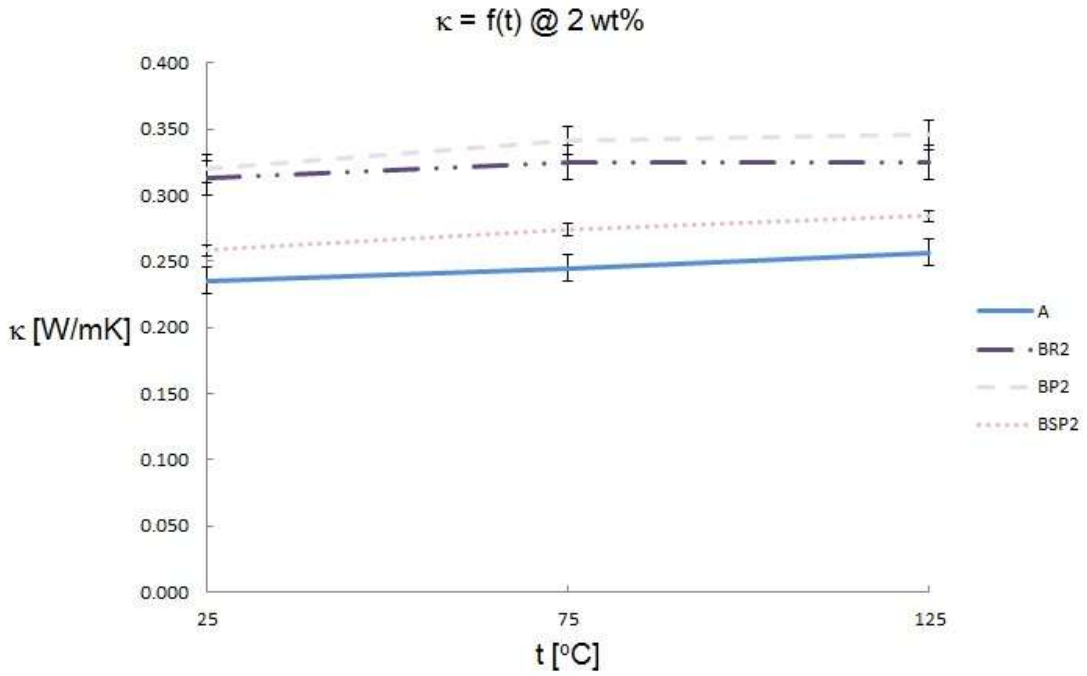

Fig. 5.14: 2 wt% samples thermal conductivity as a function of temperature.

At 2 wt% loading, 8.5% more PCNTs than RCNTs are transporting 2.2% to 6.6% more heat energy. The difference in thermal conductivity is realised with 8.5% difference in nominal heat transport potential available. If we take into account 8.5% more phonon scattering sites in the form of ash content incorporated in the BR2 samples than in the BP2 samples as well, obtained is total of 17% less phonon paths in BR2 samples. As this difference is not realised, conclusion can be drawn that individual RCNTs are transporting more heat energy than individual PCNTs. At 25 ^{o}C it would be 14.8%, at 75 ^{o}C 11.8% and at 125 ^{o}C 10.4%.

Results for 3 wt% of CNTs are graphically presented in Fig. 5.15.

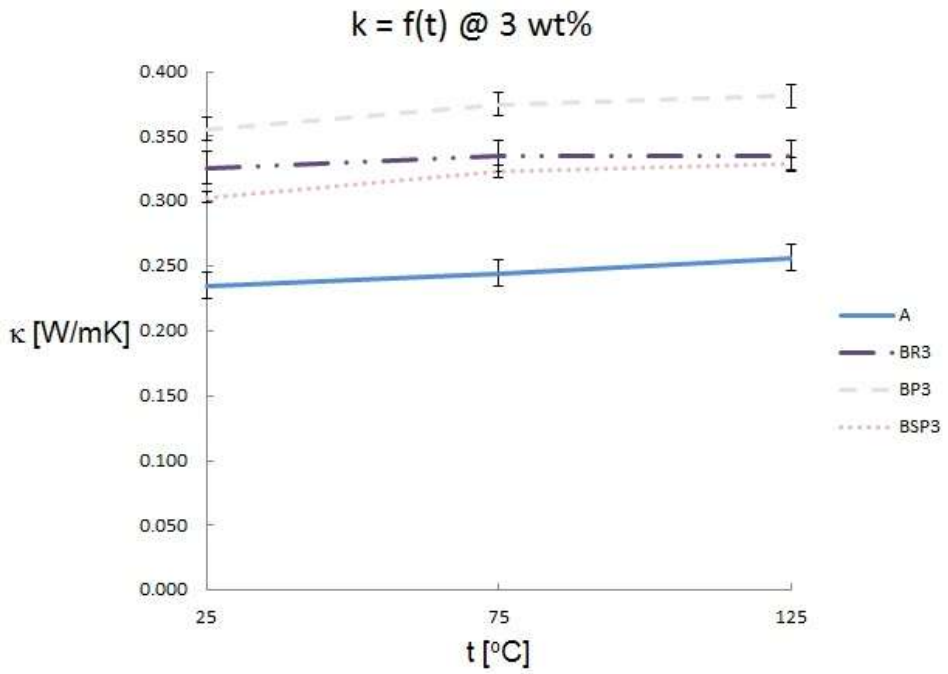

Fig. 5.15: 3 wt% samples thermal conductivity as a function of temperature.

From Fig. 5.15 can be seen that thermal conductivities for BR3 and BSP3 samples are close one to another. BR3 samples exhibit somewhat higher thermal conductivity than BSP3 samples. The difference is higher at 25 ^{o}C, 7.6%, than either at 75 ^{o}C, 3.9% or 125 ^{o}C, 1.7%. At all temperature points it hovers in the vicinity of error margin, being just above at 25 ^{o}C and just within at 125 ^{o}C. However, BP3 samples exhibit thermal conductivity higher than the one obtained with BR3 samples. The difference ranges from 9% at 25 ^{o}C to 14.1% at 125 ^{o}C, larger than the error margin.

Simple calculation completed for previous two loading levels is carried for 3 wt% samples as well. Thermal conductivities being different for samples with R, P and SP CNTs, analysis shall be carried for samples with two different CNT materials at the time.

Consideration shall begin with BR3 and BSP3 samples, made with CNTs containing 16.5% and 4% ash respectively.

At 3 wt% loading, 12.5% less RCNTs than SPCNTs are transporting 7.6% to 1.7% more heat energy at selected verification temperatures. If we take into account as well 12.5% more phonon scattering sites in the form of ash content incorporated in the BR3 samples than in the BSP3 samples, conclusion can be drawn that individual RCNTs are transporting more heat energy than individual SPCNTs. At 25 ^{o}C 32.6%, at 75 ^{o}C 28.9% and at 125 ^{o}C 26.7% more heat energy is transported through a RCNT than through a SPCNT.

Doing the same for BR3 and BP3 samples, the following is obtained. RCNT material has 8.5% less CNTs than PCNT material. It has 8.5% more ash content – phonon scattering sites - as well, giving 17% total of nominal difference in potential phonon paths available. Completing the above simple calculation at each selected verification temperature, conclusion is as follows. At 25 ^{o}C, 8% more heat energy is transported via individual RCNT than via individual PCNT. At 75 ^{o}C this is reduced to 5.2% and at 125 ^{o}C to 2.9%.

5.1.5. Conclusion

Matrix thermal conductivity improvement was evaluated at different temperatures for different load levels and different quality of CNTs added.

Loading level impact on thermal conductivity was evaluated for all three CNT materials added to the matrix. At all selected verification temperatures TC is increased with addition of CNTs. Exception is increase from 1 to 2 wt% of SPCNTs, however, this is considered an anomaly. As expected, more CNTs are creating denser heat transportation network resulting in increased thermal conductivity.

Change of thermal conductivity with temperature was the next variable investigated. Temperature was increased 50 ^{o}C twice. Each temperature increase resulted in lower thermal conductivity increase compared to the previous one. It could be said that thermal conductivity is almost the same at 125 ^{o}C as it is at 75 ^{o}C. This is attributed to phonon-phonon scattering that is increased with the temperature rise.

The following parameter whose impact on thermal conductivity was evaluated was CNT quality. At all loading levels and at all selected verification temperatures individual RCNTs were transporting more heat energy than either individual PCNTs or individual SPCNTs. This is confirmation of hypothesis that CNT quality as defined with respect to thermal conductivity has major impact on thermal conductivity.

5.2. Type D Samples

Type D samples were manufactured from carbon fibre preforms, CNTs and matrix. Samples are differentiated with respect to incorporated carbon nanotube purification level and carbon nanotube weight loading.

5.2.1. DR Samples

Samples DR1, DR2 and DR3 contain 1 wt%, 2 wt% and 3 wt% of raw CNTs respectively.

Obtained thermal conductivity results for type C and DR samples are presented in Table 5.4.

Table 5.4: Thermal conductivity for Type C and DR samples.

		κ [w/mK]			κ - Relative Increase [%]		
T [^{o}C]	25	75	125		25	75	125
Sample							
Type C	0.711±0.179	0.978±0.000	1.127±0.042				
DR1	1.058±0.088	1.179±0.092	1.265±0.120		48.8	20.5	12.2
DR2	1.534±0.097	1.626±0.091	1.746±0.042		115.6	66.2	55.0
DR3	1.710±0.009	1.842±0.010	1.943±0.001		140.4	88.3	72.4

Thermal conductivity varies both with CNTs weight content and temperature.

5.2.1.1. CNTs Loading Level Impact

To evaluate impact of CNTs loading level, defined as wt% of carbon fibre preform with incorporated CNTs weight, thermal conductivity was measured for type C and samples with each of the three different weight loadings: 1, 2 and 3 wt%. Obtained values are compared at each of the three temperature measurement points. Fig. 5.16 depicts results at 25 ^{o}C.

Fig. 5.16 shows that thermal conductivity curve slope is almost constant between type C samples and samples with 1wt% of CNTs and samples with 1 wt% and samples with 2 wt% of CNTs. Relative TC increase for these two loading intervals is nearly the same, 48.8% and 44.9% respectively. Samples with 3 wt% of CNTs have thermal conductivity 11.5% higher than samples with 2 wt% loading. Thermal conductivity increase is in all cases larger than the error margin, confirming improvement in heat transfer network with higher quantity of CNTs.

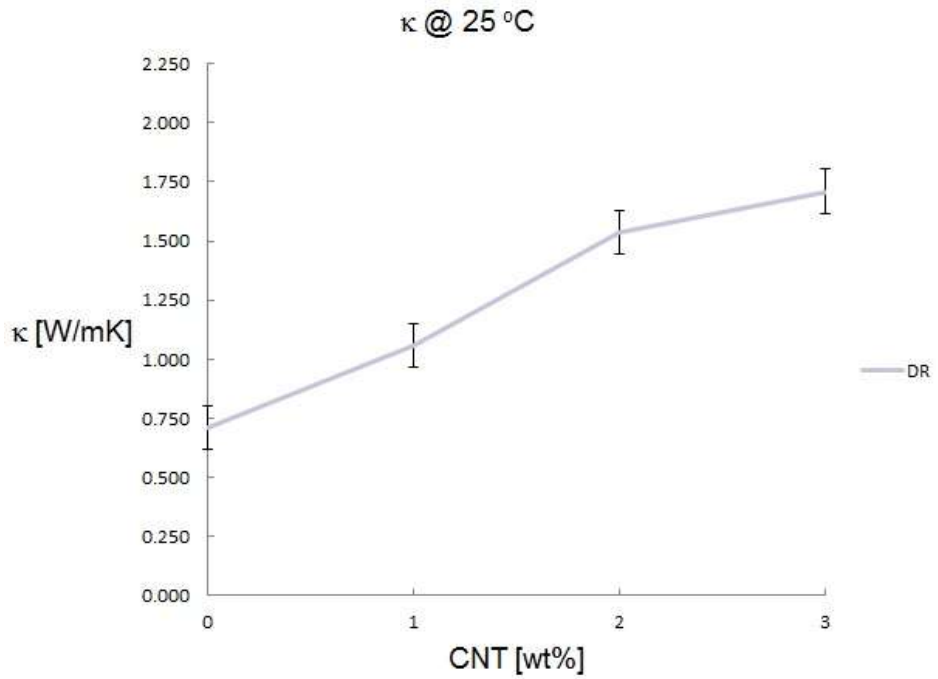

Fig. 5.16: Thermal conductivity at 25 °C plot for C and DR samples as a function of CNT loading.

For measurement point at 75 °C, thermal conductivity curve is presented in Fig. 5.17.

Fig. 5.17 shows that thermal conductivity increase is significant with addition of 1 wt% of CNTs, 20.5%. However, samples with 2wt% of CNTs exhibit 37.9% thermal conductivity increase compared to 1 wt% samples. Thermal conductivity of samples with 3 wt% loading is the highest at 1.842 W/mK with increase of 13.3% compared to 2 wt% samples. Each of the thermal conductivity increases is larger than the error margin, confirming improvement in heat transfer network with higher quantity of CNTs.

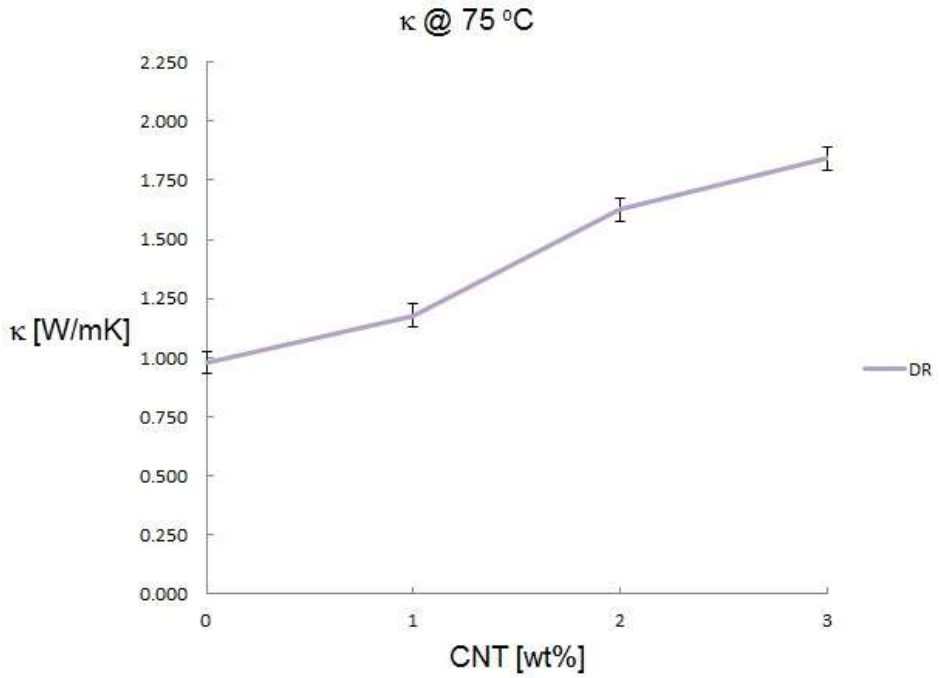

Fig. 5.17: Thermal conductivity at 75 °C plot for C and DR samples as a function of CNT loading.

For measurement point at 125 °C, thermal conductivity curve is presented in Fig. 5.18.

Fig. 5.18 shows thermal conductivity increase with addition of 1 wt% of CNTs, 12.2%. It should be noted that this increase is within the error margin. However, samples with 2 wt% of CNTs exhibit 38.1% thermal conductivity increase compared to 1 wt% samples. Thermal conductivity of samples with 3 wt% loading is the highest at 1.943 W/mK with increase of 11.2% compared to 2 wt% samples. Each of the thermal conductivity increases with 2 and 3 wt% is higher than the error margin, confirming improvement in heat transfer network with higher quantity of CNTs.

From the above presented, a conclusion can be drawn that RCNTs increase thermal conductivity of CFRP when added in quantity of 1 wt% or more. Heat transfer network is readily established with 1 wt% of RCNTs. With higher loading levels, heat transfer network is improved giving higher thermal conductivity levels. It should be noted that TC

rise is substantial for all loading levels verified at each temperature point. The TC increase is very significant, reaching 140.4% at 25 ^{o}C with 3 wt% of CNTs added. The highest thermal conductivity level was obtained with 3 wt% loading at 125 ^{o}C, 1.943 W/mK. Per obtained data, thermal conductivity can be expected to increase further with increased RCNT content. With increased CNT quantity, number of heat transportation channels would be increased and thermal conductivity would rise, being a function of number of heat transportation channels.

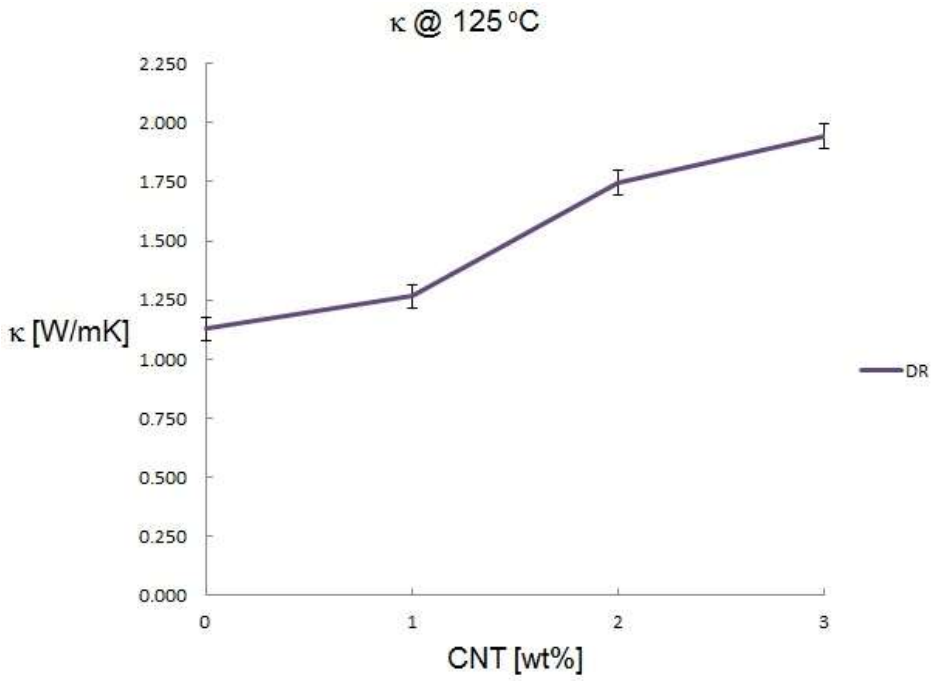

Fig. 5.18: Thermal conductivity at 125 ^{o}C plot for C and DR samples as a function of CNT loading.

5.2.1.2. Temperature Impact

To evaluate impact of temperature on thermal conductivity, thermal conductivity was measured at three different points: 25, 75 and 125 ^{o}C for type C and DR1, DR2 and DR3 samples. Thermal conductivity plot as a function of temperature in Fig. 5.19 depicts results graphically.

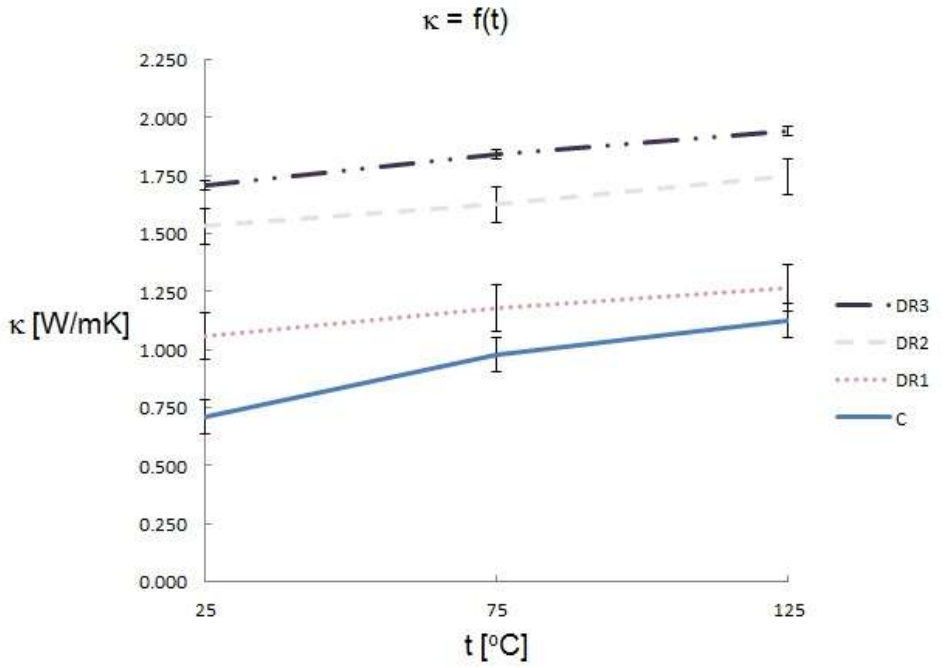

Fig. 5.19: Thermal conductivity of C and DR samples as a function of temperature.

While 1 and 3 wt% samples thermal conductivity exhibits similar behaviour with temperature change for each loading level, type C and DR2 samples thermal conductivity change with temperature increase is somewhat different.

Type C samples have more than twice as high TC increase with temperature rise from 25 to 75 ^{o}C than with the rise from 75 to 125 ^{o}C, 37.5% and 15.2% respectively. DR1 and DR3 samples have similar TC increase trend with temperature rise from 25 to 75 ^{o}C and from 75 to 125 ^{o}C, the former being larger than the latter. In contrast to type C samples, this increase is more modest and the difference lower between two consecutive temperature points. For these two intervals TC increases are 11.4% and 7.3% and 7.7% and 5.5% for DR1 and DR3 samples respectively. DR2 samples thermal conductivity is the only one that exhibits higher increase with temperature rise from 75 to 125 ^{o}C than with temperature rise from 25 to 75 ^{o}C, 7.4% and 6.0% respectively. However, the DR2 TC increase is the only one of the investigated TC for four groups of samples that is

within the error margin. Hence, this change in TC increase trend should be taken with reserve.

Thermal conductivity increase with temperature could be observed for all samples, with or without CNTs. However, the TC increase in samples without CNTs is higher than in samples with CNTs. It could be concluded that CNTs heat transportation network adversely affects thermal conductivity with temperature increase. Difference between type C and DR samples is due to modified material properties with CNT incorporation. Smaller DR samples TC increase with temperature rise is attributed to phonon-phonon scattering in CNTs.

5.2.2. DP Samples

Samples DP1, DP2 and DP3 contain 1 wt%, 2 wt% and 3 wt% of purified CNTs respectively.

Obtained thermal conductivity results for type C and DR samples are presented in Table 5.5.

Table 5.5: Thermal conductivity for Type C and DP samples.

		κ [w/mK]			κ - Relative Increase [%]		
T [^{o}C]	25	75	125		25	75	125
Sample							
Type C	0.711±0.179	0.978±0.000	1.127±0.042				
DP1	1.335±0.033	1.472±0.050	1.621±0.074		87.6	50.4	43.8
DP2	1.095±0.225	1.215±0.204	1.361±0.140		54.0	24.2	20.8
DP3	0.978±0.149	1.134±0.112	1.289±0.111		37.4	15.9	14.3

Thermal conductivity varies both with CNTs weight content and temperature.

5.2.2.1. CNTs Loading Level Impact

To evaluate impact of CNTs loading level, defined as wt% of carbon fibre preform with incorporated CNTs weight, thermal conductivity was measured for type C and samples with each of the three different weight loadings: 1, 2 and 3 wt%. Obtained values are compared at each of the three temperature measurement points. Fig. 5.20 depicts results at 25 ^{o}C.

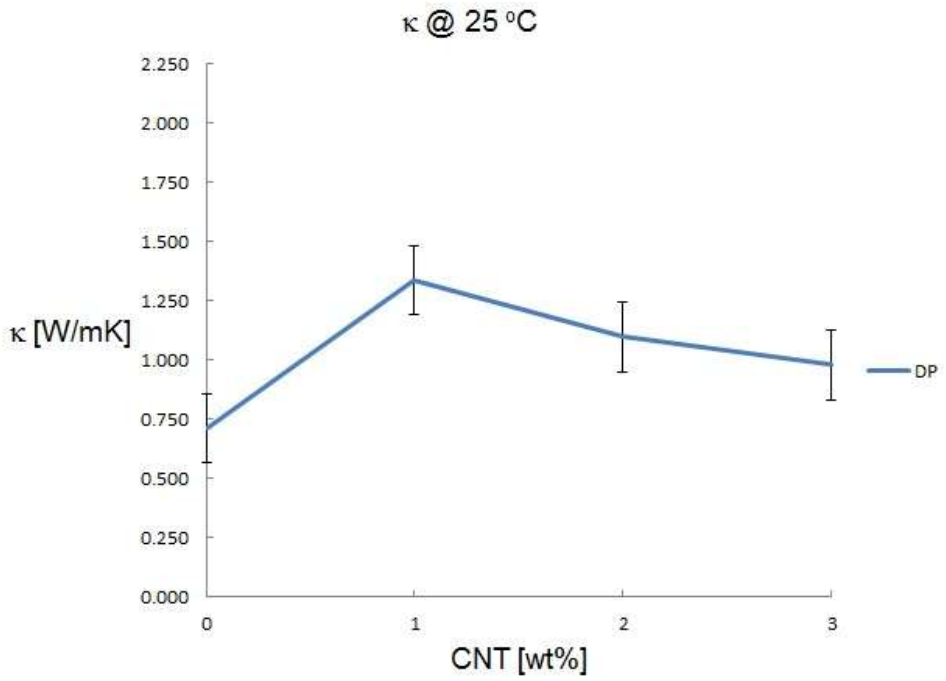

Fig. 5.20: Thermal conductivity at 25 ^{o}C plot for C and DP samples as a function of CNT loading.

Fig. 5.20 shows that thermal conductivity increase is 87.6% for samples with 1 wt% of PCNTs. This is the highest TC increase achieved with PCNTs. It is larger than the error margin and could be considered substantial. 2 wt% samples have 17.9% lower TC than DP1 samples, while DP3 samples TC is 10.7% lower than DP2 samples TC. Thermal conductivity decrease is in both cases smaller than the error margin.

For measurement point at 75 ^{o}C, thermal conductivity curve is presented in Fig. 5.21.

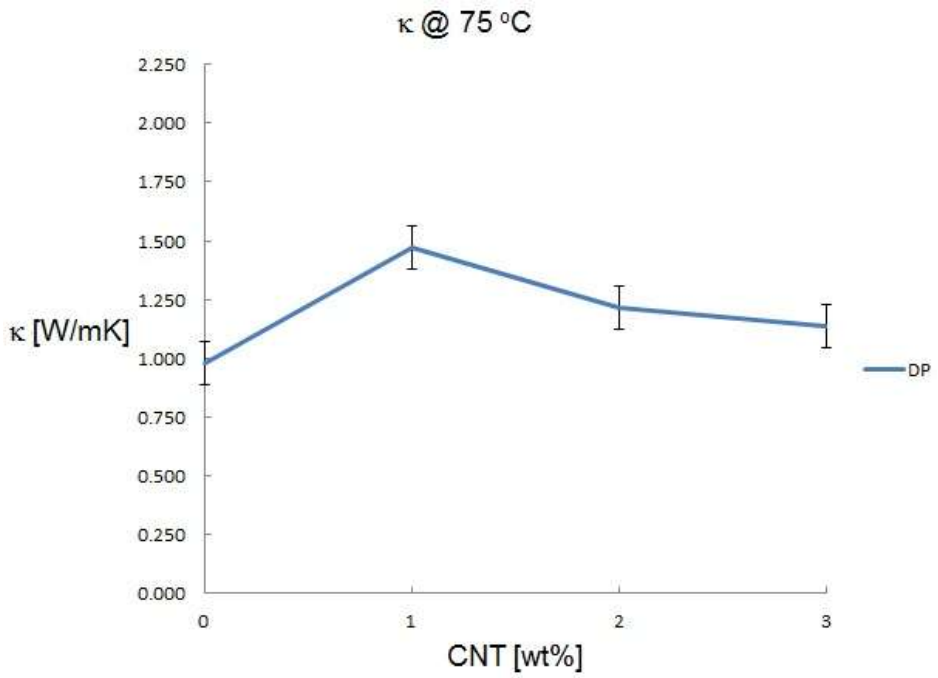

Fig. 5.21: Thermal conductivity at 75 °C plot for C and DP samples as a function of CNT loading.

Fig. 5.21 shows that thermal conductivity increase is significant with addition of 1 wt% of CNTs, 50.4%. Samples with 2 wt% of CNTs exhibited 17.5% thermal conductivity decrease compared to 1 wt% samples. Both of these changes are larger than the error margin. Thermal conductivity of samples with 3 wt% loading is 6.7% lower than the DP2 samples TC, decrease smaller than the error margin.

For measurement point at 125 °C, thermal conductivity curve is presented in Fig. 5.22.

Fig. 5.22 shows thermal conductivity increase with addition of 1 wt% of CNTs, 43.8%. DP1 sample TC at 125 °C is the highest at 1.621 W/mK. Samples with 2 wt% of CNTs exhibited 16.0% thermal conductivity decrease compared to 1 wt% samples. Both of these two changes are larger than the error margin. Thermal conductivity of samples with 3 wt% loading is 5.3% lower compared to 2 wt% samples. This change is smaller than the error margin.

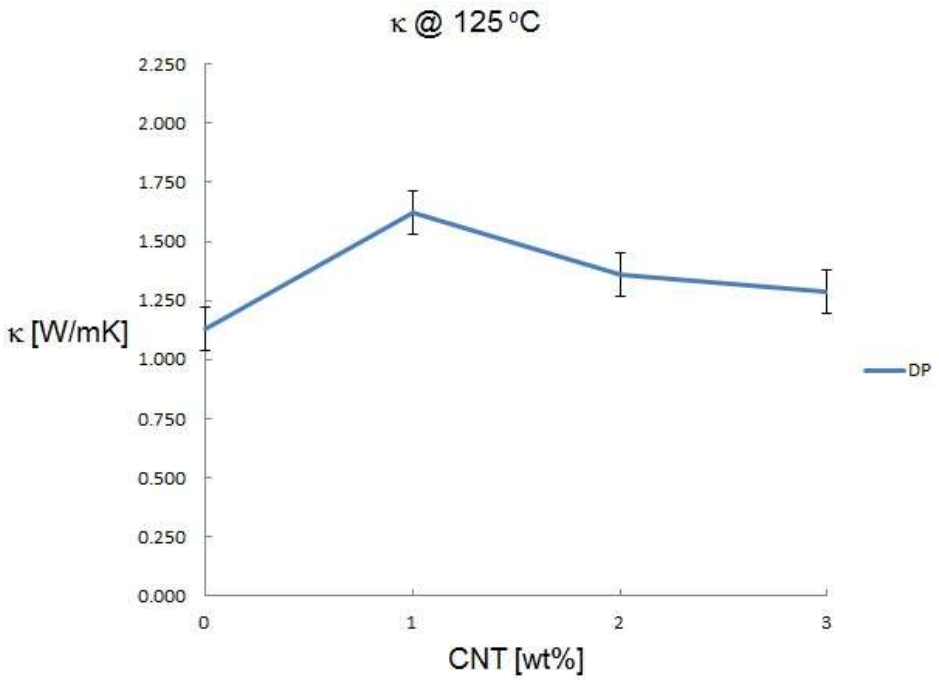

Fig. 5.22: Thermal conductivity at 125 °C plot for C and DP samples as a function of CNT loading.

From the above presented, a conclusion can be drawn that PCNTs increase thermal conductivity of CFRP when added in quantity of 1 wt% or more. Heat transfer network is readily established with 1 wt% of PCNTs. At all selected verification temperatures DP1 samples thermal conductivity is the highest one, reaching the highest value of 1.621 W/mK at 125 °C. Further loading increase is reducing thermal conductivity, equally applicable throughout investigated temperature range. Heat transfer network degradation is attributed to strong intertube coupling.

5.2.2.2. Temperature Impact

To evaluate impact of temperature on thermal conductivity, thermal conductivity was measured at three different points: 25, 75 and 125 °C for type C and DP1, DP2 and DP3

samples. Thermal conductivity plot as a function of temperature in Fig. 5.23 depicts results graphically.

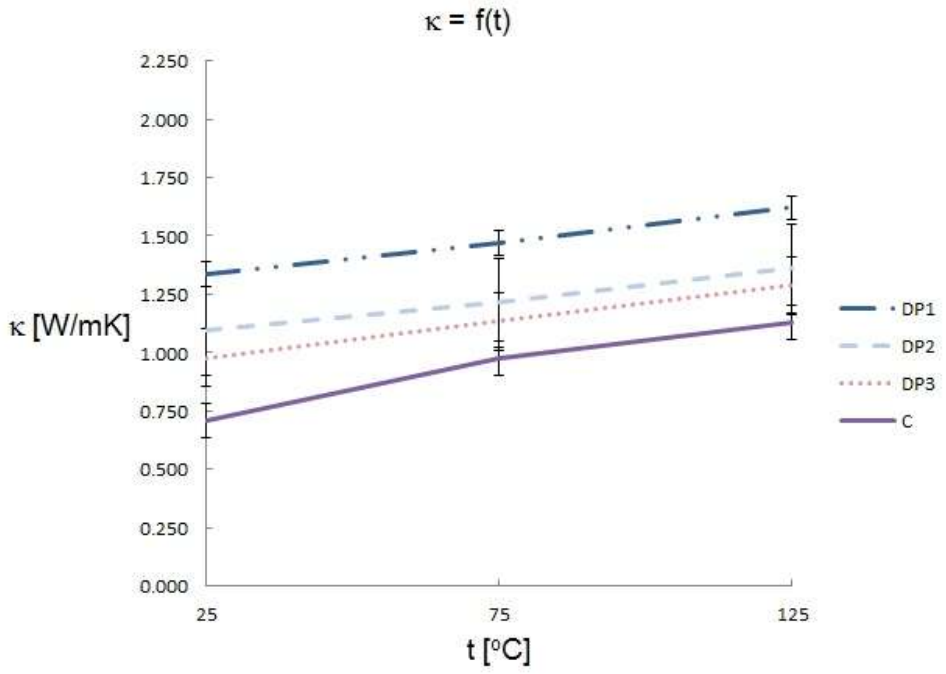

Fig. 5.23: Thermal conductivity of C and DP samples as a function of temperature.

While PCNT loaded samples thermal conductivity exhibits similar behaviour with temperature change for each loading level, type C samples thermal conductivity change with temperature increase is somewhat different, as described in section 5.2.1.2.

DP samples have similar TC increase with temperature rise from 25 to 75 ^{o}C and from 75 to 125 ^{o}C, the difference being no more than 2% between these two intervals TC changes. For 1 and 2 wt% samples TC increase with each of the temperature increments is 10%-12% while it stands at 13.7%-16.0% for DP3 samples.

DP1 samples TC change with temperature is larger than the error margin. DP2 and DP3 samples TC change with temperature is lower than the error margin. However, the trend

is the same for all three loading levels and hence the TC change with temperature is considered real. In addition to that, it follows expectations of increase with temperature.

Thermal conductivity increase with temperature could be observed for all samples, with or without CNTs. However, the TC increase in samples without CNTs is higher than in samples with CNTs with the temperature increase from 25 to 75 ^{o}C and almost the same with temperature increase from 75 to 125 ^{o}C. It could be concluded that CNTs heat transportation network adversely affects thermal conductivity with temperature increase. Difference between type C and DP samples is due to modified material properties with CNT incorporation. Smaller DP samples TC increase with temperature rise is attributed to phonon-phonon scattering in CNTs.

5.2.3. DSP Samples

Samples DSP1, DSP2 and DSP3 contain 1 wt%, 2 wt% and 3 wt% of super purified CNTs respectively.

Obtained thermal conductivity results for type C and DSP samples are presented in table 5.6.

Table 5.6: Thermal conductivity for Type C and DSP samples.

		κ [w/mK]			κ - Relative Increase [%]		
T [^{o}C]	25	75	125		25	75	125
Sample							
Type C	0.711±0.179	0.978±0.000	1.127±0.042				
DSP1	1.148±0.068	1.288±0.091	1.421±0.066		61.4	31.7	26.1
DSP2	0.980±0.087	1.092±0.071	1.185±0.085		37.7	11.6	5.1
DSP3	0.890±0.108	1.017±0.103	1.108±0.109		25.0	4.0	-1.7

Thermal conductivity varies both with CNTs weight content and temperature.

5.2.3.1. CNTs Loading Level Impact

To evaluate impact of CNTs loading level, defined as wt% of carbon fibre preform with incorporated CNTs weight, thermal conductivity was measured for type C and samples with each of the three different weight loadings: 1, 2 and 3 wt%. Obtained values are compared at each of the three temperature measurement points. Fig. 5.24 depicts results at 25 ^{o}C.

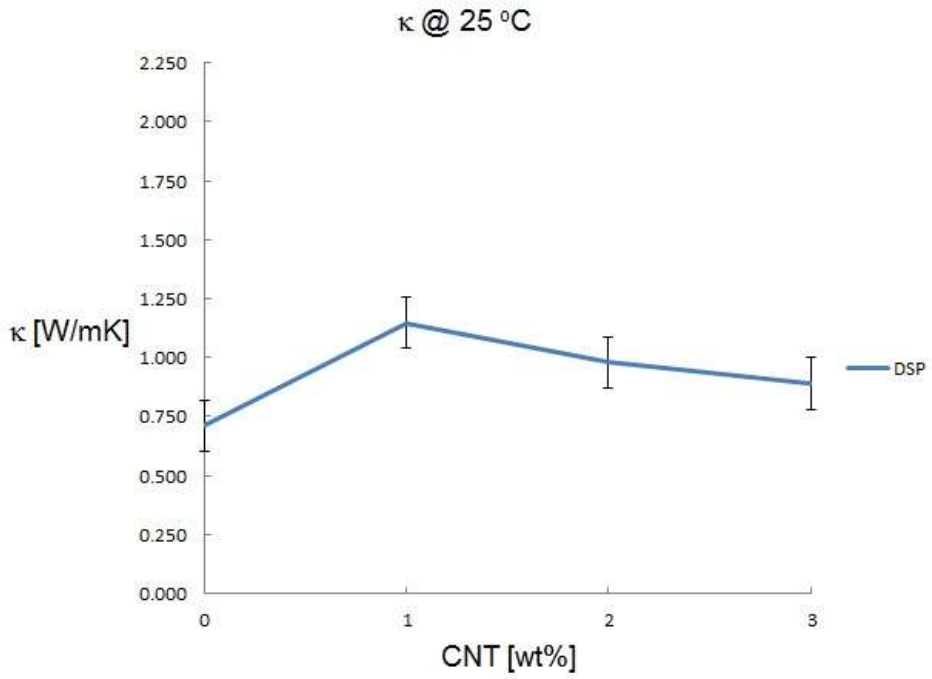

Fig. 5.24: Thermal conductivity at 25 ^{o}C plot for C and DSP samples as a function of CNT loading.

Fig. 5.24 shows that thermal conductivity increase is 61.4% for samples with 1 wt% of SPCNTs. This is the highest TC increase achieved with SPCNTs. It is larger than the error margin and could be considered substantial. 2 wt% samples have 14.7% lower TC than DSP1 samples, while DSP3 samples TC is 9.2% lower than DSP2 samples TC. Thermal conductivity decrease is larger than the error margin in the former and smaller than the error margin in the latter case.

For measurement point at 75 ^{o}C, thermal conductivity curve is presented in Fig. 5.25.

Fig. 5.25 shows that thermal conductivity increase is significant with addition of 1 wt% of CNTs, 31.7%. Samples with 2 wt% of CNTs exhibited 15.2% thermal conductivity decrease compared to 1 wt% samples. Both of these changes are larger than the error margin. Thermal conductivity of samples with 3 wt% loading is 6.8% lower than the DSP2 samples TC, decrease smaller than the error margin.

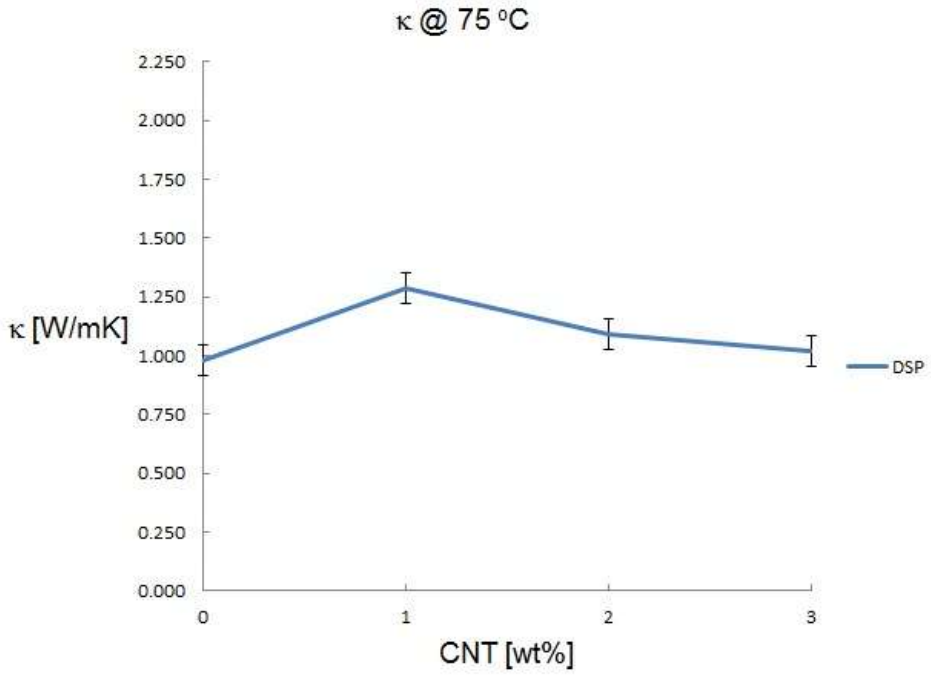

Fig. 5.25: Thermal conductivity at 75 ^{o}C plot for C and DSP samples as a function of CNT loading.

For measurement point at 125 ^{o}C, thermal conductivity curve is presented in Fig. 5.26.

Fig. 5.26 shows thermal conductivity increase with addition of 1 wt% of CNTs, 26.1%. DSP1 sample TC at 125 ^{o}C is the highest at 1.421 W/mK. Samples with 2 wt% of CNTs exhibited 16.6% thermal conductivity decrease compared to 1 wt% samples. Both of these two changes are larger than the error margin. Thermal conductivity of samples with

3 wt% loading is 6.5% lower compared to 2 wt% samples. This change is smaller than the error margin.

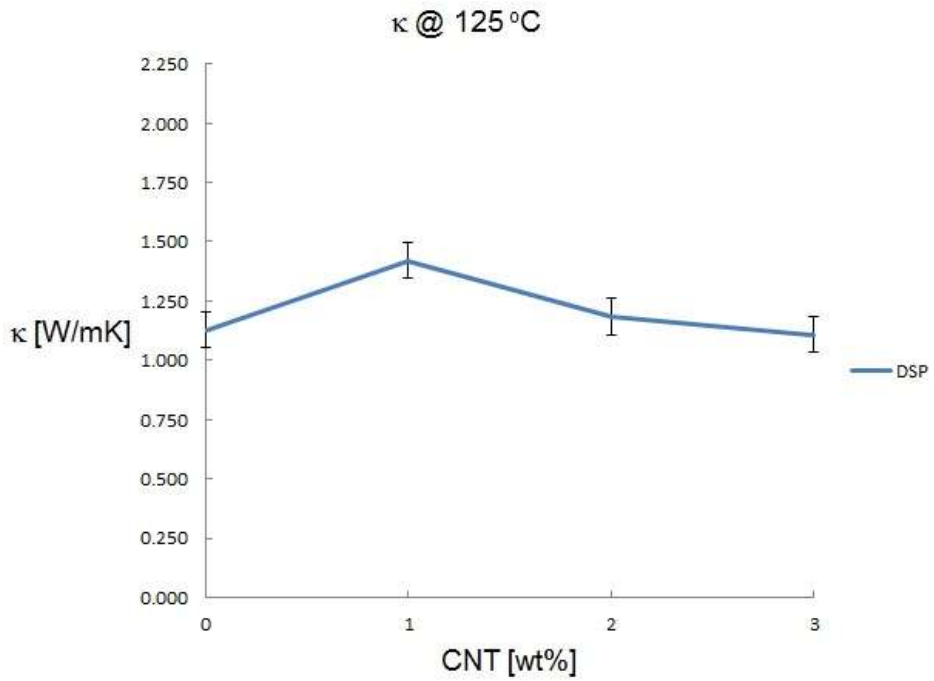

Fig. 5.26: Thermal conductivity at 125 °C plot for C and DSP samples as a function of CNT loading.

From the above presented, a conclusion can be drawn that SPCNTs increase thermal conductivity of CFRP when added in quantity of 1 wt% or more. Heat transfer network is readily established with 1 wt% of SPCNTs. At all selected verification temperatures DSP1 samples thermal conductivity is the highest one, reaching the highest value of 1.421 W/mK at 125 °C. Further loading increase is reducing thermal conductivity, equally applicable throughout investigated temperature range. Heat transfer network degradation is attributed to strong intertube coupling.

5.2.3.2. Temperature Impact

To evaluate impact of temperature on thermal conductivity, thermal conductivity was measured at three different points: 25, 75 and 125 °C for type C and DSP1, DSP2 and

DSP3 samples. Thermal conductivity plot as a function of temperature in Fig. 5.27 depicts results graphically.

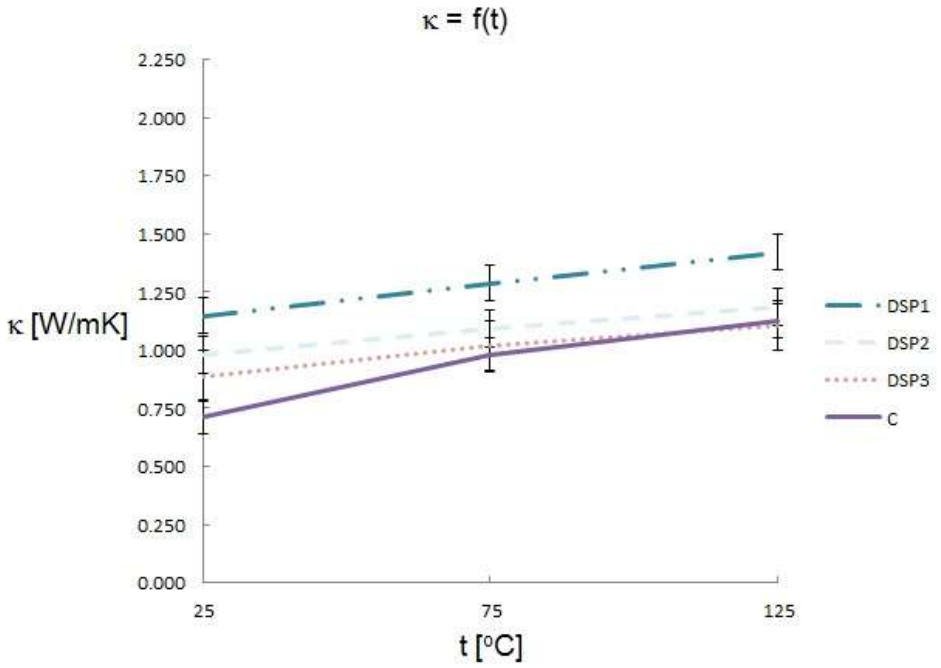

Fig. 5.27: Thermal conductivity of C and DP samples as a function of temperature.

While SPCNT loaded samples thermal conductivity exhibits similar behaviour with temperature change for each loading level, type C samples thermal conductivity change with temperature increase is somewhat different, as described in section 5.2.1.2.

DSP samples have similar TC increase with temperature rise from 25 to 75 ^{o}C and from 75 to 125 ^{o}C, the change being 2% to 5.5% higher for the former than the latter of the two temperature intervals. The TC increase is between 8.5% and 14.3%. Each increase is within the error margin. However, the trend is the same for all three loading level samples and hence the TC change with temperature is considered real. It follows expectations of increase with temperature as well.

Thermal conductivity increase with temperature could be observed for all samples, with or without CNTs. However, the TC increase in samples without CNTs is higher than in samples with CNTs. It could be concluded that CNTs heat transportation network adversely affects thermal conductivity with temperature increase. Difference between type C and DSP samples is due to modified material properties with CNT incorporation. Smaller DSP samples TC increase with temperature rise is attributed to phonon-phonon scattering in CNTs.

Lower thermal conductivity in DSP3 samples than in C samples at 125 ^{o}C should be noted. This is attributed to combination of strong intertube coupling and phonon-phonon scattering.

5.2.4. CNTs Quality Impact

To evaluate CNTs quality impact on thermal conductivity, thermal conductivities of samples made with the same weight loading of different quality CNTs were compared across investigated temperature range.

Results for 1 wt% samples are graphically presented in Fig. 5.28.

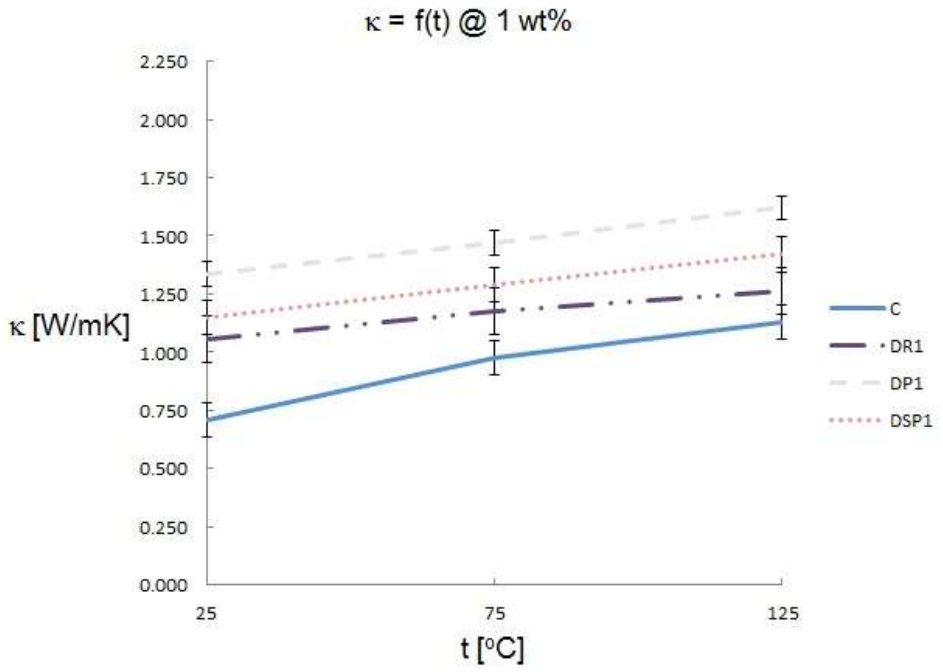

Fig. 5.28: 1 wt% samples thermal conductivity as a function of temperature.

From Fig. 5.28 can be seen that thermal conductivity for samples made with 1 wt% of PCNTs is higher than the TC for samples made with other two CNT materials. At 25 ^{o}C DP1 TC is 26.1% and 16.2% higher than DR1 and DSP1 TC respectively. At 75 ^{o}C these differences are 24.8% and 14.3%. At 125 ^{o}C the differences are 28.1% and 14.1% respectively. All differences are higher than the error margin.

With low load level of 1 wt% PCNTs established the most efficient heat transfer network, giving the highest thermal conductivity levels at all temperature test points. The highest number of the lowest quality SPCNTs established less efficient heat transport network. The number of higher quality RCNTs was insufficient to establish network equally efficient as the other two CNT materials. It should be noted that difference between DR1 and DP1 thermal conductivities is lower than the error margin. Thermal conductivity behaviour is similar to B type samples with CNTs well distributed throughout the matrix.

Results for 2 wt% of CNTs are graphically presented in Fig. 5.29.

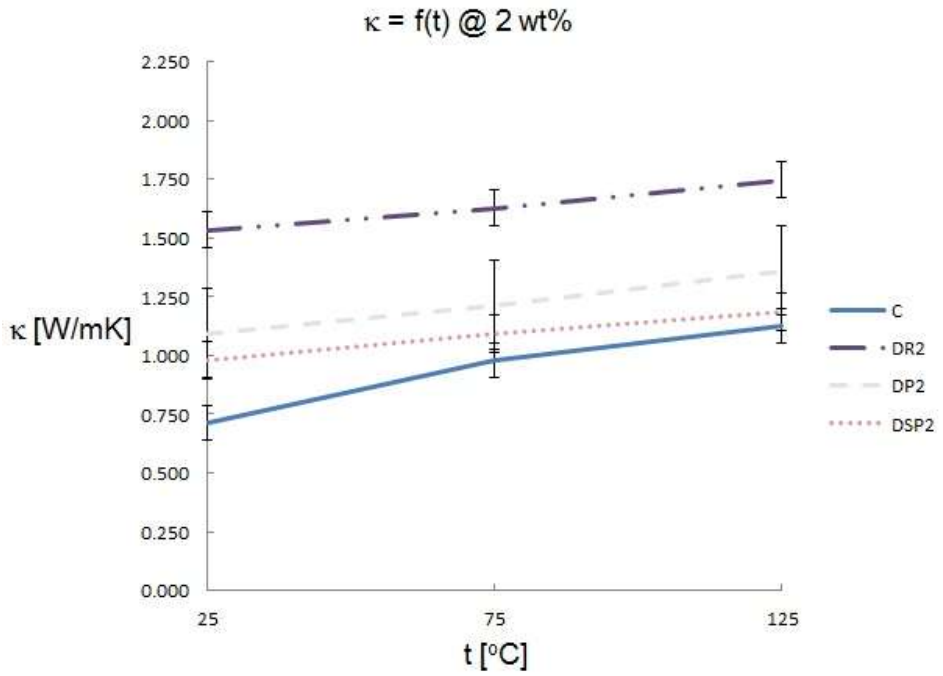

Fig. 5.29: 2 wt% samples thermal conductivity as a function of temperature.

From Fig. 5.29 can be seen that thermal conductivities of samples made with 2 wt% of RCNTs are significantly higher than thermal conductivities of samples made with either PCNTs or SPCNTs. The difference is more pronounced at 25 ^{o}C (40%-56%) than at other two testing temperature points. Sufficient quantity of better quality CNTs is making substantially more efficient heat transport network. The lowest thermal conductivity was achieved with the lowest quality SPCNTs.

Results for 3 wt% of CNTs are graphically presented in Fig. 5.30.

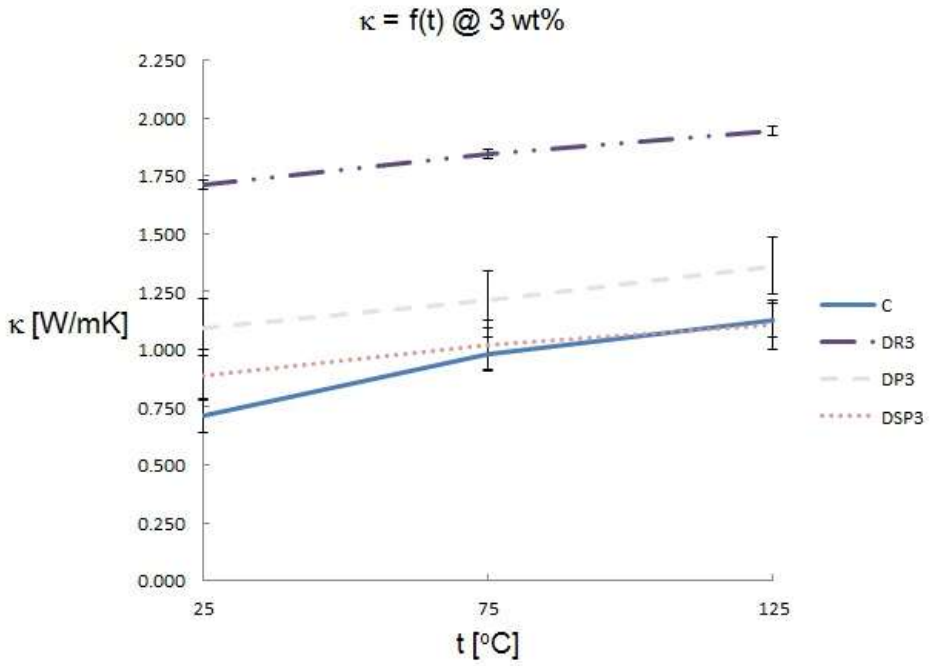

Fig. 5.30: 3 wt% samples thermal conductivity as a function of temperature.

From Fig. 5.30 can be seen that thermal conductivities of samples made with 3 wt% of RCNTs are significantly higher than thermal conductivities of samples made with either PCNTs or SPCNTs. The difference is more pronounced at 25 ^{o}C (75%-92%) than at other two testing temperature points. The difference at 125 ^{o}C is 51% and 75% with respect to DP3 and DSP3 samples respectively. With increased number of better quality CNTs heat transport network is even more efficient than with 2 wt% of RCNTs. The difference can be considered very significant.

Another step to assess CNT quality impact on thermal conductivity is the comparison of highest thermal conductivities achieved with addition of different CNT materials to the matrix. Maximum thermal conductivity values achieved with different CNT materials are graphically presented in Fig. 5.31 as a function of temperature. The highest thermal conductivity of all samples is obtained with 3 wt% of RCNTs loading.

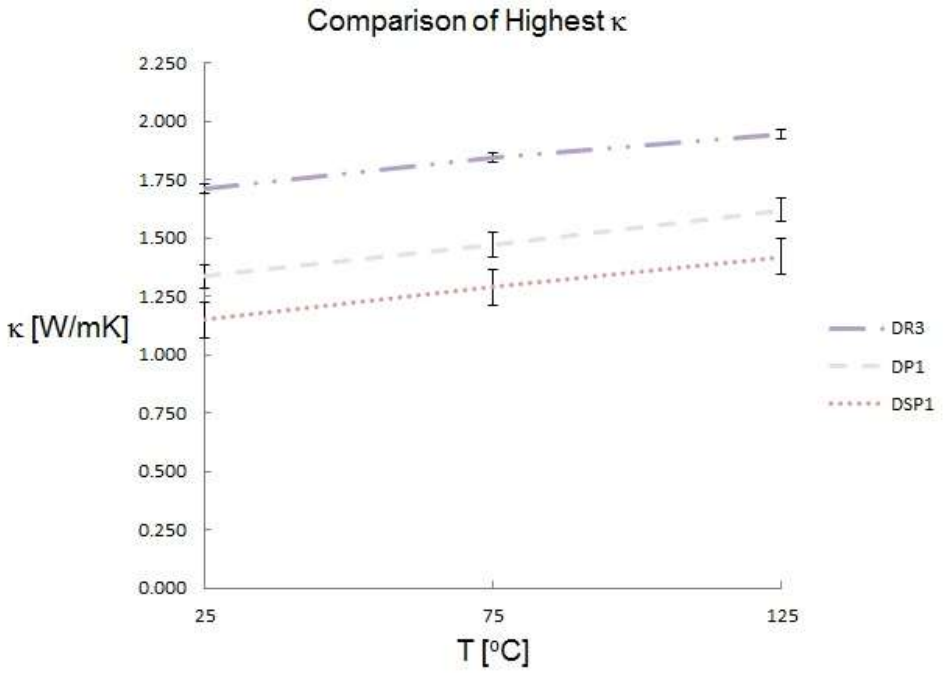

Fig. 5.31: Comparison of highest thermal conductivities obtained with different CNTs materials.

At 3 wt%, RCNTs were best suited to create high number of heat transportation channels, thus yielding the highest thermal conductivity of tested samples. Improvement over thermal conductivity of samples made without CNTs is 140.4% at 25 ^{o}C, the highest overall relative increase. The highest value of thermal conductivity was obtained at 125 ^{o}C, 1.943 W/mK, a 72.4% increase compared to type C samples.

Compared to DP1 sample the difference in thermal conductivity achieved with DR3 sample is ranging from 28.1% at 25 ^{o}C to 19.9% at 125 ^{o}C. DR3 thermal conductivity is 48.9% to 36.7% higher than DSP1 TC from 25 ^{o}C to 125 ^{o}C.

SEM picture (Fig 5.32) shows good CNTs dispersion in CFRP nanocomposites. Bright pixels are carbon nanotubes on the surface and outside of the matrix, carbon nanotubes within the matrix are lighter shade of gray.

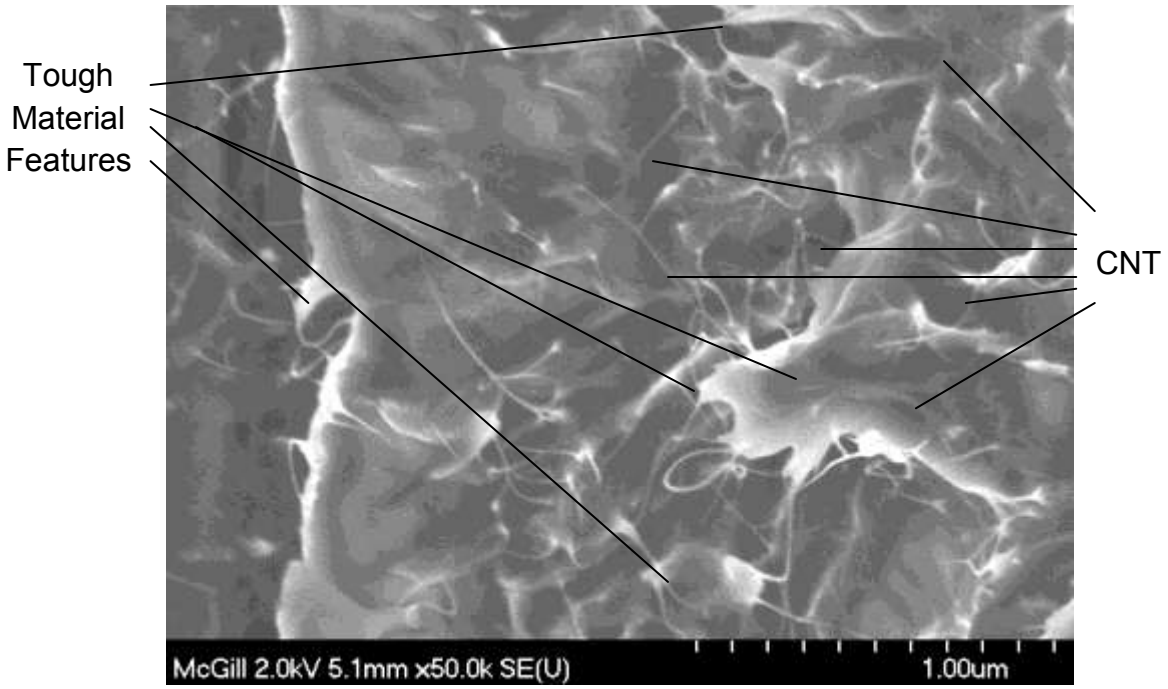

Fig. 5.32: Good distribution of CNTs in the CFRP nanocomposites. Surface is featuring tough material characteristics.

Surface in the Fig. 5.32 is uneven, a feature of a tough material surface. Epoxy matrix is known for its brittleness. Hence, it could be concluded that carbon nanotubes increased material toughness as well.

5.2.5. Conclusion

CFRP thermal conductivity improvement was evaluated at different temperatures for different load levels and different quality of CNTs added.

Loading level impact on thermal conductivity was evaluated for all three CNT materials added to the matrix. Thermal conductivity change with increased loading level is different for samples made with RCNTs and either PCNTs or SPCNTs. Increasing RCNT quantity above 1 wt% is increasing TC while the same loading levels of either PCNTs or SPCNTs reduce TC. This is equally applicable at all selected verification temperatures.

The observed difference is attributed to difference in intertube coupling which is weak between raw CNTs and strong between both purified and super purified CNTs.

Change of thermal conductivity with temperature was the next variable investigated. Temperature was increased 50 ^{o}C twice. The general trend is higher TC increase with the temperature increase from 25 ^{o}C to 75 ^{o}C than with temperature increase from 75 ^{o}C to 125 ^{o}C. This is attributed to phonon-phonon scattering that is increased with the temperature rise. Thermal conductivity increase with temperature could be observed for all samples, with or without CNTs. However, the TC increase in samples without CNTs is higher than in samples with CNTs with the temperature increase from 25 to 75 ^{o}C and almost the same with temperature increase from 75 to 125 ^{o}C. It could be concluded that CNTs heat transportation network adversely affects thermal conductivity with temperature increase. The adversity is attributed to phonon-phonon scattering in CNTs. With temperature increase, phonon-phonon scattering is more affecting thermal transport. Difference between type C and D samples is due to modified material properties with CNT incorporation. In type D samples phonon-phonon scattering is taking place at lower temperatures due to incorporated CNTs.

The following parameter whose impact on thermal conductivity was evaluated was CNT quality. Adding 3 wt% of RCNTs yielded the highest thermal conductivity improvement in this configuration. Improvement over thermal conductivity of samples made without CNTs is 140.4% at 25 ^{o}C, the highest overall relative increase. The highest value of thermal conductivity was obtained at 125 ^{o}C, 1.943 W/mK, a 72.4% increase compared to type C samples.

With low load level of 1 wt%, PCNTs established the most efficient heat transfer network giving the highest thermal conductivity levels at all temperature test points. The number of higher quality RCNTs was insufficient to establish equally efficient network.

At higher loading levels, the filler content quality came into effect. The most efficient heat transfer network was established with RCNTs. Due to low number of defect sites on CNTs walls, weak intertube coupling facilitated phonon propagation. Thermal conductivity of samples with CNTs with higher number of defect sites was reduced by strong intertube coupling. This is equally applicable to DP and DSP samples. This is another confirmation of hypothesis that CNT quality as defined with respect to thermal conductivity has major impact on thermal conductivity.

5.3. Conclusion

Thermal conductivity of epoxy composites was tested. Testing was completed at three different temperatures: 25 ^{o}C, 75 ^{o}C and 125 ^{o}C. Three different CNT materials were added to both epoxy matrix and epoxy based CFRP in 1 wt% increments, from 1 to 3 wt%. Adding carbon nanotubes to either pristine matrix or CFRP increases composites thermal conductivity.

Pristine matrix thermal conductivity is increased 53.4% at 75 ^{o}C, to reach value of 0.375 W/mK with 3 wt% of purified carbon nanotubes. The highest thermal conductivity in this configuration was achieved with BP3 samples at 125 ^{o}C, 0.382 W/mK.

Addition of 3 wt% of raw carbon nanotubes to carbon fibre preform increases composite thermal conductivity 140.4% to 1.710 W/mK at 25 ^{o}C. The highest thermal conductivity value of 1.943 W/mK is achieved at 125 ^{o}C for the DR3 sample. Compared to the state of

the art [51], obtained thermal conductivity value is lower. However, it should be noted that materials used to produce composite material in the course of these two studies were different, both carbon fibres and epoxy matrix. Hence the difference in reference material thermal conductivity, 0.711 W/mK at 25 ^{o}C for the material used in this research vs. 1.82 W/mK obtained for the material used in [51]. On the other side, thermal conductivity relative increase obtained in this study is by far exceeding ~44% obtained in [51].

A difference in thermal conductivity behaviour with temperature increase, different carbon nanotube weight loading and quality is observed between M+CNT and CF+CNT+M composites. Overall filler content is lower in M+CNT composites and individual CNTs are equally distributed throughout the liquid matrix, thus creating heat transfer network over the larger volume of material. Hence, at low to moderate loading level of 1-3 wt%, well distributed CNTs are not creating many intertube coupling sites. Phonons are transported through the network of individual carbon nanotubes. Therefore, strong intertube coupling that is taking place with lower quality CNTs does not have much effect on thermal conductivity. Hence, PCNTs with low ash content and moderately damaged side walls exhibited steady increase in thermal conductivity with content increase and provided the highest value of samples made with matrix and CNTs. Nonetheless, simple calculation employed to evaluate thermal conductivity differences with respect to CNT quality confirmed that highest quantity of heat energy is transported via the least imperfect – individual raw CNTs.

However, when CNTs are added to CF preforms, they fill much smaller space between solid CFs. Initially, individual CNTs are attached to CFs. The next phase is attachment of CNTs one to another thus forming CNT bridges between fibres. The number of bridges

being formed is function of CNT loading. At low loading levels it means that determining factor for thermal conductivity improvement is the actual number of CNTs available to form heat transfer network. Hence, at 1 wt% the highest improvement was achieved with moderately damaged PCNTs which were slightly lower in numbers than more damaged SPCNTs. Higher quality RCNT were in insufficient numbers to form equally efficient heat transfer network. However, with the weight loading increase, CNTs began to attach one to another in higher numbers and more bridges were being formed. At the attachment points, intertube coupling takes place. With increased number of attachment points intertube coupling effect is more pronounced. In the case of higher quality RCNTs, this coupling is weak, promoting heat transfer. However, in the case of PCNTs and SPCNTs with many defect sites, this coupling is strong, thus reducing thermal conductivity.

Thermal conductivity obtained with RCNTs, PCNTs and SPCNTs added to pristine matrix as well as the carbon fibre preform composites strongly supports hypothesis that carbon nanotube quality plays major role in epoxy composites thermal conductivity improvement.

Uneven surface observed in SEM pictures is pointing to improved toughness of the material with carbon nanotubes. Usually limp carbon fibres were stiff in photograph 3.6 b), indicating increased stiffness of new material.

Chapter 6

6. Conclusion, Contributions and Future Work

6.1. Conclusion

Epoxy composites thermal conductivity behavior with the addition of SWNTs was the object of this study. Single wall carbon nanotubes were incorporated in pristine matrix and carbon fibre reinforced epoxy. Carbon nanotubes, raw, purified and super purified, with different level of ash content were purchased from the same supplier. Up to 3 wt% of carbon nanotubes were added to the base material. Three roll mill was used to disperse carbon nanotubes in the pristine matrix. Ultrasound was employed to incorporate carbon nanotubes into the carbon fibre preform thus creating novel material. The novel material exhibits increased stiffness. This novel material was subsequently impregnated by matrix. Carbon nanotubes were attached to carbon fibres and henceforth one to another, as observed in SEM images. Nanocomposite material fracture surface is uneven, a feature of a tough material.

Thermal conductivity was obtained by multiplying three measured properties: density, specific heat capacity and thermal diffusivity. Thermal diffusivity was measured by flash method and specific heat capacity was measured using DSC. Density was calculated from measured mass and volume of a coupon. Obtained values indicate that more than one parameter affects thermal conductivity. Carbon nanotube weight content, testing temperature and carbon nanotube quality level of impact were evaluated in this study. An effort was made to look into these parameters separately, however, they appear to be

coupled, not only one to another but to other parameters as well. One of these parameters is ash content and another one is the composite composition.

Thermal conductivity in nanocomposites made with matrix is affected in a different manner than in nanocomposites containing carbon fibre as well when different quantities of carbon nanotubes of different quality are added.

The difference is not very pronounced with testing temperature increase. CNTs added to both matrix only and carbon fibre reinforced matrix composites are adversely affecting thermal conductivity with temperature increase due to phonon-phonon scattering.

Matrix thermal conductivity increased with CNT content increase. The greatest increase was obtained with material made from matrix and 3 wt% of purified carbon nanotubes. The carbon nanotube quality importance for heat transfer was confirmed via simple calculation which confirmed that individual RCNTs transport more heat energy at each loading level throughout investigated temperature range than either PCNTs or SPCNTs.

Different composite composition with carbon fibres as a base material provided for different mechanism to form heat transfer network. Hence obtained network occupies smaller space between carbon fibres and forms greater number of intertube coupling sites. Coupling between lower quality carbon nanotubes is strong, adversely affecting heat transfer with increased loading of carbon nanotubes. Coupling between higher quality raw carbon nanotubes is weak, giving increased thermal conductivity at higher loading levels. The highest thermal conductivity value of 1.943 W/mK was obtained with 3 wt% loading at 125 ^{o}C. However, relative to reference material without carbon nanotubes, the largest increase of 140.4% was obtained at 25 ^{o}C with the same material.

Further thermal conductivity increase can be expected with further RCNT loading increase.

Based on the above, carbon nanotubes have substantial impact on thermal conductivity of composite materials to which they are added. To improve thermal conductivity of the material to which they are added, selected carbon nanotubes quality and quantity should be compatible with the material structure and components. Increased carbon fibre preform stiffness and uneven carbon fibre nanocomposite fracture surface point to improved mechanical properties of the material obtained with the addition of carbon nanotubes.

6.2. Contributions

Carbon nanotube quality importance for epoxy composites thermal conductivity was demonstrated.

New method to modify carbon fibres with carbon nanotubes was found. Employing ultrasonic bath with ice bath, combined with incremental addition of CNTs, gave good distribution of carbon nanotubes within the carbon fibre preform. Effective overcome of the filtering effect was further facilitated by selecting small thickness carbon fibre fabric made of low count tows - emulation of layer by layer method.

Novel material was created by adding carbon nanotubes to carbon fibre preform utilising above described method. This novel material exhibits increased stiffness.

New prepreg material was created by using the carbon nanotube modified carbon fibre preform as epoxy matrix reinforcement, followed by partial cure in oven.

To eliminate thermally insulating matrix accumulation against the tool plate, ancillary materials stacking sequence was improved to apply breather, bleeder and release film below as well as above the sample.

Fully cured composite material laminate produced from the above new prepreg material significantly increases composite material through thickness thermal conductivity. The through thickness thermal conductivity was increased to 1.943 W/mK at 125 ^{o}C. This value is lower than the current state of the art [51], however, the composite constituent materials are different. On the other side, obtained is 140.4% thermal conductivity relative increase at 25 ^{o}C, by far exceeding ~44% obtained in [51]. The composite material fracture surface is uneven, pointing to increased material toughness.

6.3. Future Work

Further increase in CFRP through thickness thermal conductivity could be obtained. One avenue to pursue would be RCNT content increase above 3 wt%. Another one would be incorporation of carbon nanotubes of higher quality than the ones employed in this research. Investigation could be conducted to determine the best way to obtain carbon nanotubes with the quality high enough to obtain engineering level through thickness thermal conductivity in carbon fibre reinforced composites.

Structural parts employed in areas where heat dissipation is of concern are often exposed to thermal cycling. Improved through thickness thermal conductivity impact on mechanical properties of structural parts exposed to thermal cycling could provide insight in applicability of composite materials developed in the course of this work.

Increased stiffness of carbon fibre preform and uneven surface observed in SEM pictures, a feature of a tough material, point to improved mechanical properties of the material developed in the course of this work. Evaluation of improvement of mechanical properties achieved in the novel material could be object of a future study. Parameters like carbon nanotube quality with respect to mechanical properties and loading could be optimized for mechanical properties optimisation.

Evaluation of new method using ultrasound to modify carbon fibres with carbon nanotubes applicability on other material systems can be conducted. These systems could be based on either carbon or glass fibres in any form. Nanomaterials added could be any of the known materials: carbon nanotubes, graphene, nanoclay, microcapsules or any combination of the above.

References

[1] L.V. Radushkevich, V.M. Lukyanovich: O structure ugleroda, obrazuyucegosya pri termiceskom razlogenii okisi ugleroda na zeleznom kontakte; Zurn Fizic Himii 1952, 26: 88-95.

[2] M. Monthioux,V.L. Kuznetsov: Who should be given the credit for the discovery of carbon nanotubes; Carbon 2006, 44: 1621-1623.

[3] S. Iijima, T. Ichihashi: Single-shell carbon nanotubes of 1-nm diameter; Nature 1993, 363: 603-605.

[4] D.S. Bethune, C.H. Klang, M.S. de Vries, G. Gorman, R. Savoy, J. Vasquez, R. Beyers : Cobalt-catalysed growth of carbon nanotubes with single-atomic-layer walls; Nature 1993, 363: 605-607.

[5] N. Hamada, S. Sawada, A. Oshiyama: New one-dimensional conductors: Graphitic microtubules; Physical Review Letters 1992, 68: 1579-1581.

[6] M. S. Dresselhaus, G. Dresselhaus, and R. Saito; Physics of CNTs; Carbon 1995, 33: 883-891.

[7] J. Yu, R. K. Kalia, P. Vashishta: Phonons in graphitic tubules: A tight-binding molecular dynamics study; Journal of Chemical Physics 1995, 103: 6697-6705.

[8] M. S. Dresselhaus, G. Dresselhaus, P. Eklund and R. Saito: Carbon Nanotubes, Physics Word 1998, 33.

[9] CRC Handbook of Chemistry and Physics, 9th Edition, 2013-2014

[10] J. Hone, M. Whitney, C. Piskoti, A. Zettl: Thermal conductivity of single-walled carbon nanotubes; Physical Review B 1999, 59: 2514-2516.

[11] J.M. Ziman: Electrons and Phonons: The Theory of Transport Phenomena in Solids, Oxford Scholarship Online, 2007.

[12] B.T. Kelly: Physics of Graphite, Applied Science Publishers, 1981.

[13] J. Hone, M.C. Llaguno, M.J. Biercuk, A.T. Johnson, B. Batlogg, Z. Benes, J.E. Fischer: Thermal properties of carbon nanotubes and nanotube-based materials; Appl. Phys. A 2002, 74: 339–343.

[14] P. Kim, L. Shi, A. Majumdar, P.L. McEuen: Thermal Transport Measurements of Individual Multiwalled Nanotubes; Physical Review Letters 2001, 87: 215502-1 215502-4.

[15] E. Pop, D. Mann, J. Cao, Q. Wang, K. Goodson, H. Dai: Negative Differential Conductance and Hot Phonons in Suspended Nanotube Molecular Wires; Physical Review Letters 2005, 95: 155505-1- 155505-4.

[16] C. Yu, L. Shi, Z. Yao, D. Li, A. Majumdar: Thermal Conductance and Thermopower of an Individual Single-Wall Carbon Nanotube, Nano Letters 2005, 5: 1842-1846.

[17] M.T. Pettes, L. Shi: Thermal and Structural Characterizations of Individual Single-, Double-, and Multi-Walled Carbon Nanotubes; Advanced Functional Materials 2009, 19: 3918–3925.

[18] A.E. Aliev, M.H Lima, E. M. Silverman, R.H. Baughman: Thermal conductivity of multi-walled carbon nanotube sheets: radiation losses and quenching of phonon modes; Nanotechnology 2010, 21: 035709 – 1-11.

[19] J. Guo, X. Wang: Thermal characterization of microscale conductive and nonconductive wires using transient electrothermal technique; Journal of Applied Physics 2007, 101: 063537-1 - 063537-7.

[20] T. Wang, X. Wang, J. Guo, Z. Luo, K. Cen: Characterization of thermal diffusivity of micro/nanoscale wires by transient photo-electro-thermal technique; Applied Physics A 2007, 87: 599–605.

[21] J. Guo, X. Wang, D.B. Geohegan, G. Eres, and C. Vincent: Development of pulsed laser-assisted thermal relaxation technique for thermal characterization of microscale wires; Journal of Applied Physics 2008, 103: 113505-1 - 113505-9.

[22] M.B. Jakubinek, M.B. Johnson, M.A. White, C. Jayasinghe, G. Li, W. Cho, M.J. Schulz, V. Shanov: Thermal and electrical conductivity of array-spun multi-walled carbon nanotube yarns; Carbon 2012, 50: 244-248.

[23] J. Hone, M.C. Llaguno, N.M. Nemes, A.T. Johnson, J.E. Fischer, D.A. Walters, M.J. Casavant, J. Schmidt, and R.E. Smalley: Electrical and thermal transport properties of magnetically aligned single wall carbon nanotube films; Applied Physics Letters 2000, 77: 666-668.

[24] B. Zhao, D.N. Futaba, S. Yasuda, M. Akoshima, T. Yamada, and K. Hata: Exploring Advantages of Diverse Carbon Nanotube Forests with Tailored Structures Synthesized by Supergrowth from Engineered Catalysts; ACS Nano 2008, 3: 108-114.

[25] M. Akoshima, K. Hata, D.N. Futaba, K. Mizuno, T. Baba, M. Yumura: Thermal diffusivity of SWNT Forests Measured by Laser Flash Method; Japanese Journal of Applied Physics 2009, 48: 05EC07 – 1-6.

[26] M.B. Jakubinek, M.A. White, G. Li, C. Jayasinghe, W. Cho, M.J. Schulz, V. Shanov: Thermal and electrical conductivity of tall, vertically aligned carbon nanotube arrays; Carbon 2010, 48: 3947-3952.

[27] S. Berber, Y-K Kwon, D. Tománek: Unusually High Thermal Conductivity of Carbon Nanotubes; Physical Review Letters 2000, 84: 4613-4616.

[28] R.A. Shelly, K. Toprak, Y. Bayazitoglu: Nose-Hoover thermostat length effect on thermal conductivity of single wall carbon nanotubes; International Journal of Heat and Mass Transfer 2010, 53: 5884–5887.

[29] X.H. Yan, Y. Xiao, Z.M. Li: Effects of intertube coupling and tube chirality on thermal transport of carbon nanotubes; Journal of Applied Physics 2006, 99: 124305-1 – 124305-4

[30] M. J. Biercuk, M. C. Llaguno, M. Radosavljevic, J. K. Hyun, A. T. Johnson, J. E. Fischer: Carbon nanotube composites for thermal management; Applied Physic Letters 2002, 80: 2767-2769.

[31] N.A Kotov, A.A Memedov, M. Prato, D.M. Guldi, J. Wicksted, A. Hirsch: Designing Ultrastrong Materials for Space Applications; SPIE Proceedings 2004, 5166: 228-237.

[32] F. Du, C. Guthy, T. Kashiwagi, J. E. Fischer, K. I. Winey: An Infiltration Method for Preparing Single-Wall Nanotube/Epoxy Composites with Improved Thermal

Conductivity; Journal of Polymer Science: Part B: Polymer Physics 2006, 44: 1513–1519.

[33] M. Wirts-Riitters, M. Heimann, J. Kolbe, K.-J. Wolter: Carbon nanotube (CNT) filled adhesives for microelectronic packaging; 2nd Electronics System Integration Technology Conference 2008, 1057-1062.

[34] W.-T. Hong, N.-H. Tai: Investigations on the thermal conductivity of composites reinforced with carbon nanotubes; Diamond & Related Materials 2008, 17: 1577-1581.

[35] Kai Yang, Mingyuan Gu, Yiping Guo, Xifeng Pan, Guohong Mu: Effects of carbon nanotube functionalization on the mechanical and thermal properties of epoxy composites; Carbon 2009, 47: 1723-1737.

[36] S. Wang, R. Liang, B. Wang, C. Zhang: Dispersion and thermal conductivity of carbon nanotube composites; Carbon 2009, 47: 53-57.

[37] S.-Y. Yang, C.-C.M. Ma, C.-C. Teng, Y.-W. Huang, S.-H. Liao, Y.-L. Huang, H.-W. Tien, T.-M. Lee, K.-C. Chiou: Effect of functionalized carbon nanotubes on the thermal conductivity of epoxy composites; Carbon 2010, 48: 592-603.

[38] Ramsha R., Saqib A., Fiaz A., Shafiq U., J.T. Grant, Javed I.: Advance polymeric carbon nanocomposite films with enhanced thermo-mechanical properties; Polymer Composites 2011: 1757-1765.

[39] B.-H. Chen, C.-H.Lan, M.-S. Jeng, C.-J.Huang, M.-L. Chang, F.-H. Tsau, J.-R. Ku, S.-Y.Lin: Influence of biphenyl chemisorption on the thermal properties of single-walled carbon nanotube; International Symposium on Computer, Communication, Control and Automation 2010, 314-317.

[40] S. Inoue, Y. Matsumura: MD Study of Functionalized Single-Walled Carbon Nanotube; Journal of Thermal Science and Technology 2011, 6: 256-267.

[41] E. S. Choi, J. S. Brooks, D. L. Eaton, M. S. Al-Haik, M. Y. Hussaini, K. Dahmen: Enhancement of thermal and electrical properties of carbon nanotube polymer composites by magnetic field processing; Journal of Applied Physics 2003, 94: 6034-6039.

[42] J.J. Vilatela, R. Khare, A.H. Windle: The hierarchical structure and properties of multifunctional carbon nanotube fibre composites; Carbon 2011, 50: 1227-1234.

[43] V. Datsyuk, I. Firkowska, K. Gharagozloo-Hubmann, M. Lisunova, A.-M. Vogt, A. Boden, M. Kasimir, S. Trotsenko, G. Czempiel, S. Reich: Carbon nanotubes based engineering materials for thermal management applications; 27th IEEE SEMI-THERM Symposium 2011: 325-332.

[44] V. Datsyuk, S. Trotsenko, S. Reich: Carbon-nanotube-polymer nanofibers with high thermal conductivity; Carbon 2013, 52: 605-608.

[45] Y. A. Kim, S. Kamio, T. Tajiri, T. Hayashi, S. M. Song, and M. Endo: Enhanced thermal conductivity of carbon fiber/phenolic resin composites by the introduction of carbon nanotubes; Applied Physics Letters 2007, 90: 093125-1 - 93125-3.

[46] M. Theodoore, J. Fielding, K. Green, D. Dean, N. Horton, A. Noble, S. Miller: Nanostructured Coupling Agents for Multifunctional Composites; SAMPE Conference Proceedings 2009, 54: 18 pages.

[47] L. Yoo, H. Kim: Conductivities of Graphite Fiber Composites with Single-Walled Carbon Nanotube Layers; International Journal of Precision Engineering and Manufacturing 2011, 12: 745-748.

[48] S. Han, D.D.L. Chung: Increasing the through-thickness thermal conductivity of carbon fiber polymer-matrix composite by curing pressure increase and filler incorporation; Composites Science and Technology 2011, 71: 1944–1952.

[49] M. Zimmer, Q. Cheng, S. Li, J. Brooks, R. Liang, B. Wang, C. Zhang: Comparative Characterization of Multiscale Carbon Fiber Composite with Long and Short MWCNTs at Higher Weight Fractions; Journal of Nanomaterials 2012, 532080 – 1-9.

[50] K. Naito, J.-M. Yang, Y. Xu, Y. Kagawa: Enhancing the thermal conductivity of polyacrylonitrile- and pitch-based carbon fibers by grafting carbon nanotubes on them; Carbon 2010, 48: 1849-1857.

[51] R.B. Mathur, B.P. Singh, P.K. Tiwari, T.K. Gupta: Enhancement in the thermomechanical properties of carbon fibre-carbon nanotube-epoxy hybrid composites; International Journal of Nanotechnology 2012, 9: 1040-1049.

[52] Class for Physics of the Royal Swedish Academy of Sciences: Scientific background on the Nobel Prize in Physics 2010.

[53] A.A. Balandin, S. Ghosh, W. Bao, I. Calizo, D. Teweldebrhan, F. Miao, C.N. Lau: Superior Thermal Conductivity of Single-Layer Graphene; Nano Letters 2008, 8: 902-907.

[54] A. Yu, P. Ramesh, X. Sun, E. Bekyarova, M.E. Itkis, R.C. Haddon: Enhanced thermal conductivity in a hybrid graphite nanoplatelet - Carbon nanotube filler for epoxy composites; Advanced Materials 2008, 20: 4740-4744.

[55] K.M.F. Shahil, V. Goyal, R. Gulotty, A.A. Balandin: Graphene Fillers for Ultra-Efficient Thermal Interface Materials; 2012 IEEE Silicon Nanoelectronics Workshop (SNW), p 2 pp., 2012.

[56] Ke Chu ·Wen-sheng Li · Hongfeng Dong: Role of graphene waviness on the thermal conductivity of graphene composites; Applied Physics A 2013, 111: 221-225.

[57] X. Huang, C. Zhi, P. Jiang: Toward Effective Synergetic Effects from Graphene Nanoplatelets and Carbon Nanotubes on Thermal Conductivity of Ultrahigh Volume Fraction Nanocarbon Epoxy Composites; The Journal of Physical Chemistry 2012, 116: 23812-23820.

[58] L. Yu, J.S. Park, Y.-S. Lim, C.S. Lee, K. Shin, H.J. Moon, C.-M. Yang, Y.S. Lee, J.H. Han: Carbon Hybrid Fillers Composed of Carbon Nanotubes Directly Grown on Graphene Nanoplatelets for Effective Thermal Conductivity in Epoxy Composites; Nanotechnology 2013, 24: 155604 (7pp).

[59] S.H. Song, K.H. Park, B.H. Kim, Y.W. Choi, G. H. Jun, D.J. Lee, B.-S. Kong, K.-W. Paik, S. Jeon: Enhanced Thermal Conductivity of Eoxy-Graphene Composites by Using Non-Oxidized Grahene Flakes with Non-Covalent Functionalisation; Advanced Materials 2013, 25: 732-737.

[60] S. Ganguli,, A.K. Roy, D.P. Anderson: Improved thermal conductivity for chemically functionalized exfoliated graphite-epoxy composites; Carbon 2008, 46: 806-817.

[61] M. Martin-Gallego, M.M. Bernal, M. Hernandez, R. Verdejo, M.A. Lopez-Manchado: Comparison of filler percolation and mechanical properties in graphene

and carbon nanotubes filled epoxy nanocomposites; European Polymer Journal 2013, 49: 1347–1353.

[62] Z. He, X. Zhang, M. Chen, M. Li, Y. Gu, Z. Zhang, Q. Li: Effect of the Filler Structure of Carbon Nanomaterials on the Electrical, Thermal, and Rheological Properties of Epoxy Composites; Journal of Applied Polymer Science 2013: 3366-3372.

[63] H. Rong, Z. Liu, Q. Wua, Y.-H. Lee: A facile and efficient gas phase process for purifying single-walled carbon nanotubes; Current Applied Physics 2010, 10: 1231–1235.

[64] Toho-Tenax Properties of filaments – Data available on Toho-Tenax web site.

[65] Certificate of Analysis – Unidym, 29 March 2012.

[66] Certificate of Analysis – Unidym Carbon nanotubes, 10 March 2008.

[67] Certificate of Analysis – Carbon Nanotechnologies Incorporated Carbon nanotubes, 28 January 2008.

[68] Resolution Performance Products Product Bulletin: SC:1183-02 / EPIKOTE™ Resin 862/EPIKURE™ Curing Agent W System.

[69] Carl Glezen, Hexion Specialty Chemicals, Inc., Houston Technology Center – e-mail (14 February 2008).

[70] I. Rosca, S.V. Hoa: Highly conductive multiwall carbon nanotube and epoxy composites produced by three-roll milling; Carbon 2009, 47: 1958-1968.

[71] Operating instructions LFA 447^{TM} Nanoflash – Netzsch.